Ontwerp van groene draadloze toegangsnetwerken
voor outdooromgevingen: optimalisatie van
energieverbruik en elektromagnetische bestraling van de mens

Design of Green Wireless Access Networks
for Outdoor Environments: Optimization towards
Power Consumption and Electromagnetic Exposure for Human Beings

Margot Deruyck

Promotoren: prof. dr. ir. L. Martens, prof. dr. ir. W. Joseph
Proefschrift ingediend tot het behalen van de graad van
Doctor in de Ingenieurswetenschappen: Computerwetenschappen

Vakgroep Informatietechnologie
Voorzitter: prof. dr. ir. D. De Zutter
Faculteit Ingenieurswetenschappen en Architectuur
Academiejaar 2014 - 2015

UNIVERSITEIT
GENT

ISBN 978-90-8578-757-0
NUR 986
Wettelijk depot: D/2015/10.500/1

Universiteit Gent
Faculteit Ingenieurswetenschappen en Architectuur
Vakgroep Informatietechnologie

Promotoren: Prof. Dr. Ir. Luc Martens
Prof. Dr. Ir. Wout Joseph

Universiteit Gent
Faculteit Ingenieurswetenschappen en Architectuur

Vakgroep Informatietechnologie
Gaston Crommenlaan 8 bus 201, B-9050 Gent, België

Tel.: +32-9-331.49.00
Fax.: +32-9-331.48.99

Proefschrift tot het behalen van de graad van
Doctor in de Ingenieurswetenschappen:
Computerwetenschappen
Academiejaar 2014-2015

Dankwoord

Na vijf jaar is de finishlijn bereikt! Eindelijk heb ik “mijn” boek in handen. Mijn naam staat ook inderdaad op de flap van dit boek, maar het is niet enkel het resultaat van mijn zweet, bloed en tranen... Een doctoraat schrijf je namelijk helemaal niet alleen. Ik sta hier in de schijnwerpers, maar er zijn heel wat mensen die “achter de schermen” aan dit doctoraat hebben bijgedragen. Het is dan ook maar normaal dat deze eerste pagina’s gewijd worden aan het bedanken van al deze mensen. Toen ik bijna een jaar geleden startte met het schrijven van dit boek, dacht ik dan ook dat dit dankwoord zichzelf zou schrijven. In mijn hoofd wist ik perfect wie ik waarvoor zou bedanken, al dan niet met een vrolijke kwinkslag. Het op papier zetten van deze laatste woorden valt me echter zwaarder (en emotioneler) dan ooit gedacht en misschien is het resultaat nog niet 100% wat ik voor ogen had, weet dat ik jullie allemaal bijzonder dankbaar ben! Ooit dacht ik dat het de bedoeling was om die mensen te bedanken die actief hebben meegeholpen aan het onderzoek, maar na het lezen van de vele dankwoorden van mijn voorgangers, begrijp ik dat dit dankwoord juist een opportuniteit biedt om ook die mensen die in je privé sfeer een positieve bijdrage hebben geleverd te bedanken. Uiteraard wil ik deze traditie dan ook niet verbreken... Ik ga hier niet iedereen bij naam noemen, maar ik ga ervan uit dat iedereen wel weet wanneer hij/zij zich moet aangesproken voelen. Het risico is wellicht reëel dat ik in deze lijst nog iemand vergeet, alvast sorry daarvoor, maar toch een welgemeende merci!

Een doctoraat gaat hand in hand met een promotor en ik had de eer en het genoegen om er maar liefst twee te hebben. Luc en Wout, bedankt voor alle kansen die jullie mij aangeboden hebben, voor het nalezen van die duizenden woorden en mijn werk waar nodig bij te sturen. Bedankt!

Een hele speciale dankjewel voor mijn ouders. Bedankt om mij te steunen tijdens mijn ingenieursstudies en in mijn keuze om voor een doctoraat te gaan. Bedankt om mij op zovele manieren bij te staan, zonder jullie steun[1] zou ik vandaag niet staan waar ik nu sta. Het is onmogelijk om alle dingen waarvoor ik jullie wil bedanken op papier te zetten, dus uit het diepste van mijn hart: dankjewel!

De Wireless & Cable, aka WiCa, collega’s en ex-collega’s! Bedankt om iedere dag in een aangename sfeer te laten verlopen. Bedankt voor de werkgerelateerde

[1] ’Per ardua ad astra’ ;-)

discussies, over de iets minder werkgerelateerde discussies, tot de fantasierijke gesprekken aan de WiCa eettafel in de gang voor onze deur. Toen ik vijf jaar geleden begon bij de WiCa, waren we nog maar met een tiental. Intussen zijn we bijna verdubbeld. De bureau verandert hierdoor op sommige dagen in een klein "kiekenkot", maar desalniettemin maken jullie het verschil. Gezien de grootte van de groep is er een aanzienlijk risico dat ik een dierbare (ex-)collega zou vergeten in het lijstje, maar ik reken erop dat jullie het mij allen vergeven dat ik er slechts enkelen bij naam noem om even in de bloemetjes te zetten met een special thanks!
Als eerste uiteraard Emmeric! Zes jaar geleden kreeg ik je totaal onverwachts als begeleider van mijn master thesis. De ellenlange mailtjes van toen zijn intussen vervangen door een inleidend "Emmeric, heb je een minuutje?". Bedankt Emmeric, voor die vele minuutjes, om te helpen bij het uitwerken van wetenschappelijke uitdagingen en praktische zaken, om mijn levende encyclopedie te zijn als ik een Matlab commando zocht, om teksten te herlezen en zoveel keer mijn Engels te verbeteren, om bevestiging te geven waar nodig!
Ook een special thanks naar Simon! Van het examen Discrete Wiskunde over onze masterproef en IWT verdediging tot uiteindelijk onze doctoraatsverdediging. Tijdens onze opleiding legden we een identiek traject af (tot zelfs identiek dezelfde examens ;-)). In ons onderzoek gingen we qua onderwerp ieder onze eigen weg, maar bedankt om zoveel jaar mijn "running mate" te zijn en het beantwoorden van de vele vragen en mailtjes tijdens de laatste loodjes van ons doctoraat!
Isabelle, voor het bijstaan bij alle adminstratieve zaken. Ik probeerde mijn onkostennota's zo duidelijk mogelijk te maken, maar er was altijd wel weer een onvoorziene omstandigheid waarvoor ik je hulp nodig had.
Tot slot, Leen en Kris, voor het installeren van mijn "infrastructuur" en ervoor te zorgen dat dat bestand dat ik weer eens had verwijderd toch nog ergens te vinden was. Het maakte het werken zoveel aangenamer!

Ook buiten de WiCa groep zijn er enkele Green ICT (ex-)collega's die ik wens te bedanken: Willem, Sofie, Ward en Bart. Bedankt voor de vele vruchtbare samenwerkingen!

Rebecca, thanks voor de "dates" met of zonder mannen, voor het praten over de kleine en de grote dinges des levens en de occasionele vrouwentalk. Laten we deze gewoonte zeker verder zetten in de toekomst!

De studievrienden en hun vriendinnen! Intussen zijn we al enkele jaren afgestudeerd en zien we elkaar belange na niet meer dagelijks. Het is niet altijd even gemakkelijk om met zijn allen af te spreken, maar als we bij elkaar zijn, hebben we altijd een gezellige tijd die veel te snel voorbij is. Bedankt voor die gezellige tijden, de interesse in het onderzoek en de bemoedigend woordjes op de juiste tijdstippen. We moeten vaker afspreken!

Graag bedank ik ook de "bende van Torhout" (hoewel er momenteel niemand meer in Torhout woont ;-)). Ook hier geldt dat we elkaar veel te weinig zien, maar

dat het toch altijd gezellig is. Bedankt voor die gezellige avonden, BBQs en uiteraard... de oudejaarsavondfeestjes!

Iedereen gaat me nu ongetwijfeld compleet gek verklaren: Arsenio en Valioso de la Canardière, mijn paarden, op jullie rug kreeg ik vaak de meest verrijkende inzichten!

Een doctoraatsdankwoord wordt typisch met het beste afgesloten dus de laatste woorden zijn voor Alex(ander)! Bedankt om er altijd voor mij te zijn, om de traantjes te drogen bij verdriet en in vreugde te delen, om niet van mijn zijde te wijken tijdens mijn eerste 20km van Brussel, om mij de ruimte te geven die ik nodig heb en ze soms juist niet te geven, bedankt voor zovele dingen, veel te veel om op te noemen! Ik kan me niemand anders naast mijn zijde voorstellen!

Gent, januari 2015
Margot Deruyck

Table of Contents

List of Figures

List of Tables

List of Symbols and Acronyms

0-9

2G Second Generation

3G Third Generation

3GPP Third Generation Partnership Project

4G Fourth Generation

A

AC Alternating Current

B

BER Bit Error Rate

BIPT Belgian Institute for Postal services and Telecommunications

BS Base Station

C

CA Carrier Aggregation

D

DC Direct Current

DSL Digital Subscriber Line

E

EIRP Equivalent Isotropically Radiated Power

EM electromagnetic

ETSI European Telecommunications Standards Institute

F

FEC Forward Error Correction

FPGA Field-Programmable Gate Array

G

GPRS General Packet Radio Service

GPS Global Positioning System

GRAND Green Radio Access Network Design

GSM Global System for Mobile Communications

H

HSPA High Speed Packet Access

I

ICNIRP International Commission on Non-Ionizing Radiation Protection

ICT Information and Communication Technology

L

LoS Line-of-Sight

LTE Long Term Evolution

M

MIMO Multiple-Input Multiple-Output

MMS Multimedia Messaging Service

MS Mobile Station

M2M Machine-to-Machine

N

nLoS non-Line-of-Sight

O

OFDMA Orthogonal Frequency Division Multiple Access

P

PC Personal Computer

PRB Physical Resource Block

Q

QAM Quadrature Amplitude Modulation

QPSK Quadrature Phase Shifting Key

R

RF Radio-Frequent

Rx Receiver

S

SISO Single-Input Single-Output

SMS Short Messaging Service

SNR Signal-to-Noise Ratio

SOFDMA Scalable Orthogonal Frequency Division Multiple Access

T

Tx Transceiver

U

UMTS Universal Mobile Telecommunication System

W

WAP Wireless Access Protocol

W-CDMA Wideband Code Division Multiple Access

WI Walfish-Ikegami

WiFi Wireless Fidelity

WiMAX Worldwide Interoperability for Microwave Access

WMAN Wireless Metropolitan Access Network

WNIC Wireless Network Interface Card

WWAN Wireless Wide Area Network

Nederlandstalige samenvatting

In het laatste decennia zagen we een enorme groei in mobiele toestellen. Vandaag de dag beschikken we niet langer enkel maar over een standaard GSM of smartphone, maar ook over een laptop, een tablet, en misschien wel een smart watch en een armband die toeziet op onze fitheid. In de loop der tijd zijn mobiele toestellen steeds krachtiger geworden en hoeven we ons niet langer te beperken tot enkel het telefoneren of surfen op het internet, maar kunnen we ook veeleisendere diensten gaan gebruiken. Denk bijvoorbeeld aan het streamen van muziek en video of de zogenaamde videochat waarbij we onze gesprekpartner ook kunnen zien tijdens het telefoneren. Deze twee trends, de groei in mobiele toestellen en het krachtiger worden van deze toestellen, hebben uiteraard een directe invloed op de draadloze toegangsnetwerken die deze toestellen bedienen. Enerzijds zullen de netwerken moeten uitgebreid worden om deze extra vraag ten gevolge van de toevloed aan mobiele toestellen te kunnen opvangen, anderszijds moeten ze ook voldoende capaciteit leveren zodat de eindgebruiker tevreden blijft. Uiteraard is er een keerzijde van de medaille. In 2008 waren communicatienetwerken al verantwoordelijk voor 15% van het ICT energieverbruik. Maar liefst 77% van dit verbruik werd veroorzaakt door de draadloze telecommunicatienetwerken van operatoren. Momenteel wordt het meeste van onze energie gewonnen uit het verbranden van fossiele brandstoffen. Niet alleen is er maar een beperkte hoeveelheid van deze brandstoffen beschikbaar, bij de verbranding ervan komt CO_2 vrij wat het natuurlijke broeikasteffect versterkt met klimaatsverandering tot gevolg. Het is dan ook belangrijk dat we in elk aspect van onze samenleving ons energieverbruik proberen te reduceren en dus in de toekomst draadloze toegangsnetwerken met een minimaal verbruik gaan ontwerpen. Naast het energieverbruik zien we dat de mens steeds vaker bezorgd is om mogelijke gezondsheidseffecten door de elektromagnetische straling van deze netwerken. Daarom is het ook belangrijk om draadloze toegangsnetwerken uit te rollen met een zo laag mogelijke straling voor de mens. Het doel van dit werk is om toekomstige groene draadloze toegangsnetwerken te ontwerpen waarbij zowel het energieverbruik als de straling van het netwerk geminimaliseerd is.

In de eerste fase van dit werk wordt het energieverbruik van de grootste verbruiker binnen draadloze toegangsnetwerken i.e., het basisstation, gekarakteriseerd. Hiervoor wordt de architectuur van drie verschillende types van basisstations (macrocell, microcell en femtocell basisstation) opgesteld. Op basis van deze architectuur wordt een model voor het energieverbruik van elk type ontworpen.

Een macrocell basisstation gebruikt typisch tussen de 1200 en 1600 W, terwijl een microcell basisstation ongeveer 4 keer minder vermogen verbruikt en een femtocell basisstation maar liefst 100 keer minder dan een macrocell basisstation. Uiteraard is energieverbruik niet de enige parameter van belang. Ook de performantie van het basisstation is belangrijk. Zo kan een basisstation meer energie verbruiken, maar ook een groter gebied bedienen met een hogere capaciteit dan een ander basisstation. Om dit op te vangen worden energie-efficiëntie metrieken gedefinieerd die niet alleen energieverbruik maar ook andere performantie parameters zoals dekking en capaciteit in rekening brengen. Deze metrieken laten ons toe om een vergelijking te maken tussen verschillende types basisstations, technologieën en netwerken. Het vergelijken van verschillende technologieën toont aan dat het afhankelijk is van de vereiste bit rate welke technologie het meeste energie-efficiënt is. Voor de verschillende basisstation types wordt aangetoond dat voor de metriek "energieverbruik per gedekt gebied" de gebruikte technologie bepaalt welk basisstation het meest energie-efficiënt is. Dit neemt echter niet weg dat het introduceren van een type basisstations met een lagere energie-efficiëntie in het netwerk kan leiden tot een lager energieverbruik van het complete netwerk omdat dit type bijvoorbeeld een lager energieverbruik heeft. Om de energie-efficiëntie van een basisstation te verhogen, kan MIMO gebruikt worden.

Voor het valideren van onze resultaten werden metingen van het energieverbuik uitgevoerd op een bestaand macrocell en microcell basisstation. Door het combineren van deze meetresultaten met de traffiek gegevens gedurende de meetperiode wordt de invloed van variaties in traffiek op het energieverbruik onderzocht.

In de tweede fase worden energie-efficiënte netwerken i.e., met een minimaal energieverbruik, ontworpen. Hiervoor wordt een netwerkplanningstool voorgesteld. Twee verschillende algoritmes worden voorgesteld: een dekkingsgebaseerd algoritme en een capaciteitsgebaseerd algoritme. Het doel van het dekkingsgebaseerd algoritme is om een bepaald gebied te dekken met een minimaal energieverbruik en voor een vooropgestelde bit rate. Het capaciteitsgebaseerd algoritme gaat reageren op de bit rate die vereist wordt door de eindgebruiker actief in het vooropgestelde gebied. De modellen voor het energieverbuik van de verschillende types van basisstations uit de vorige fase zullen in deze algoritmes gebruikt worden.

Door het dekkingsgebaseerde algoritme toe te passen op een realistisch voorbeeld in België (een greenfield ontwerp voor Gent en een optimalisatie van een bestaand netwerk in Brussel) wordt aangetoond dat LTE de energie-efficiëntste is van de beschouwde technologieën. Daarnaast wordt aangetoond dat het optimaliseren van bestaande netwerken naar energieverbruik al kan leiden tot een reductie in energieverbruik van 33%. Een zorgvuldige keuze van de locaties voor de basisstations kan dus al leiden tot een significante besparing. De energie-efficiëntie van de bekomen netwerken kan verhoogd worden door het introduceren van "small cell" basisstations.

Daarnaast wordt ook een uitbreiding van het dekkingsgebaseerde algoritme voorgesteld door het introduceren van sleep modes en cell zooming (ook wel cell breathing genaamd) in het netwerk. Beiden zijn energiebesparende technieken en

kunnen leiden tot een bijkomende reductie van 14% voor een greenfield ontwerp en 2% voor een bestaand netwerk geoptimaliseerd naar energieverbruik. Ook zonder de optimalisatie naar energieverbruik, kunnen deze technieken maar liefst 8% energie besparen. Het is dus aangeraden dat toekomstige netwerken sleep modes en cell zooming zullen ondersteunen.

Het capaciteitsgebaseerd algoritme wordt gebruikt om de invloed van drie LTE-Advanced functies te onderzoeken namelijk: carrier aggregation (wat toelaat om de bit rate per basisstation te verhogen), heterogene netwerken (waarbij macrocell en femtocell basisstations in één netwerk gebruikt worden) en verbeterde ondersteuning voor MIMO (tot 8 zend- en 8 ontvangstantennes). Er wordt vergeleken met LTE op zowel het basisstation niveau als op het netwerkniveau.

In het algemeen zal een hogere bit rate leiden tot een lagere energie-efficiëntie voor het basisstation. Maar wanneer er carrier aggregation wordt gebruikt is het echter wel mogelijk om een hogere energie-efficiëntie te bekomen bij een hogere bit rate. Dit kan nog verder verhoogd worden door het gebruik van MIMO.

Op het netwerkniveau wordt het laagste energieverbruik (en de hoogste energie-efficiëntie) bekomen wanneer de drie functies, een heterogeneen netwerk waarbij het femtocell basisstation zowel MIMO als carrier aggregation ondersteunt, samen worden aangewend. Het introduceren van femtocell basisstations die geen carrier aggregation en MIMO ondersteunen levert echter ook al tot een significantie energiebesparing.

In de derde fase wordt de blootstelling voor de mens aan elektromagnetische (EM) velden straling in rekening gebracht. Hiervoor worden twee uitbreidingen van het capaciteitsgebaseerd algoritme voorgesteld. De eerste uitbreiding ontwerpt netwerken die geoptimaliseerd zijn naar energieverbruik maar waarbij wordt voldaan aan een vooropgestelde blootstellingsnorm, terwijl de tweede uitbreiding netwerken ontwerpt waarbij de EM straling voor de mens geminimaliseerd is. De resultaten van deze twee uitbreidingen worden vergeleken met die waarbij het netwerk geoptimaliseerd is naar energieverbruik. Wanneer we optimaliseren naar energieverbruik bekomen we een netwerk dat bestaat uit een laag aantal basisstations met een hoog zendvermogen, terwijl de optimalisatie naar straling resulteert in een netwerk met een hoog aantal basisstation maar met een laag zendvermogen. Wanneer we optimaliseren naar energieverbruik maar rekening houden met een bepaalde blootstellingsnorm wordt een compromis bereikt tussen de twee andere optimalisaties.

Tenslotte worden er groene draadloze netwerken ontworpen waarbij zowel het energieverbruik als de straling geoptimaliseerd wordt. Zoals hierboven vermeld legt een dergelijke optimalisatie contrasterende vereisten op aan het netwerk. Een trade-off is dus noodzakelijk. Het capaciteitsgebaseerd algoritme wordt uitgebreid met een fitness functie die de performantie van het netwerk evalueert. Door het kiezen van geschikte wegingsfactoren wordt de gewenste afweging tussen de optimalisatie naar energieverbruik en de optimalisatie naar straling bekomen. Dit laaste algoritme laat ons toe om de gewenste toekomstige groene draadloze netwerken

te ontwerpen waarbij zowel EM blootstelling als energieverbruik geoptimaliseerd wordt.

English summary

The last few decades, a considerable increase in mobile devices ranging from mobile phones and smart phones, over laptops and tablets, to smart watches and fitness devices has been noticed. Besides this, these devices are becoming very powerful, allowing also more demanding services such as streaming music and videos, video calling, etc. These two trends have of course their influence on the wireless access networks serving those mobile devices. The network will not only have to expand in size to cope with these extra demands, but also has to provide a higher capacity to keep the end user satisfied. In 2008, communication networks were already responsible for 15% of the ICT power consumption, moreover, 77% of this consumption was caused by telecommunication operator networks. To preserve our fossil fuels and reduce CO_2 emission, every aspect of our society has to contribute and it is thus important to develop future wireless access networks with a minimal power consumption. On the other side, people are becoming more concerned about the health effects of those networks. Exposure awareness to electromagnetic fields is currently growing, so it is desirable that future wireless access networks have also a minimal global exposure for human beings. The main focus of this dissertation is to design future green wireless access networks minimizing both power consumption and global exposure for human beings.

In the first phase, the power consumption of the largest power consumer in wireless access networks i.e., the base station is characterized. Therefore, the architecture of three different base station types (macrocell, microcell, and femtocell base station) is determined. Based on this architecture, a power consumption model for each base station type is developed. A macrocell base station consumes typically around 1200 to 1600 W, while a microcell base station consumes approximately 4 times less power and a femtocell base station even 100 times compared to the macrocell base station. However, power consumption is not the only parameter when developing an energy-efficient network. For example, a base station can have a higher power consumption but also offering a higher coverage and higher capacity compared to another base station. Therefore, appropriate energy efficiency metrics, taking into account both power consumption and performance parameters (such as coverage, capacity, etc.), are defined to determine and compare the energy efficiency of different base stations, wireless technologies, and networks. Comparing different wireless technologies shows that it depends on the required bit rate which one is the most energy-efficient. For the different base station types, it was found that for the energy efficiency metric "power consumption per covered

area", it depends on the considered technology which base station type is the most energy-efficient. However, introducing a less energy-efficient base station type in the network can reduce the overall network power consumption because it has for example a lower power consumption. To increase the energy efficiency of a single base station, MIMO can be used.

To validate the power consumption values obtained by our models for the different base station types, measurements were performed on an actual macrocell and microcell base station. By combining the results of these power consumption measurements with the traffic data of the measurement time period, it was possible to investigate the influence of traffic variations on the base station's power consumption.

In the second phase, energy-efficient wireless access networks are developed. To this end, a deployment tool for the design of wireless access networks optimized towards power consumption is proposed. Two algorithms are presented: a coverage-based algorithm, using a genetic search algorithm and a capacity-based algorithm. The purpose of the coverage-based algorithm is to cover a specific (geometrical) area with a minimal power consumption for a certain predefined bit rate. Analogously, the capacity-based algorithm develops networks optimized towards power consumption but responding to the instantaneous bit rate request of the users active in the considered area, rather than providing coverage to a certain area. The power consumption model of the different base station types is used by both algorithms when developing and evaluating the network.

When applying the coverage-based algorithm on realistic cases in Belgium (a greenfield deployment in Ghent and optimizing an existing network in Brussels), the highest energy efficiency was obtained by LTE (amongst the considered technologies and for the considered cases and assumptions). Optimizing an existing network towards power consumption can reduce the consumed power by 33%. A careful selection of the base station locations can thus already result in a significant saving. The energy efficiency of all the considered scenarios can further be increased when introducing small cell base stations in the network. Furthermore, an extension on the coverage-based algorithm is proposed, combining sleep modes and cell zooming (or cell breathing). Both these techniques are power reducing and can result in an additional power saving of 14% for the considered greenfield deployment, and 2% for an existing network optimized towards power consumption. Introducing sleep modes and cell zooming in an existing network not optimized towards power consumption can reduce the power consumption by 8%. For future networks, it is recommended to support sleep modes and cell zooming.

The capacity-based algorithm is used to investigate the influence of three features added to LTE-Advanced on the power consumption and energy efficiency. A comparison with LTE is made. These three features are carrier aggregation (to increase the bit rate of the base station), improved support for heterogeneous networks (consisting of a mixture of macrocell and femtocell base stations), and extended support for MIMO (even up to 8 transmitting and 8 receiving antennas). This investigation is performed on the base station level and on the network level.

In general, for a single base station, a higher bit rate results in a lower energy efficiency. However, by using carrier aggregation, LTE-Advanced allows to obtain higher bit rates for even a higher energy efficiency. Furthermore, MIMO can also increase the energy efficiency of a single base station.

On the network level, the highest power reduction (and energy efficiency improvement) is obtained when applying the three features together i.e., a heterogeneous network where the femtocell base station supports both carrier aggregation and MIMO. However, adding femtocell base station without carrier aggregation and MIMO can already reduce the power consumption significantly.

In the third phase, global exposure for human beings is taken into account when developing networks. To do this, two extensions of the capacity-based algorithm are proposed. The first extension develops networks optimized towards power consumption satisfying a certain exposure limit, while the second extension optimizes networks towards global exposure for human beings. The results obtained with those two extensions are compared to the results when optimizing only towards power consumption. This comparison shows that when optimizing towards power consumption, the network consists of a low number of high-power base stations, while optimizing towards global exposure results in a network consisting of a high number of low-power base stations. When optimizing towards power consumption while satisfying a certain exposure limit, a compromise between the other two optimizations is obtained.

In the last phase, green wireless access networks optimizing towards both power consumption and global exposure are developed . As mentioned above, the optimization towards power consumption and towards global exposure imposes conflicting requirements on the network. A trade-off between these two parameters has to be made. The capacity-based algorithm is extended with a fitness function evaluating the performance of the network. By choosing appropriate weight factors in the fitness function, the required trade-off between the importance of optimizing towards power consumption and towards global exposure can be obtained. This last algorithm allows to design the desired future green wireless access networks minimizing both power consumption and global exposure.

1 Introduction

1.1 Context and motivation

In 1993 the mobile phone entered the commercial market. The idea of calling (or being called) wherever you are, was innovative resulting in a very quick adoption of this device, not only in the professional world but also privately. Merely ten years after his introduction, already 1.5 billion subscriptions were sold worldwide. In 20 years, the mobile phone has incredibly changed from a device only used for calling to today's smart phone which is a small computer on its own with possibilities far beyond voice calls. However, the wireless world has not stopped with mobile phones and smart phones. Laptops, tablets, gaming consoles, etc. all have wireless access to the internet and has become very popular. Although it seems that wireless devices are already hugely involved in our daily life, it is still expected that the number of global mobile devices will grow significantly. By 2017, 8.6 billion handheld or personal devices and 1.7 billion Machine-to-Machine (M2M) connections (such as Global Positioning System (GPS) systems in cars, tracking systems in shipping sector, medical or health applications, smart homes, etc.) will exist which is a growth of 13% compared to 2012 as shown in Fig. 1.1 [1].

As mentioned above, mobile devices are nowadays very powerful. People are using their mobile devices for other activities than voice calls as well such as reading or sending mails, visiting social network sites, streaming music or video, making video calls, downloading apps, etc. Fig. 1.2 gives an overview of the most

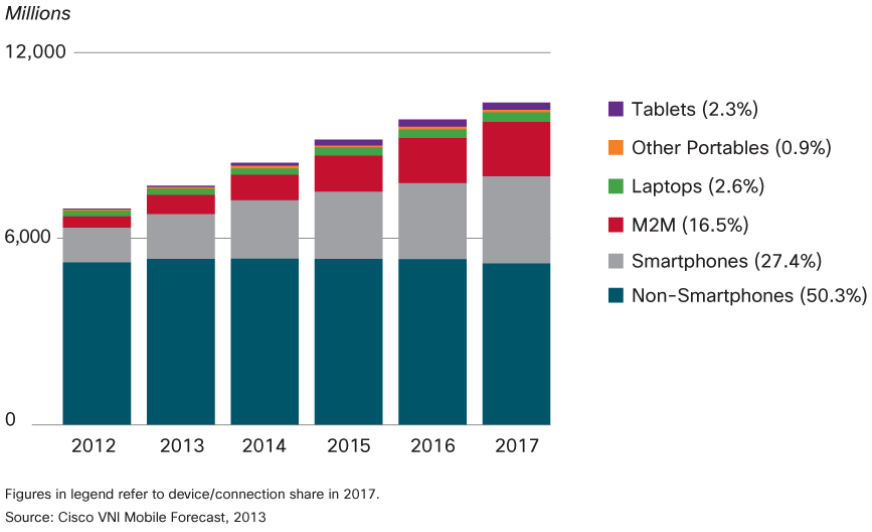

Figure 1.1: Growth and growth prediction of global mobile devices [1].

popular activities on a smart phone and indicates how many (as a percentage) of the surveyed people execute the activity on a daily base [2]. Besides the fact that people are using their mobile devices in an other way than ten years ago, these activities also result in higher traffic demands than before. For example, a higher bit rate will be required when making a video call than an ordinary voice call. This has of course a direct influence on the amount of mobile data traffic. In two years time, the global mobile data traffic has tripled, and Cisco predicts a 13-fold increase by 2017 as shown in Fig. 1.3 [1].

It is obvious that this extreme growth in data traffic and user devices has its influence on the network. Wireless technologies are of course evolving as well, providing higher data rates, but the network must also be able to serve this amount of users and their demands. In 2008, communication networks (both wired and wireless) were already responsible for 15% of the electricity consumption of Information and Communication Technology (ICT) [3]. Within communication networks, telecommunication operator networks (i.e., cellular networks) consume 77% of the power as shown in Fig. 1.4 [4]. From 2007 to 2012, the power consumed by these networks increased by 10%. Within those networks, or more general wireless access networks, the base stations, which is the equipment to communicate with the mobile devices and the backhaul network, are large power consumers. Currently most of the energy is produced by burning fossil fuels such as natural gas, oil, wood, etc. which are non-renewable energy resources with only a limited amount

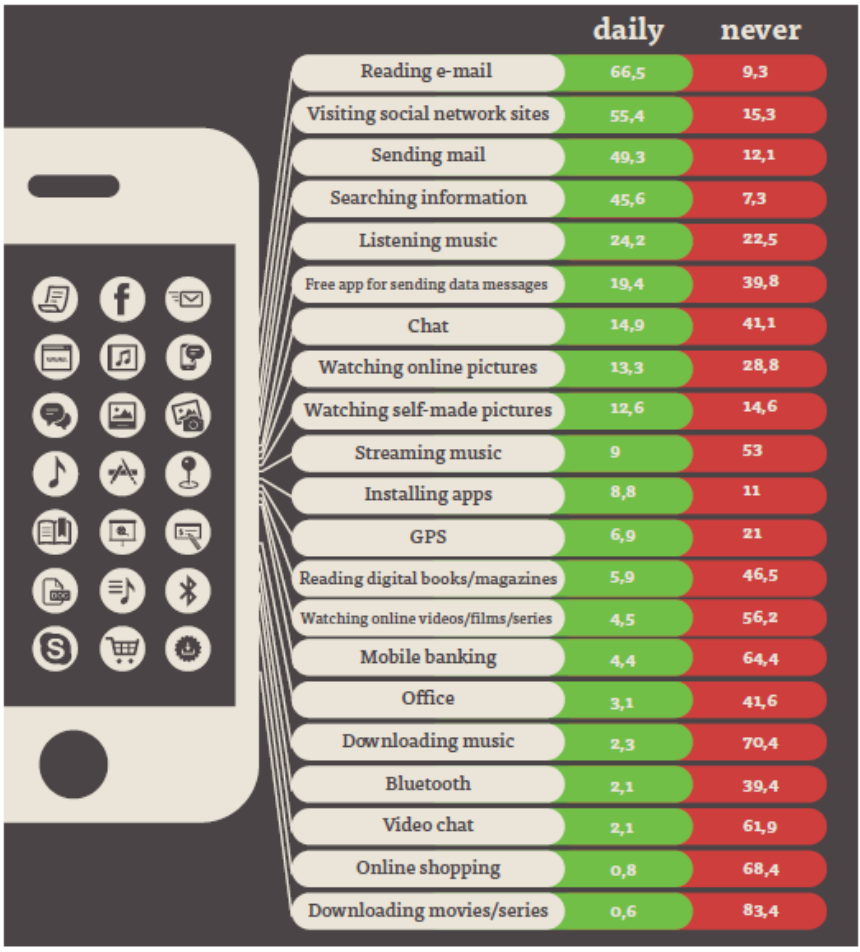

Figure 1.2: Overview of the most popular activities on a smart phone and the percentage of surveyed people executing this activity in 2012 [2].

available. The burning processes of these fuels cause the emission of carbon dioxide (i.e., CO_2). As CO_2 emission directly contributes to the climate change, it is important that future wireless access networks try to reduce their power consumption and ecological footprint.

Besides power consumption, people are also more and more concerned about possible health effects due to electromagnetic (EM) radiation. A recent study in Flanders, Belgium, showed that about 5% of the respondents does not have a mobile phone [2]. Fig. 1.5 shows the reasons for not adopting a mobile phone. Approximately 6% of the non-adopters is worried about his/her health. EM field

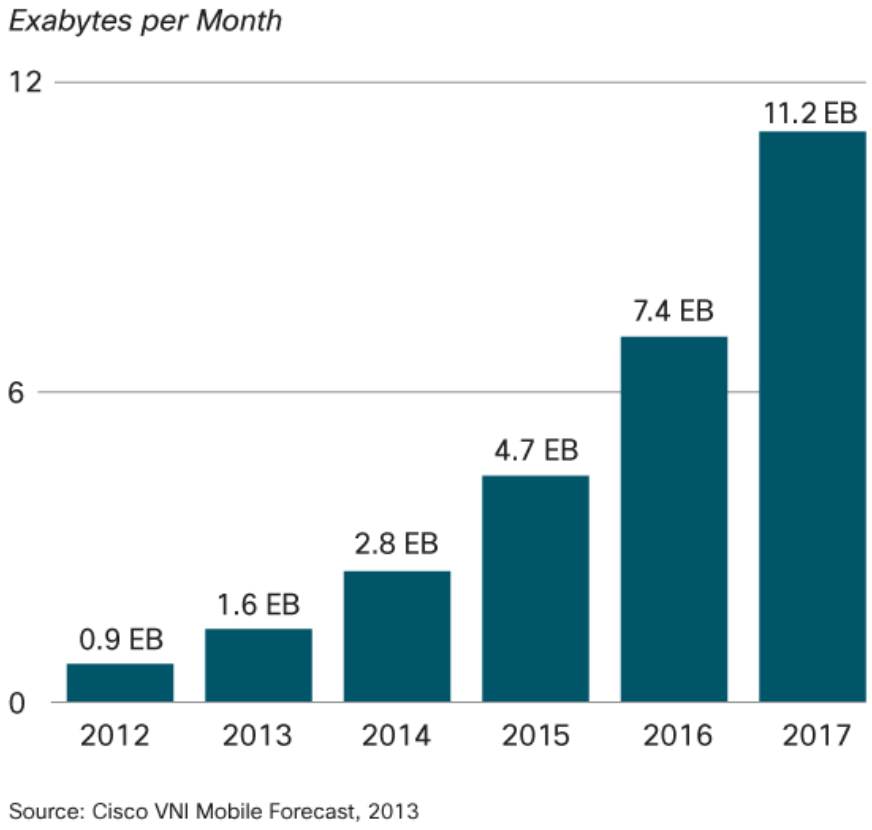

Figure 1.3: Growth and growth prediction of the global mobile data traffic per month [1].

exposure awareness has significantly increased in the last few years. International organizations such as International Commission on Non-Ionizing Radiation Protection (ICNIRP) provide safety guidelines and national authorities define laws and norms to limit the exposure of the electromagnetic fields caused by wireless networks [5]. Although no unambiguously answer is been given whether or not electromagnetic radiation from wireless networks can result in long-term health effects, it is still beneficial as a precautionary principle to minimize the exposure of human beings in future wireless access networks.

In conclusion, future wireless access networks should thus be developed with a minimal power consumption and a minimal exposure for human beings, without compromising the quality of service for the end user(s). Such networks are called green networks. **The goal of this dissertation is to design green wireless access networks with a minimal power consumption and/or a minimal exposure of**

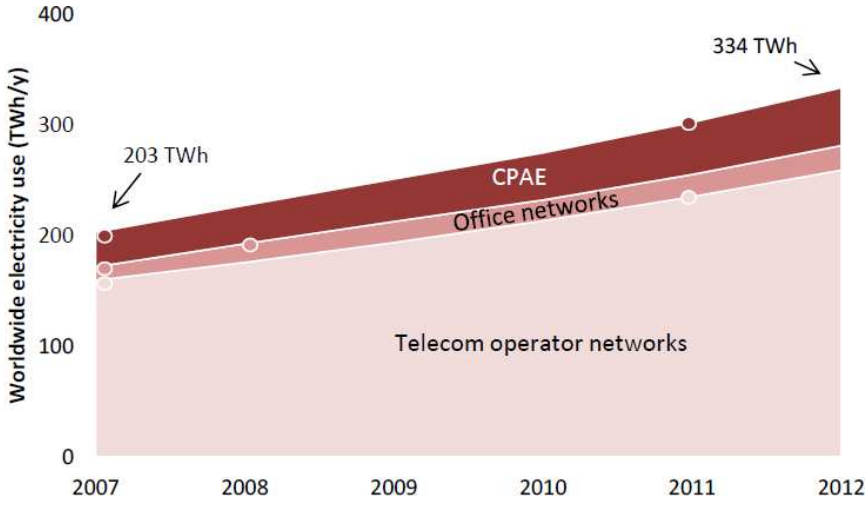

Figure 1.4: Overview of the power consumption of communication networks from 2007 to 2012 (CPAE = Customer Premises Access Equipment) [4].

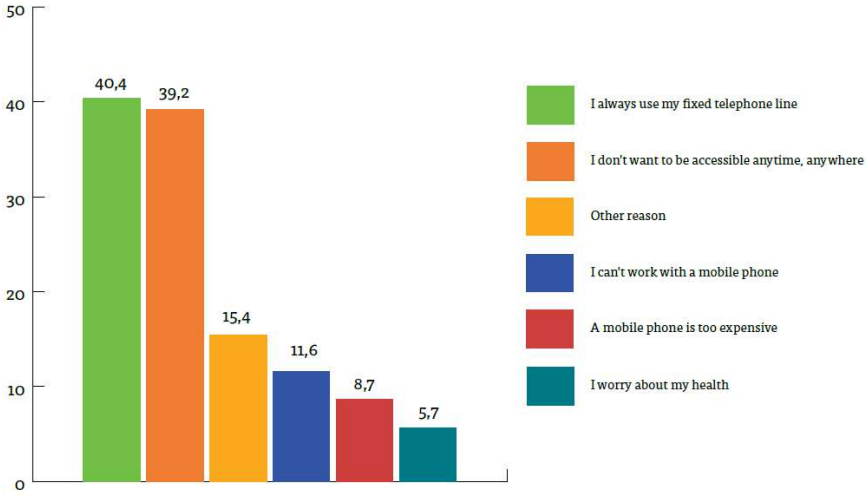

Figure 1.5: Reasons for not adopting a mobile phone [2].

human beings.

1.2 Wireless technologies

An important parameter when developing wireless access networks is of course the selected technology. When we look only to downlink peak data rates, we

already see a tremendous evolution: from 14.4 kbps to 100 Mbps in less than thirty years. In this dissertation, different wireless technologies are considered. It is of course not possible to consider them all, so we have focused on the most recent Wireless Metropolitan Access Network (WMAN) and Wireless Wide Area Network (WWAN) technologies which provide mobile data communication in a large geographical area, spanning a whole city or country. An overview of the considered technologies is given here.

1.2.1 IEEE 802.16

The wireless technology based on the IEEE 802.16 standard is probably better known as Worldwide Interoperability for Microwave Access (WiMAX). The characteristics of this technology and the product certification is specified by the WiMAX forum to ensure the interoperability between different manufacturers. Within this IEEE 802.16 standard, two important profiles can be distinguished: IEEE 802.16-2004 which is better known as fixed WiMAX [6], and IEEE 802.16e or mobile WiMAX [7].

Fixed WiMAX provides support for the so called fixed or nomadic access. This means that the sender and the receiver are located on a fixed position and are not moving during communication. Because of this, fixed WiMAX offers a good alternative for fixed wired networks. In Belgium, fixed WiMAX uses the 3.5 GHz band.

In the IEEE 802.16e interface the support for mobility is added. The users can now move while they are communicating. The most important difference between fixed and mobile WiMAX is the use of Scalable Orthogonal Frequency Division Multiple Access (SOFDMA). Due to this technique, it is possible to allow multiple users to the medium at the same time. One of the big advantages of SOFDMA over Orthogonal Frequency Division Multiple Access (OFDMA), which is used by fixed WiMAX, is the scalability. This means that mobile WiMAX can choose between different bandwidths according to the channel quality. Besides this, mobile WiMAX supports also higher bit rates and has an improved support for Multiple-Input Multiple-Output (MIMO) whereby multiple antennas are used to transmit and receive the signal. Furthermore, a power management system is added allowing longer battery operation time for mobile devices and there is also support for handovers between different base stations which is important for the user mobility. Mobile WiMAX uses the 2.5 GHz band in Belgium.

1.2.2 UMTS

Universal Mobile Telecommunication System (UMTS), also known as Third Generation (3G), is the successor of Global System for Mobile Communications (GSM) and General Packet Radio Service (GPRS) and is developed by the European

Telecommunications Standards Institute (ETSI) [8]. GSM is also known as Second Generation (2G) and is the first wireless technology that allowed digital mobile telephony [9]. GPRS is an extension on GSM and allowed some new services over GSM such as internet browsing, Wireless Access Protocol (WAP) allowing web services on mobile devices, and Multimedia Messaging Service (MMS) which is a more advanced Short Messaging Service (SMS) whereby the message could be accompanied by a picture or a short video.

UMTS in turn is specified as a solution that allows both mobile telephony as data traffic. It provides mobile operators enough capacity and broadband purposes to serve both voice and data users, especially in urban environments. UMTS typically uses the 900 MHz and 2.1 GHz band.

1.2.3 HSPA

High Speed Packet Access (HSPA) is the successor of the widely deployed UMTS and promises higher data rates, increased cell and user throughput, and a lower delay during transmission [10]. Just as UMTS, it operates in the 900 MHz and 2.1 GHz bands.

1.2.4 LTE

The newest commercial technology in this overview is Long Term Evolution (LTE), commercially often denoted as Fourth Generation (4G), although it is actually 3.9G. LTE-Advanced, the successor of LTE, is 4G. The LTE technology is standardized by Third Generation Partnership Project (3GPP) and different releases were defined during the last few years. Release 8 and 9 is better known as LTE, while Release 10 is known as LTE-Advanced [11–13]. This last release is discussed in details in the next section.

Just like mobile WiMAX, LTE uses SOFDMA enabling the adaptation of the modulation scheme, coding rate, and bandwidth according to the channel quality. LTE features five different bandwidths resulting in a peak downlink data rate up to 300 Mbps. LTE currently uses the 1.8 GHz and 2.6 GHz frequency bands, but it can also use the 700 MHz and 800 MHz bands.

1.2.5 LTE-Advanced

As mentioned above, Release 10 is better known as LTE-Advanced [13]. Note that LTE and LTE-Advanced are actually based on the same technology and thus is LTE-Advanced equipment backward compatible with LTE. This means that LTE-Advanced devices can communicate with LTE devices but not the other way around, as LTE devices can not use functionalities defined in LTE-Advanced. The four main features added to LTE-Advanced are carrier aggregation, extended sup-

port for heterogeneous networks and MIMO, and relaying [14].

Carrier aggregation allows to extend the bandwidth used for transmission by sending different so called component carriers to a device. These component carriers consist of control data and user data. Up to five component carriers (not necessarily of the same bandwidth) can be sent to a device. By using carrier aggregation, higher bit rates can be obtained.

In a heterogeneous network, different base station types will cooperate within the same network. LTE based heterogeneous networks typically consists of two layers with macrocell (or eNodeB) and femtocell (or home-eNodeB) base stations. Although this was already supported in LTE, LTE-Advanced introduces a better interference management between the different cells in the network.

Also MIMO was already supported by LTE, but LTE-Advanced extends this support up to 8 transmitting and 8 receiving antennas (i.e., 8x8 MIMO).

Finally, LTE-Advanced introduces relaying in the network. This means that a terminal communicates with the network through a relay node instead of communicating directly with the base station. This relay node is in fact a small base station on its own, wirelessly connected to the base station. The advantage of such a node is that it can ameliorate the coverage on locations that can be difficult to reach by wireless signals such as for example indoors. The terminal notices no difference. It looks like it is communicating directly with the base station.

1.3 Outline

The general topic of this dissertation is designing green wireless access networks optimized towards power consumption and/or exposure of human beings. This section sums up the different chapters in this doctoral thesis.

As mentioned above, the base stations are the largest power consumers within wireless access networks. To develop energy-efficient networks, it is thus important to have a realistic quantification of its power consumption. In Chapter 2, the architecture of three different base station types is established. Based on this architecture, a power consumption model for each base station type is defined. The performance of the above described technologies and the different base station types is compared. To this end, appropriate energy efficiency metrics are defined. These metrics allow us to determine if a solution is more energy-efficient than another by not only considering power consumption but also other performance parameters (such as coverage, number of served users, offered capacity, etc.). Such a metric is essential as otherwise it is very difficult to define the best solution: one technology could have a higher power consumption but also a higher coverage, while another technology could have a lower coverage for also a lower power consumption.

Chapter 3 proposes a deployment tool for energy-efficient wireless access networks. A coverage-based algorithm is proposed, which uses a genetic search al-

gorithm. The purpose of this algorithm is to cover a specific (geometrical) area as energy-efficiently as possible. The base station power consumption model of Chapter 2 is used in this algorithm to evaluate the network's power consumption. Furthermore, a comparison is made between different technologies when considering a greenfield deployment and when optimizing an existing network towards power consumption.

In Chapter 4, measurements are performed on two different base station types. These measurements are used to evaluate the proposed power consumption model of Chapter 2. Furthermore, an extension of the model is proposed, taking into account the dependency of the base station on the variation in traffic. The influence of introducing sleep modes and cell zooming or cell breathing is also investigated.

Chapter 5 investigates the influence of three different features added to LTE-Advanced (carrier aggregation, extended support for MIMO, and heterogeneous networks) on the power consumption and energy efficiency. A comparison with LTE is also made. This study is done on base station level and on network level. For the network level, a capacity-based deployment tool is proposed. The purpose of this tool is to respond to the instantaneous bit rate request of the users in a geometrical area as energy-efficiently as possible rather than providing coverage to a certain area which is the purpose of the coverage-based tool. The power consumption model of Chapter 2 is again used to evaluate the power consumption of the network.

In Chapter 6, three extensions of the capacity-based deployment of Chapter 5 are proposed. The first extension develops networks optimized towards power consumption but satisfying a certain exposure limit, while the second extension optimizes networks towards global exposure for human beings. The last extension develops future green wireless access networks: the network is optimized towards both power consumption and global exposure. The three algorithms along with the capacity-based algorithm of Chapter 5 are applied on a realistic suburban case in Belgium and it is investigated how optimizing towards a certain parameter influences the performance of the network.

Finally, Chapter 7 summarizes my scientific contributions and briefly discusses interesting future work.

1.4 Publications

The following list provides an overview of the publications published in scientific journals and presented at international conferences during my PhD research.

1.4.1 Journal

(publications in journals listed in the ISI Web of Science)

1.4.1.1 As first author

[MD1] **M. Deruyck**, E. Tanghe, W. Joseph, and L. Martens, "Modelling and Optimization of Power Consumption in Wireless Access Networks," *Elsevier Computer Communications*, Vol. 34, No. 17, pp. 2036-2046, November 2011.

[MD2] **M. Deruyck**, E. Tanghe, W. Joseph, W. Vereecken, M. Pickavet, L. Martens, and B. Dhoedt, "Model for Power Consumption of Wireless Access Networks," *IET Science, Measurement & Technology*, Vol. 5, No. 4, pp. 155-161, July 2011.

[MD3] **M. Deruyck**, E. Tanghe, W. Joseph, and L. Martens, "Characterization and Optimisation of the Power Consumption in Wireless Access Networks by Taking Daily Traffic Variations into Account," *EURASIP Journal on Wireless Communications and Networking*, 2012, Article ID 248, 12 pages, doi: 10.1186/1687-1499-2012-248.

[MD4] **M. Deruyck**, W. Joseph, and L. Martens, "Power Consumption Model for Macrocell and Microcell Base Stations," *European Transactions on Emerging Telecommunications*, Vol. 25, No. 3, pp. 320-333, March 2014, doi: 10.1002/ett.2565.

[MD5] **M. Deruyck**, E. Vanhauwaert, D. Pareit, B. Lannoo, W. Joseph, I. Moerman, and L. Martens, "WiMAX Based Monitoring Network for a Utility Company: a case study," *European Transactions on Emerging Telecommunications*, Vol. 25, No. 3, pp. 343-353, March 2014, doi: 10.1002/ett.2573.

[MD6] **M. Deruyck**, W. Vereecken, W. Joseph, B. Lannoo, M. Pickavet, and L. Martens, "Reducing the Power Consumption in Wireless Access Networks: Overview and Recommendations," *Progress In Electromagnetics Research - PIER*, Vol. 132, pp. 255-274, 2012.

[MD7] **M. Deruyck**, W. Joseph, B. Lannoo, D. Colle, and L. Martens, "Designing Energy-Efficient Wireless Access Networks: LTE and LTE-Advanced," *IEEE Internet Computing*, Vol. 17, No. 5, pp. 39-45, September-October 2013.

[MD8] **M. Deruyck**, W. Joseph, E. Tanghe, and L. Martens, "Reducing the Power Consumption in LTE-Advanced Wireless Access Networks by a Capacity Based Deployment Tool," *Radio Science*, Vol. 49, No. 9, pp. 777-787, 2014.

1.4.1.2 As co-author

[MD9] W. Vereecken, W. Van Heddeghem, **M. Deruyck**, B. Puype, B. Lannoo, W. Joseph, D. Colle, L. Martens, and M. Pickavet, "Power Consumption in Telecommunication Networks: Overview and Reduction Strategies," *IEEE Communications Magazine*, Vol. 49, No. 6, pp. 62-69, June 2011.

[MD10] D. Pareit, **M. Deruyck**, E. Tanghe, W. Joseph, I. Moerman, L. Martens, and P. Demeester, "Detailed Modeling of MAC Throughput and Ranges for Mobile WiMAX," *IEEE Communications Letters*, Vol. 15, No. 8, pp. 839-841, August 2011.

[MD11] W. Vereecken, **M. Deruyck**, D. Colle, W. Joseph, M. Pickavet, L. Martens, and P. Demeester, "Evaluation of the Potential for Energy Saving in Macrocell and Femtocell Networks using a Heuristic Introducing Sleep Modes in Base Stations," *EURASIP Journal on Wireless Communications and Networking*, 2012, Article ID 170, 14 pages, doi: 10.1186/1687-1499-2012-170.

[MD12] S. Aleksic, **M. Deruyck**, W. Vereecken, W. Joseph, M. Pickavet, and L. Martens, "Energy Efficiency of Femtocell Deployment in Combined Wireless/Optical Access Networks," *Elsevier Computer Networks*, Vol. 57, No. 5, pp. 1217-1233, April 2013.

1.4.2 Conference

1.4.2.1 As first author

[MD13] **M. Deruyck**, E. Tanghe, W. Joseph, D. Pareit, I. Moerman, and L. Martens, "Performance Analysis of WiMAX for Mobile Applications," in *IEEE Wireless Communications and Networking Conference*, Sydney, AU, April 2010.

[MD14] **M. Deruyck**, W. Vereecken, E. Tanghe, W. Joseph, M. Pickavet, L. Martens, and P. Demeester, "Power Consumption in Wireless Access Networks," in *European Wireless Conference*, Lucca, IT, April 2010, pp. 924-931.

[MD15] **M. Deruyck**, W. Vereecken, E. Tanghe, W. Joseph, M. Pickavet, L. Martens, and P. Demeester, "Comparison of Power Consumption of Mobile WiMAX, HSPA and LTE Access Networks," in *9th Conference on Telecommunications Internet and Media Techno Economics*, Ghent, BE, June 2010.

[MD16] **M. Deruyck**, E. Tanghe, W. Joseph, W. Vereecken, M. Pickavet, B. Dhoedt, and L. Martens, "Towards a Deployment Tool for Wireless Access Networks with Minimal Power Consumption," in *IEEE 21st International Symposium on Personal, Indoor and Mobile Radio Communications*, Istanbul, TR, September 2010, pp. 295-300.

[MD17] **M. Deruyck**, E. Tanghe, W. Joseph, and L. Martens, "Modelling the Energy Efficiency of Microcell Base Stations," in *First International Conference on Smart Grids, Green Communications and IT Energy-aware Technologies*, Venice, IT, May 2011.

[MD18] **M. Deruyck**, D. De Vulder, W. Joseph, and L. Martens, "Modelling the Power Consumption in Femtocell Networks," in *IEEE Wireless Communications and Networking Conference*, Paris, FR, April 2012, pp. 30-35.

[MD19] **M. Deruyck**, W. Joseph, E. Tanghe, and L. Martens, "Designing Advanced Energy-Efficient Wireless Access Networks by a Capacity Based Deployment Tool," in *Future Network & Mobile Summit - Workshop on Management Frameworks for Future Mobile Communication Networks - Session 11e: COST ICT: Networks and More (Presentation)*, Lissabon, PT, July 2013.

[MD20] **M. Deruyck**, W. Joseph, E. Tanghe, D. Plets, and L. Martens, "Designing Green Wireless Access Networks: Optimizing towards Power Consumption versus Exposure of Human Beings," in *11th International Symposium on Wireless Communication Systems*, Barcelona, SP, August 2014.

1.4.2.2 As co-author

[MD21] W. Vereecken, I. Haratcherev, **M. Deruyck**, W. Joseph, M. Pickavet, L. Martens, and P. Demeester, "The Effect of Variable Wake Up Time on the Utilization of Sleep Modes in Femtocell Mobile Access Networks," in *9th Annual Conference on Wireless On-demand Network Systems and Services*, Courmayeur, IT, January 2012, pp. 63-66.

[MD22] S. Aleksic, **M. Deruyck**, and W. Joseph, "Energy Efficiency of Optically Backhauled LTE: a case study," in *International Conference on Electromagnetics in Advanced Applications*, Torino, IT, 2013, pp. 390-393.

[MD23] D. Plets, W. Joseph, K. Vanhecke, G. Vermeeren, S. Aerts, **M. Deruyck**, and L. Martens, "Whole-body and Localized SAR and Dose Prediction Tool for Indoor Wireless Network Deployments," in *11th International Symposium on Wireless Communication Systems*, Barcelona, SP, August 2014.

1.4.3 Other

1.4.3.1 As first author

[MD23] **M. Deruyck**, W. Joseph, and L. Martens, "Characterization of Green Wireless Access Networks," in *11de UGent - FirW Doctoraatssymposium*, Ghent, BE, December 2010.

[MD24] **M. Deruyck**, E. Tanghe, W. Joseph and L. Martens, "Energy Efficiency of 802.11n versus LTE Advanced femtocell networks based on a 3D deployment tool," in *COST IC1004 4th Management Committe Meeting*, Lyon, FR, May 2012, ref.: TD(12)04015.

[MD25] **M. Deruyck**, W. Joseph, B. Lannoo, D. Colle, and L. Martens, "Designing Energy-Efficient Wireless Access Networks: LTE and LTE-Advanced," in *COST IC1004 6th Management Committee Meeting*, Malaga, ES, February 2013, ref.: TD(13)06012.

[MD26] **M. Deruyck**, W. Joseph, E. Tanghe, and L. Martens, "Taking User Capacity Demands into Account to Reduce Power Consumption in Wireless Access Networks," in *GREENETS joint COST IC1004 workshop on SON Algorithms for Energy Efficiency*, Ilmenau, DE, May 2013.

[MD27] **M. Deruyck**, W. Joseph, E. Tanghe, D. Plets, and L. Martens, "Designing Green Wireless Access Networks: Optimizing towards Power Consumption versus Exposure of Human Being," in *COST IC1004 8th Management Committee Meeting*, Ghent, BE, September 2013, ref.: TD(13)08010.

References

[1] Cisco. *Cisco Visual Networking Index: Global Mobile Data Traffic Forecast Update 2012-2017, White paper*. Technical report, 2012.

[2] S. De Moor, D. Schuurman, and L. De Marez. *Digimeter report 5: Adoption and usage of Media & ICT in Flanders - Wave 5*. Technical report, August – September 2012.

[3] M. Pickavet, W. Vereecken, S. Demeyer, P. Audenaert, B. Vermeulen, C. Develder, D. Colle, B. Dhoedt, and P. Demeester. *Worldwide Energy Needs for ICT: the Rise of Power-Aware Networking*. In 2nd International Symposium on Advanced Networks and Telecommunication Systems, pages 1–3, Bombay, India, 2008.

[4] W. Van Heddeghem, S. Lambert, B. Lannoo, D. Colle., M. Pickavet, and P. Demeester. *Trends in worldwide ICT electricity consumption from 2007 to 2012*. Computer Communications, 50:64–76, September 2014.

[5] ICNIRP. *Guidelines for limiting exposure to time-varying electric, magnetic, and electromagnetic fields (up to 300 GHz)*. Health Physics, 74(4):494–522, April 1998.

[6] IEEE Computer Society, the IEEE Microwave Theory, and Techniques Society. *Air interface for Fixed Broadband Wireless Access Systems*, October 2004.

[7] IEEE Computer Society, the IEEE Microwave Theory, and Techniques Society. *Part 16: Air Interface for Fixed and Mobile Broadband Wireless Access Systems: Amendment 2: Physical and Medium Access Control Layers for Combined Fixed and Mobile Operation in Licensed bands and Corrigendum 1*, February 2006.

[8] 3GPP. *3rd Generation Partnership Project: Technical Specification Group Radio Access Network, UE Radio Transmission and Reception (TDD) Release 1999, TR 25.102 v3.13.0*, October 2006.

[9] ETSI. *Digital cellular telecommunications system (Phase 2+); GSM Cordless Telephony System (CTS), Phase 1; CTS radio interface layer 3 specification (GSM 04.56 version 7.1.1 Release 1998), ETSI EN 302 406 v7.1.1*, August 2000.

[10] 3GPP. *3rd Generation Partnership Project: Technical Specification Group Radio Access Network: Physical Layer Aspects of UTRA High Speed Downlink Packet Access (Release 4), TR 25.848 v4.0.0.*, March 2001.

[11] 3GPP. *3rd Generation Partnership Project: Technical Specification Group Radio Access Network: Evolved Universal Terrestrial Radio Access (E-UTRA): User equipment (UE) Radio Transmission and Reception, TS 36.101 v8.17.0 Release 8*, 2008.

[12] 3GPP. *3rd Generation Partnership Project: Technical Specification Group Radio Access Network: Evolved Universal Terrestrial Radio Access (E-UTRA): User equipment (UE) Radio Transmission and Reception, TS 36 101 v9.1.0*, 2009.

[13] 3GPP. *3rd Generation Partnership Project: Technical Specification Group Radio Access Network: Evolved Universal Terrestrial Radio Access (E-UTRA): User equipment (UE) Radio Transmission and Reception, TS 36.101 v10.1.0 Release 10*, 2011.

[14] E. Dahlman, S. Parkvall, and J. Sköld. *4G LTE/LTE-Advanced for Mobile Broadband*. Academic Press, 2011.

2

Power consumption model for a base station

In general, a wireless cellular access network can consist of three different base station types: macrocell, microcell, and small cell (femtocell or picocell) base stations. The largest coverage area is obtained by a macrocell base station. This base station type can often be found along highways. The microcell base station has a smaller coverage area and is typically used in densely populated areas such as historical city centres, shopping malls, metro stations, etc. A small cell base station has the smallest coverage area and is mostly placed indoor in offices and large buildings to provide indoor coverage [1]. To determine the power consumption in a wireless access network, it is important to know how much power each base station type consumes. Therefore, the power consumption for each base station type is modeled and an appropriate energy efficiency metric is proposed to make a realistic comparison between different configurations of the base station and different wireless technologies. The models are developed based on private interviews with an operator and power measurements of base stations and are thus representative for currently deployed wireless access networks. This power consumption model will be used as a basis for the next chapters.

2.1 Power consumption model for a macrocell base station

Fig. 2.1 shows the six power-consuming components of the macrocell base station:

- *Rectifier*: converts Alternating Current (AC) to Direct Current (DC) and is also known as the AC-DC converter.
- *Digital signal processing*: converts the signal to a sequence of bits or symbols and processes these signals.
- *Transceiver*: is responsible for transmitting and receiving the signals.
- *Power amplifier*: converts the DC input power into a Radio-Frequent (RF) signal.
- *Air conditioning*: regulates the temperature in the base station cabin.
- *Backhaul*: is responsible for the communication with the backhaul network. This is often a microwave link but is sometimes replaced by a fiber link.

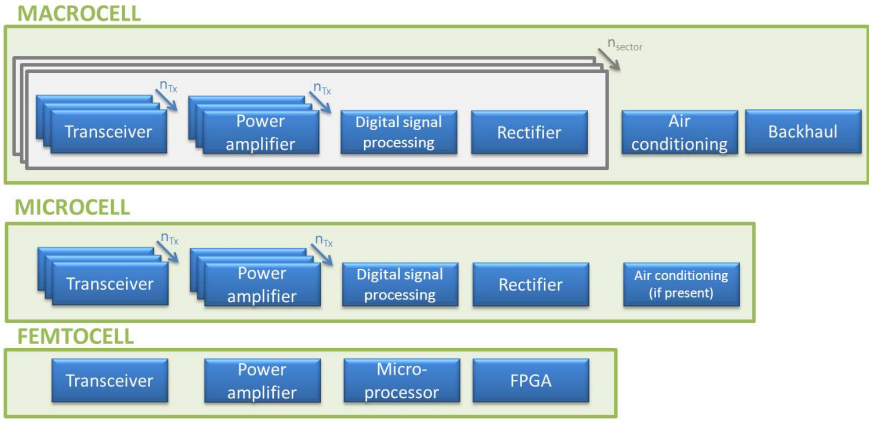

Figure 2.1: Architecture of the macrocell, microcell, and femtocell base station.

If we determine the sum of the power consumption of all those components, we can determine the base station's power consumption. However, as shown in Fig. 2.1, some of the components are used multiple times depending on the configuration of the base station. The power consumption of these components should thus be multiplied by their number of occurrences. Which components and how many of them are needed depend on two factors: the number of sectors n_{sector}

and the number of transmitting antennas n_{Tx}.
Firstly, the influence of n_{sector} is discussed. The area covered by a base station is called a cell which is further divided into a number of sectors n_{sector}. Each sector is covered by one antenna and needs therefore one rectifier, one digital signal processor, one transceiver, and one power amplifier. The power consumption of these components must thus be multiplied by n_{sector}.
Secondly, we discuss the influence of n_{Tx}. As mentioned above each sector is covered by one antenna. However, in the future, multiple transmitting antennas will be used per sector. This technique is called MIMO. For each transmitting antenna, one transceiver and one power amplifier are needed. This means that the power consumption of these two components must not only be multiplied by n_{sector} but also by n_{Tx}.

Each of the base station's components has a typical power consumption value which is given in Table 2.1. The power consumption of the backhaul connection and the rectifier(s) is assumed to be constant throughout time. The power consumption of the air conditioning is not influenced by the time but rather by the temperature inside and outside the base station cabin. It is assumed that the heat generation rate inside the cabin and the temperature outside the cabin is constant, which results in a constant power consumption for the air conditioning.

The power consumption of the digital signal processing, the transceiver, and the power amplifier can fluctuate during time due to variations in load on the base station. The load represents the number of active users and the requirements of the services they use in the base station cell. The higher the load, the higher the base station's power consumption. To take this into account, we define the *load factor*. The power consumption of these three components must be multiplied by this load factor to determine the base station's power consumption at a certain time of the day. Furthermore, the power consumption of the power amplifier is also dependent on the input power of the antenna P_{Tx}. The higher P_{Tx}, the higher the power consumption of the power amplifier and thus also of the base station.

Based on the discussion above, the following formula is derived to determine the power consumption $P_{el/macro}$ of the macrocell base station (in Watt):

$$\begin{aligned} P_{el/macro} &= n_{sector} \cdot (P_{el/rect} + F \cdot (n_{Tx} \cdot (P_{el/amp} + P_{el/trans}) \\ &+ P_{el/proc}) + P_{el/back} + P_{el/airco} \end{aligned} \tag{2.1}$$

with n_{sector} the number of sectors, F the load factor, n_{Tx} the number of transmitting antennas, and $P_{el/rect}$, $P_{el/amp}$, $P_{el/trans}$, $P_{el/proc}$, $P_{el/back}$, and $P_{el/airco}$ the power consumption (in Watt) of the rectifier, the power amplifier, the transceiver, the digital signal processor, the backhaul connection, and the air conditioning, respectively.

A power consumption of 1279.1 W per macrocell base station is obtained assuming P_{Tx} = 35 dBm (e.g., for WiMAX) and 1672.6 W assuming P_{Tx} = 43 dBm

(e.g., for LTE). Here, we assume a load factor of 1.0, corresponding with the maximal power consumption of the base station. The worst-case scenario will thus be investigated. In [2, 3], P_{el} of 1500 W is found for the traditional 3G (UMTS) base station, which is similar to the P_{el} obtained with our model. In [4], P_{el} for a one-sector base station with one antenna is 783 W. With our model, similarly, P_{el} = 761 W is obtained. Furthermore, a good agreement between our P_{el} and confidential data from an operator about the power consumption of 3G base stations is obtained.

Component	**Macrocell BS**	**Microcell BS**	**Femtocell BS**
Number of sectors	3	1	1
Digital signal processing	100 W	100 W	7.9 W (Microprocessor + FPGA)
Power amplifier	24.7 W (P_{Tx} = 35 dBm) 156.3 W (P_{Tx} = 43 dBm)	16.6 W	2.4 W
Transceiver	100 W	100 W	1.8 W
Rectifier	100 W	100 W	—
Air conditioning	225 W	60 W	—
Backhaul	80 W	—	—

Table 2.1: Power consumption of the components for the different base station types [5–11].

2.2 Power consumption model for a microcell base station

Fig. 2.1 shows that the same components are used for a microcell base station as for a macrocell base station except for the backhauling. The backhaul connection of a microcell base station is typically established through the overlaying macrocell network. Furthermore, a microcell base station supports only one sector covered by one antenna. The power consumption of the different components are shown in Table 2.1 and are similar to those of the macrocell base station except for the power amplifier and the air conditioning. As less devices are present in the base station's cabin, a less powerful air conditioning with a lower power consumption can be used. Note that the air conditioning is not always necessary in a microcell base station but, as mentioned above, the worst-case scenario is investigated so the air conditioning is here included. The power amplifier consumes also less than the one of the macrocell base station because the input power P_{Tx} of the antenna is typically around 33 dBm. Furthermore, a load factor of 1.0 is assumed and the backhaul connection is through the overlaying macrocell network.

Based on the discussion above, the following formula is derived for the power consumption $P_{el/micro}$ of a microcell base station (in Watt):

$$P_{el/micro} = P_{el/rect} + P_{el/airco} + F \cdot (P_{el/amp} + P_{el/trans} + P_{el/proc}) \quad (2.2)$$

with F the load factor, and $P_{el/rect}$, $P_{el/airco}$, $P_{el/amp}$, $P_{el/trans}$, and $P_{el/proc}$ the power consumption of the rectifier, the air conditioning, the power amplifier, the transceiver, and the digital signal porcessing (in Watt), respectively.

This results in a typical power consumption of 376.6 W for a microcell base station.

2.3 Power consumption model for a femtocell base station

The size of a femtocell base station is much smaller than that of a macrocell and microcell base station and is comparable to that of a Wireless Fidelity (WiFi) access point. Therefore, the power-consuming components are different from those of a macrocell and microcell base station as shown in Fig. 2.1. The femtocell base station consists of a microprocessor, a Field-Programmable Gate Array (FPGA), a transceiver, and a power amplifier [5]. The microprocessor is responsible for implementing and managing the standardized radio protocol stack and the baseband processing and also takes care of the communication with the backhaul network [5]. The FPGA is responsible for a number of features such as data encryption, hardware authentication, etc. The power consumption of these components is also listed in Table 2.1. It is assumed that the connection with the backhaul network is done through Digital Subscriber Line (DSL) or cable network which is beyond the scope of this study.

The following formula is derived to determine the power consumption $P_{el/femto}$ of the femtocell base station (in Watt) [5]:

$$P_{el/femto} = P_{el/mp} + P_{el/FPGA} + P_{el/trans} + P_{el/amp} \tag{2.3}$$

with $P_{el/mp}$, $P_{el/FPGA}$, $P_{el/trans}$, and $P_{el/amp}$ the power consumption of the microprocessor, FPGA, transceiver, and power amplifier (in Watt), respectively.

Taking into account the values of Table 2.1 results in a femtocell base station power consumption of 12 W.

2.4 Energy efficiency metric for a base station and/or network

If multiple technologies are compared, it is very difficult to determine which one is the most energy-efficient: one technology could have a higher power consumption but also higher coverage ranges, while another one could have a smaller range but also a lower power consumption. Therefore, we define different energy efficiency metrics which takes the performance of the base station or network into account.

A first metric defines the power consumed to cover 1 m^2 (in W/m^2) [12, 13]:

$$PC_{area} = \frac{P_{el}}{A} \tag{2.4}$$

P_{el} presents the power consumption of the base station (in Watt) and $A = \pi \cdot R^2$ with R the range of the considered base station (in metres). When considering a network, $P_{el} = \sum_{i=1}^{n} P_i$ with P_i the power consumption of base station i (in Watt) and n the number of base stations present in the network and A is the area covered by the network (in m^2). The lower PC_{area}, the more energy efficient the base station or network is. As an alternative, one can also use the inverse function of eq. (2.4), which is known as the *coverage effectiveness* (in m^2/W). This parameter tells us how much area is covered when 1 W power is consumed. The higher the coverage effectiveness, the more energy-efficient the base station is.
It is also possible to express the energy efficiency in terms of covered users when consuming 1 W power (in 1/W) [14, 15]:

$$PC_{users} = \frac{U}{P_{el}} \tag{2.5}$$

with U the number of covered users by the base station or the network. The higher PC_{users}, the more energy efficient the network or base station is.
The offered bit rate is also typically taken into account as a performance parameter. The energy efficiency metric expresses then the physical bit rate available when 1 W power is consumed (in Mbps/W) [12, 16]:

$$PC_{bitrate} = \frac{B}{P_{el}} \tag{2.6}$$

with B the physical bit rate offered by the individual base station (in Mbps) or $B = \sum_{i=1}^{n} B_i$ with B_i the physical bit rate offered by base station i (in Mbps) and n the number of base stations present in the network when considering a network. The higher $PC_{bitrate}$, the more energy-efficient the base station or network is.
One can also combine the different performance parameters in one energy efficiency metric (in ($m^2 \cdot$ Mbps)/W):

$$PC_{product_1} = \frac{A \cdot B \cdot U}{P_{el}} \tag{2.7}$$

with the parameters A, B, U, and P_{el} as described above. The higher PC, the more energy efficient the network or base station is.
When combining the performance parameters, one can also normalize each performance parameter:

$$PC_{norm} = \frac{\frac{A}{A_{max}} \cdot \frac{B}{B_{max}} \cdot \frac{U}{U_{max}}}{\frac{P_{el}}{P_{max}}} \tag{2.8}$$

with the parameters A, B, U, and P_{el} as defined above. A_{max} equals then the complete area that needs to be covered, B_{max} is the sum of all the bit rates when each base station offers the highest possible bit rate, U_{max} is the total number of users active in the considered area, and P_{max} is the network power consumption whereby each base station is operating at its highest power consumption mode. The higher PC, the more energy-efficient the base station or network is.

The definition to combine all performance parameters used above (Eq. (2.7)) is of course just one way to combine them. Eq. (2.8) for example normalizes each parameter. Furthermore, it also possible to take the sum of the normalized parameters instead of multiplying them:

$$PC_{sum} = \frac{\frac{A}{A_{max}} + \frac{B}{B_{max}} + \frac{U}{U_{max}}}{\frac{P_{el}}{P_{max}}} \tag{2.9}$$

or by multiplying the nominators and denominators of PC_{area}, $PC_{bitrate}$, and PC_{users}:

$$PC_{product_2} = \frac{A \cdot B \cdot U}{P_{el}^3} \tag{2.10}$$

Note that not all of these energy efficiency metrics will be used simultaneously, but it will depend on the purpose of the comparison (e.g., comparing different technologies, different network topologies, different base station types) which energy efficiency metric will be used.

2.5 Comparison between different wireless technologies and base station types

In this section, the energy efficiency of different wireless technologies and base station types is compared based on the above described models and metric (PC_{area}).

2.5.1 Configuration

For the macrocell base station, five different technologies are investigated: fixed and mobile WiMAX, UMTS, HSPA, and LTE. For the microcell and femtocell base station, only three technologies are compared: mobile WiMAX, HSPA, and LTE. Only the most recent technologies were here considered.

2.5.1.1 Macrocell base station

As discussed in Section 2.4, the power consumption P_{el} of the base station is related to the wireless range R covered by this base station to determine the energy efficiency. To this end, a link budget has to be constructed. A link budget takes all

of the gains and the losses of the transmitter through the medium to the receiver into account. Firstly, we calculate the maximum allowable path loss PL_{max} (in dB) to which a transmitted signal can be subjected while still being detectable at the receiver. The path loss is the ratio of the radiated power to the received power of the signal; it includes all of the possible elements of loss associated with interactions between the propagating wave and any objects between the transmit and receive antennas [17]. To determine PL_{max}, the parameters of Table 2.2 are taken into account. Table 2.2 lists all the gains and losses that occur. These parameters are retrieved from the specifications and/or typical values proposed by the operators themselves to make a fair comparison between the considered technologies.

Some of these parameters need a short explanation, for example, the fading margin. The fading margin accounts for temporal fading (e.g., due to varying weather conditions) and is determined based on the projected yearly availability of the system. The noise figure is a measure of degradation of how much the Signal-to-Noise Ratio (SNR) degrades due to the different components in the equipment. The receiver SNR determines the required SNR at the receiver for a certain Bit Error Rate (BER) and the physical bit rate which is determined by the transmission mode. In mobile telecommunication systems, the Mobile Station (MS) typically supports different transmission modes. These transmission modes are determined by a coding rate and a modulation scheme. For wireless communication, the binary bit stream has first to be translated into an analogue signal, which can be performed by using a modulation scheme such as Quadrature Phase Shifting Key (QPSK) and 16-Quadrature Amplitude Modulation (QAM) or 64-QAM. Furthermore, a coding rate is used for Forward Error Correction (FEC), which is responsible for the correction of errors occurred. The coding rate indicates how many redundant bits will be added per number of information bits. The modulation scheme and the coding rate have an important role in the determination of the physical bit rate. Each transmission mode is characterized by a receiver SNR value, which represents the required SNR at the receiver for a certain BER (here, a BER of 10^{-6} is assumed). It is thus a determining factor for the required signal power, indicating the signal power level for acceptable communication quality. Table 2.2 gives an overview of the different transmission modes supported by each technology and the corresponding receiver SNR. The higher the modulation scheme and coding rate, the higher the required receiver SNR, the higher the bit rate, and the lower the range.

Since UMTS and HSPA use Wideband Code Division Multiple Access (W-CDMA) as multiple access technique, an extra gain needs to be taken into account. This gain is called the processing gain PG (in dB) and is defined as [19]:

$$PG = -10 \cdot log_{10}(SP) = -10 \cdot log_{10}(\frac{CR}{SR}) \tag{2.11}$$

Parameter	Mobile WiMAX	Fixed WiMAX	UMTS	HSPA	LTE	Unit
Frequency	2.5	3.5	2.1	2.1	2.6	GHz
Input power BS p_{Tx}	35	35	43	43	43	dBm
Effective input power BS p_{Tx}^{TCH}	35	35	31.5	24.7	43	dBm
Antenna gain BS	16	17	17.4	17.4	18	dBi
Antenna gain MS	2	8	0	0	0	dBi
Number of MIMO Tx antennas	1,2,3,4	1	1	1,2,3,4	1,2,3,4	—
Number of MIMO Rx antennas	1,2,3,4	1	1	1,2,3,4	1,2,3,4	—
Cyclic combining gain BS	3	3	3	3	3	dB
Soft handover gain	0	0	1.5	1.5	0	dB
Feeder loss BS	0.5	0.5	2	0	2	dB
Feeder loss MS	0	0	0	0	0	dB
Fade margin	10	10	10	10	10	dB
Yearly availability	99.995	99.995	99.995	99.995	99.995	%
Cell interference margin	2	0	0	2	2	dB
User interference margin	0	0	6	9	0	dB
Bandwidth	5	3.5	5	5	5	MHz
Receiver SNR	[6, 8.5, 11.5, 15, 19, 21][(a)]	[6.4, 9.4, 11.2, 16.4, 18.2, 22.7, 24.4][(b)]	[7, 5.5, 7][(c)]	[-3.1, 0.1, 3.4, 6.0, 7.1, 9.6, 15.6][(d)]	[-1.5, 3, 10.5, 14, 19, 23, 29.4][(e)]	dB
Used subcarriers	360	201	1	1	301	—
Total subcarriers	512	256	1	1	512	—
Noise figure MS	7	4.6	8	9	8	dB
Implementation loss MS	2	0	0	0	0	dB
Processing gain	—	—	[25.0 17.8 10][(c)]	12	—	dB
Control overhead	—	—	0.25	0.25	—	—
Target load	—	—	0.75	0.875	—	—
Max. number of users	—	—	[64 16 4][(c)]	75	—	—
Duplexing	FDD	FDD	FDD	FDD	FDD	—
Building penetration loss [18]	8.1	8.1	8.1	8.1	8.1	dB
Height BS antenna	30	30	30	30	30	m
Height MS antenna	1.5	1.5	1.5	1.5	1.5	m
Coverage requirement	90	90	90	90	90	%
Shadowing margin	13.2	13.2	13.2	13.2	13.2	dB

(a) [1/2 QPSK, 3/4 QPSK, 1/2 16-QAM, 3/4 16-QAM, 2/3 64-QAM, 3/4 64-QAM]

(b) [1/2 BPSK, 1/2 QPSK, 3/4 QPSK, 1/2 16-QAM, 3/4 16-QAM, 1/2 64-QAM, 2/3 64-QAM, 3/4 64-QAM]

(c) [AMR 12.2 Voice, CS64 data, PS64 stream, PS64 data, PS384 data]

(d) [1/4 QPSK, 1/2 QPSK, 3/4 QPSK, 3/4 8-QAM, 1/2 16-QAM, 3/4 16-QAM, 3/4 64-QAM]

(e) [1/3 QPSK, 1/2 QPSK, 2/3 QPSK, 1/2 16-QAM, 2/3 16-QAM, 4/5 16-QAM, 1/2 64-QAM, 2/3 64-QAM]

Table 2.2: Link budget table of the macrocell base station for the technologies considered

with SP being the spreading factor, which is the ratio of the chip rate CR (in Mcps) to the symbol rate SR (in Mbps). The processing gain is thus the ratio of the spreaded (RF) bandwidth to the unspreaded (baseband) bandwidth. Also the input power of the antenna for UMTS and HSPA needs to be scaled according to the control overhead, the target load and the maximum number of users [20]:

$$P_{Tx}^{TCH} = \frac{(1 - CL) \cdot P_{Tx}}{TL \cdot N_{users}} \tag{2.12}$$

with P_{Tx}^{TCH} being the power reserved by the base station for the traffic channels. CL is the control overhead, TL the target load, and N_{users} the maximum number of users. P_{Tx} is used to determine the power consumption of the base station, while P_{Tx}^{TCH} is used to determine the range of the UMTS and HSPA base station (Table 2.2). This is due to the fact that in each component some power is lost. For mobile WiMAX, fixed WiMAX, and LTE, P_{Tx} in Table 2.2 is equal to P_{Tx}^{TCH} because an OFDMA-based multiple access technology is used. Also the user interference margin UIM needs to be taken into account when using UMTS and HSPA [20]:

$$UIM = -10 \cdot log_{10}(1 - TL) \tag{2.13}$$

with TL the target load.

For mobile WiMAX, HSPA, and LTE an extra gain, the MIMO gain G_{MIMO} needs to be taken into account. Here, the theoretical MIMO gain is considered [21]:

$$G_{MIMO} = 10 \cdot log_{10}(n_{Tx} \cdot n_{Rx}) \tag{2.14}$$

with n_{Tx} the number of transmitting antennas and n_{Rx} the number of receiving antennas. Although the theoretical MIMO gain might be an overestimation for some realistic cases [22], it is used for all technologies considered to realise a fair comparison.

Once the maximum allowable path loss PL_{max} is known, the maximum range R (in metres) covered by the base station of a certain technology can be determined:

$$R = g^{-1}((PL_{max} - SM)|f, h_{BS}, h_{MS}) \tag{2.15}$$

with PL_{max} the maximum allowable path loss (in dB), SM the shadowing margin (in dB), f the frequency (in Hz), h_{BS} the height of the base station antenna (in metres) and h_{MS} the height of the mobile station antenna (in metres). The shadowing margin depends on the standard deviation of the path loss model, the coverage percentage, and the outdoor standard deviation. Here, a coverage percentage of 90% is considered. The function $g(.)$ depends on the used path loss model, for example, the HATA model and the Erceg model [23, 24]. For this study, the Erceg C model is used as this is the best suitable for suburban areas and the considered scenario.

The quantity before the '|' in Eq. (2.15) is a variable and varies over a continuous interval, whereas the quantities after the '|' are parameters that take only one discrete known value.

2.5.1.2 Microcell base station

To determine the path loss and the coverage of a microcell base station, the same procedure and parameters as in Section 2.5.1.1 are used, although the values of some parameters are different. Table 2.3 summarizes the link budget parameters for the coverage calculations of the microcell base station for all considered technologies.

Some parameters of Table 2.3 have the same value as for the macrocell base station (Table 2.2) because these parameters are either technology dependent (such as the frequency and the bandwidth), or mobile receiver dependent (such as the antenna gain and the feeder loss of the mobile receiver) or based on environmental assumptions (such as the fade margin). The same (cell) interference margin (i.e., 2 dB) is assumed for both the macrocell and the microcell base station as carried out in [4]. When the purpose is to increase throughput, the microcell base station will be mainly located within the cell covered by the macrocell base station (the so-called umbrella structure), and a more exhaustive study of the interference will be needed [25]. The values for the input power P_{Tx} of the antenna and the antenna gain of the base station differ between a macrocell and microcell base station. A microcell base station has a typical P_{Tx} of 2 W; sometimes, 6 W is used. In this study, a P_{Tx} of 2 W is selected, which corresponds with 33 dBm [4]. As mentioned earlier, a microcell base station supports only one sector; therefore, an omnidirectional antenna is considered here. The antenna gain for this antenna type varies from 4 to 6 dB depending on the technology. Furthermore, the Walfish-Ikegami (WI) propagation model is considered as this model is suitable for the microcell base station [26]. An antenna height of 6 m is chosen, which corresponds with the height of the roof-gutter of two-storied house (i.e., 3 m per floor).

2.5.1.3 Femtocell base station

To determine the path loss and the coverage of a femtocell base station, the same procedure and parameters as in Section 2.5.1.1 are used, although the values of some parameters are different. Table 2.4 summarizes the link budget parameters for the coverage calculations of the femtocell base station for all technologies considered.

Again some parameters of Table 2.4 have the same value as for the macrocell base station (Table 2.2) as mentioned in Section 2.5.1.2. Other values are specific for the femtocell base station. Instead of the Erceg and WI propagation model, the

Parameter	Mobile WiMAX	HSPA	LTE	Unit
Frequency	2.5	2.1	2.6	GHz
Input power BS p_{Tx}	33	33	33	dBm
Effective input power BS p_{Tx}^{TCH}	33	13.8	33	dBm
Antenna gain BS	6	5	4	dBi
Antenna gain MS	2	0	0	dBi
Number of MIMO Tx antennas	1	1	1	—
Number of MIMO Rx antennas	1	1	1	—
Cyclic combining gain BS	3	3	3	dB
Soft handover gain	0	1.5	0	dB
Feeder loss BS	0.5	0	2	dB
Feeder loss MS	0	0	0	dB
Fade margin	10	10	10	dB
Yearly availability	99.995	99.995	99.995	%
Cell interference margin	2	2	2	dB
User interference margin	0	9	0	dB
Bandwidth	5	5	5	MHz
Receiver SNR	[6, 8.5, 11.5, 15, 19, 21][a]	[-3.1, 0.1, 3.4, 6.0, 7.1, 9.6, 15.6][b]	[-1.5, 3, 10.5, 14, 19, 23, 29.4][c]	dB
Used subcarriers	360	360	360	—
Total subcarriers	512	512	512	—
Noise figure MS	7	9	8	dB
Implementation loss MS	2	0	0	dB
Processing gain	—	12	—	dB
Control overhead	—	0.25	—	—
Target load	—	0.875	—	—
Max. number of users	—	75	—	—
Duplexing	FDD	FDD	FDD	—
Building penetration loss [18]	8.1	8.1	8.1	dB
Height BS antenna	6	6	6	m
Height MS antenna	1.5	1.5	1.5	m
Coverage requirement	90	90	90	%
Shadowing margin	12.8	12.8	12.8	dB

[a] [1/2 QPSK, 3/4 QPSK, 1/2 16-QAM, 3/4 16-QAM, 2/3 64-QAM, 3/4 64-QAM]

[b] [1/4 QPSK, 1/2 QPSK, 3/4 QPSK, 3/4 8-QAM, 1/2 16-QAM, 3/4 16-QAM, 3/4 64-QAM]

[c] [1/3 QPSK, 1/2 QPSK, 2/3 QPSK, 1/2 16-QAM, 2/3 16-QAM, 4/5 16-QAM, 1/2 64-QAM, 2/3 64-QAM]

Table 2.3: Link budget table of the microcell base station for the technologies considered

ITU-R P.1238 model is used here [27] because femtocell base stations are typically installed indoor. This model predicts the path loss for three possible scenarios: a residential building, a commercial building or an office. Here, the office scenario is assumed.

Parameter	Mobile WiMAX	HSPA	LTE	Unit
Frequency	2.5	2.1	2.6	GHz
Input power BS p_{Tx}	23	15	21	dBm
Effective input power BS p_{Tx}^{TCH}	23	-4	21	dBm
Antenna gain BS	2	2	2	dBi
Antenna gain MS	2	0	0	dBi
Number of MIMO Tx antennas	1	1	1	—
Number of MIMO Rx antennas	1	1	1	—
Cyclic combining gain BS	3	3	3	dB
Soft handover gain	0	1.5	0	dB
Feeder loss BS	0.5	0	2	dB
Feeder loss MS	0	0	0	dB
Fade margin	10	10	10	dB
Yearly availability	99.995	99.995	99.995	%
Cell interference margin	2	2	2	dB
User interference margin	0	9	0	dB
Bandwidth	5	5	5	MHz
Receiver SNR	[6, 8.5, 11.5, 15, 19, 21][a]	[-3.1, 0.1, 3.4, 6.0, 7.1, 9.6, 15.6][b]	[-1.5, 3, 10.5, 14, 19, 23, 29.4][c]	dB
Used subcarriers	360	360	360	—
Total subcarriers	512	512	512	—
Noise figure MS	7	7	5	dB
Implementation loss MS	2	0	0	dB
Processing gain	—	12	—	dB
Control overhead	—	0.25	—	—
Target load	—	0.875	—	—
Max. number of users	—	75	—	—
Duplexing	FDD	FDD	FDD	—
Building penetration loss	0	0	0	dB
Height MS antenna	1.5	1.5	1.5	m
Coverage requirement	90	90	90	%
Shadowing margin	13.2	13.2	13.2	dB

[a] [1/2 QPSK, 3/4 QPSK, 1/2 16-QAM, 3/4 16-QAM, 2/3 64-QAM, 3/4 64-QAM]

[b] [1/4 QPSK, 1/2 QPSK, 3/4 QPSK, 3/4 8-QAM, 1/2 16-QAM, 3/4 16-QAM, 3/4 64-QAM]

[c] [1/3 QPSK, 1/2 QPSK, 2/3 QPSK, 1/2 16-QAM, 2/3 16-QAM, 4/5 16-QAM, 1/2 64-QAM, 2/3 64-QAM]

Table 2.4: Link budget table of the femtocell base station for the technologies considered

2.5.2 Comparison between the different technologies

2.5.2.1 Macrocell base station

In this section, the considered wireless technologies are compared when using a single macrocell base station. To this end, the power consumption per covered area PC_{area} (Eq. (2.4)) is investigated as a function of the bit rate offered by the base station. It is more useful to investigate PC_{area} as function of the bit rate instead of investigating $PC_{bitrate}$ (Eq. 2.6), because PC_{area} takes also the performance (i.e., the range) for this bit rate into account. The other energy efficiency metrics (Eq. (2.5, 2.7, 2.8)) are typically used to represent the energy efficiency of

networks. Fig. 2.2 shows thus the power consumption per covered area PC_{area} (Eq. (2.4)) as a function of the bit rate (in Mbps) for the considered technologies. To determine the covered area, the maximum range that can be obtained by each bit rate supported by the technology is calculated, assuming that the base station transmits with maximum allowed power. A higher bit rate typically results in a lower range. For the bit rate calculation, the aggregated physical bit rate is assumed which has to be divided between the different users.
In general, one can see that for each technology PC_{area} increases for increasing bit rates and thus the base station becomes less energy-efficient for higher bit rates. Assuming a fixed bandwidth, each bit rate is determined by the coding rate and modulation scheme. Each technology supports different combinations of coding rate and modulation schemes. Each combination is characterized by a receiver SNR. This receiver SNR is also taken into account into the link budget and influences the obtained range. The higher the receiver SNR, the smaller the range will be. The difference in receiver SNR between WiMAX and LTE on the one hand, and HSPA and UMTS on the other hand, is that WiMAX and LTE use SOFDMA as multiple access technique, while UMTS and UMTS use Wideband Code Division Multiple Access (W-CDMA).
As mentioned above, a technology becomes less energy-efficient for higher bit rates. For mobile WiMAX, fixed WiMAX, HSPA, and LTE, this can be explained by the fact that higher bit rates correspond with higher receiver SNRs as shown in Table 2.2. Higher receiver SNRs correspond with smaller ranges: from Eq. (2.15) one can see that a higher PC_{area} corresponds then with a smaller range for the same power consumption. For UMTS, the processing gain is mainly responsible for the decrease in energy efficiency when higher bit rates are used. Table 2.2 lists the processing gain for the three considered UMTS services. The higher the bit rate of the service, the lower the processing gain. A lower processing gain results in a lower range for the same power consumption and thus UMTS becomes also less energy-efficient for higher bit rates.

Based on the assumptions made for the parameters, UMTS is the most energy-efficient technology until a bit rate of 2.8 Mbps, LTE between 2.8 Mbps and 8.2 Mbps, fixed WiMAX between 8.2 Mbps and 13.8 Mbps, and finally mobile WiMAX for bit rates higher than 13.8 Mbps.

For example, for a bit rate of 2 Mbps, PC_{area} is 0.5 mW/m^2 for UMTS while PC_{area} = 0.7 mW/m^2 for fixed WiMAX and PC_{area} = 1.9 mW/m^2 for HSPA. Mobile WiMAX and LTE do not support bit rates below the 2.8 Mbps for the considered bandwidth. UMTS performs better than fixed WiMAX because of its higher ranges (1015.4 m versus 788.8 m at 2 Mbps), despite the fact that it has a higher power consumption (i.e., 1672.6 W) than fixed WiMAX (i.e., 1279.1 W). This higher range is due to the UMTS processing gain. The higher

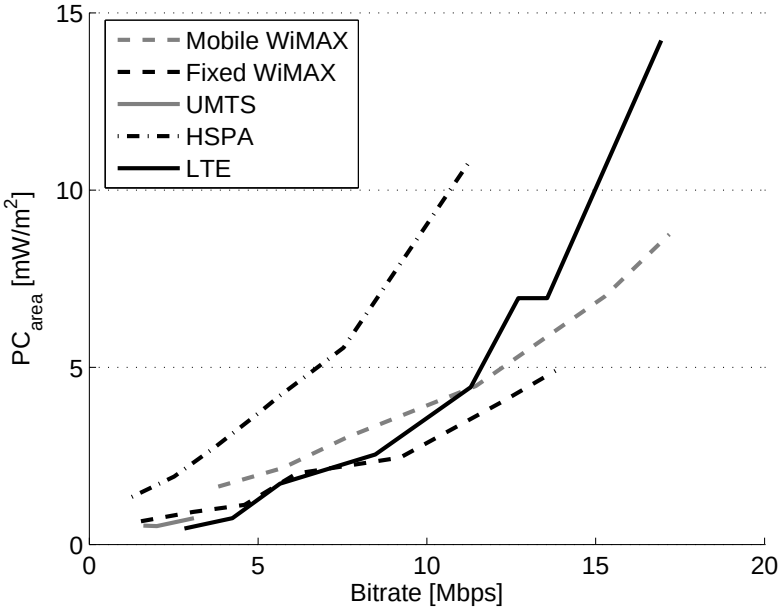

Figure 2.2: Comparison of the power consumption PC_{area} per covered area of a macrocell base station (in a 5 MHz channel) for different technologies.

power consumption of UMTS is caused by the higher input power P_{Tx} of the antenna (43 dBm versus 35 dBm for fixed WiMAX, Table 2.2): a higher P_{Tx} corresponds with a higher power consumption of the power amplifier in Eq. (2.1), resulting in a higher power consumption of the entire base station.

HSPA is the least energy-efficient technology at 2 Mbps because of its lower ranges. Table 2.2 shows that the effective input power of the antenna P_{Tx}^{TCH} is lower for HSPA (i.e., 24.7 dBm). The power consumption of the HSPA base station is the same as for the UMTS base station.

From 2.8 Mbps to 8.2 Mbps, LTE is the most energy-efficient technology. LTE has an input power of the antenna of 43 dBm resulting in higher ranges (557.0 m at 5 Mbps) and a power consumption of 1672.6 W. UMTS does not support bit rates higher than 3 Mbps.

From 8.2 Mbps to 13.8 Mbps, fixed WiMAX is the most energy-efficient solution. Fixed WiMAX performs better than LTE because of its lower receiver SNR, its higher antenna gain for the mobile station (8 dBi versus 0 dBi) and its lower noise figure (4.6 dB versus 8 dB) resulting in higher ranges (e.g., 407.7 m versus 346.3 m at 10 Mbps) due to its lower input power of the antenna P_{Tx} (35 dBm versus 43 dBm). Fixed WiMAX and mobile WiMAX have the same power con-

sumption (i.e., 1279.1 W). Fixed WiMAX has higher ranges than mobile WiMAX for the same reasons as for LTE, except for the receiver SNRs.

For bit rates higher than 13.8 Mbps, mobile WiMAX is the most energy-efficient solution based on our assumptions. Only mobile WiMAX and LTE support these higher bit rates. Mobile WiMAX performs better because of its higher range (e.g., 215.7 m versus 193.5 m at 17 Mbps) and its lower power consumption (i.e., 1279.1 W versus 1672.6 W). The higher range is due to the lower receiver SNRs. The lower power consumption is caused by the lower input power of the antenna P_{Tx} (35 dBm versus 43 dBm).

Influence of MIMO Finally, the influence of MIMO on the power consumption of the macrocell base station is investigated. The considered technologies are compared for a 2x1, 2x2, 3x2, 3x3, 4x3, and 4x4 MIMO system. Fig. 2.3 gives an overview of PC_{area} as a function of the chosen MIMO system for mobile WiMAX, HSPA, and LTE. The energy efficiency gain is also indicated in the figure. This gain, EG, indicates how much (as a percentage) PC_{area} has decreased compared to the Single-Input Single-Output (SISO) system:

$$EG = \frac{PC_{area/SISO} - PC_{area/MIMO}}{PC_{area/SISO}} \cdot 100[\%] \tag{2.16}$$

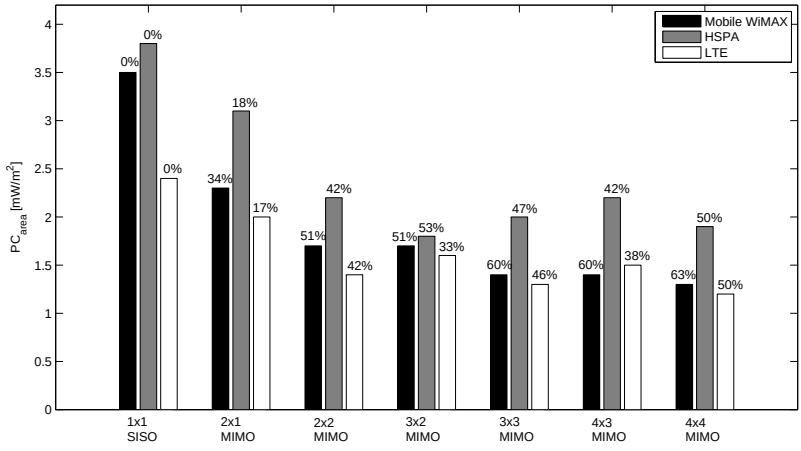

Figure 2.3: Influence of 2x1, 2x2, 3x2, 3x3, 4x3, and 4x4 MIMO on PC_{area}.

Based on the assumptions made for the parameters and the cases considered, Fig. 2.3 shows that the energy efficiency increases when MIMO is introduced. The

highest energy efficiency is obtained with a 4x4 MIMO system (up to 63%). The EG is the highest for mobile WiMAX.

Compared to the SISO system, the area covered by each technology increases with 438% when using 4x4 MIMO, because of an increase of 132% of the range, whereas the power consumption increases with only 95% for mobile WiMAX and 173% for HSPA and LTE. The increase in power consumption is lower for mobile WiMAX because of its lower input power P_{Tx} of the antenna (Table 2.2). This is also the reason why the highest EG are obtained with mobile WiMAX (34-63%) for all considered MIMO systems.

Comparing the different MIMO systems reveals that a higher MIMO array size (i.e., more transmitting and/or more receiving antennas) does not always result in a higher energy efficiency. For mobile WiMAX, EG for a 2x2 and 3x2 MIMO system are approximately equal (51%). This can be explained as follows: the power consumption P_{el} of the base station for 2x2 MIMO is lower (1689.5 W against 2495.8 W for 3x2 MIMO) because only two transmitting antennas are used. However, the range is higher for the 3x2 MIMO system (794.4 m against 576.3 m for 2x2 MIMO) because of its higher MIMO gain, resulting in similar values for PC_{area} and EG.

Analogously for LTE, the 2x2 and 3x3 MIMO system have higher EG than the 3x2 and the 4x3 MIMO system, respectively. For HSPA even lower EG values for the 3x3 and 4x3 MIMO system than respectively for the 3x2 MIMO system and the 3x3 MIMO system are obtained.

2.5.2.2 Microcell base station

Fig. 2.4 presents the power consumption PC_{area} per covered area as a function of the bit rate for the microcell base station in a 5 MHz channel. For the microcell base station, mobile WiMAX is the most energy-efficient technology for bit rates higher than 3.8 Mbps (11.5 mW/m^2 for about 5.5 Mbps versus 23.9 mW/m^2 for LTE and 38.6 mW/m^2 for HSPA). Mobile WiMAX performs better because of its higher antenna gain for both the base and the mobile stations (Table 2.3). In general and for the case considered here, HSPA is less energy-efficient (higher value for PC_{area}) than mobile WiMAX and LTE because of its lower effective input power of the antenna P_{Tx}^{TCH}.

LTE is the most energy-efficient for bit rates between 2.8 and 3.8 Mbps (PC_{area} is 7.9 mW/m^2 for about 2.5 Mbps versus 19.9 mW/m^2 for HSPA). Bit rates below 2.8 Mbps are only supported by HSPA (PC_{area} is 14.7 mW/m^2 for 1.3 Mbps) and not by mobile WiMAX or LTE.

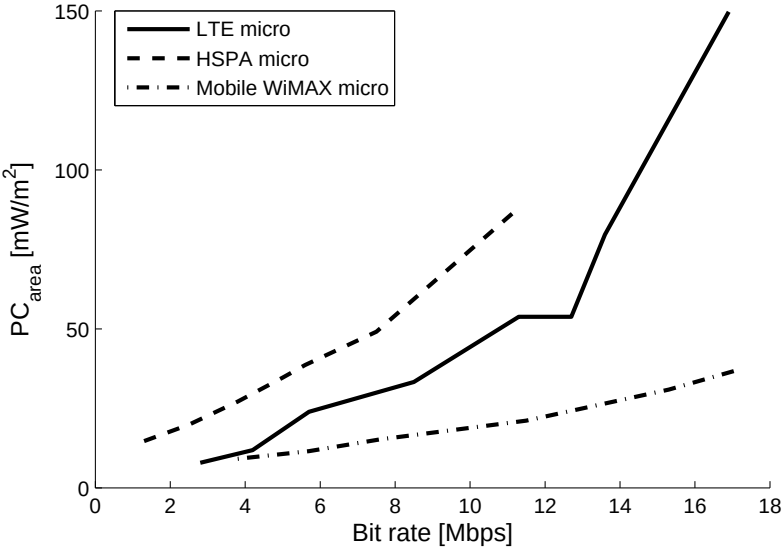

Figure 2.4: Comparison of the power consumption PC_{area} per covered area a microcell base station in a 5 MHz channel for different technologies.

2.5.2.3 Femtocell base station

Fig. 2.5 compares the power consumption PC_{area} per covered area for the considered technologies in a 5 MHz channel. The femtocell base station consumes 10.5 W, 10.0 W, and 9.7 W, respectively, for mobile WiMAX, LTE, and HSPA. The differences in power consumption are due to the differences in the input power of the antenna (Table 2.4). As mentioned above, the higher the input power of the antenna, the higher the power consumption of the power amplifier (Eq. (2.3)) and thus the higher the power consumption of the base station.

For bit rates higher than 5 Mbps, mobile WiMAX is the most energy-efficient technology (PC_{area} = 34.9 mW/m^2 versus 4.2 mW/m^2 for LTE and 2.3 mW/m^2 for HSPA and for a bit rate of approximately 11 Mbps). Although mobile WiMAX has a higher power consumption, it obtains a higher range (38.5 m versus 27.4 m and 9.4 m for LTE and HSPA respectively) due to its lower receiver SNR and its higher input power of the antenna (Table 2.4), resulting thus in a higher energy efficiency.

For bit rates between 2.8 Mbps and 5 Mbps, LTE is the most energy-efficient technology (PC_{area} = 0.4 mW/m^2 versus 0.6 mW/m^2 and 5.4 mW/m^2 for, respectively, mobile WiMAX and HSPA for a bit rate of approximately 4 Mbps). Again, a higher range is obtained with LTE (93.5 m versus 76.8 m and 24 m for mobile

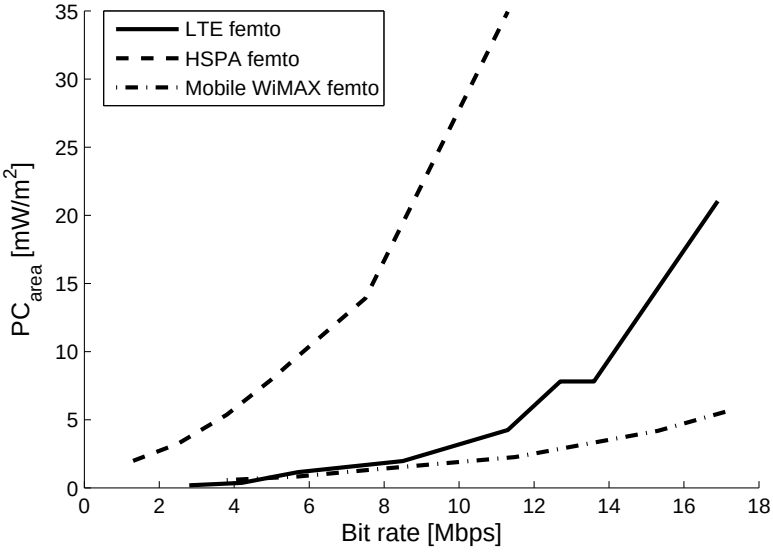

Figure 2.5: Comparison of the power consumption PC_{area} per covered area of a femtocell base station in a 5 MHz channel for different technologies.

WiMAX and HSPA respectively and for a bit rate of approximately 4 Mbps) than for the other technologies due to its lower receiver SNR for the considered bit rates (Table 2.4).

Finally, only HSPA supports bit rates below the 2.8 Mbps and the energy efficiency is shown in Fig. 2.5.

2.5.3 Comparison between the different base station types

In this section, the power consumption PC_{area} per covered area of a macrocell, microcell, and femtocell base station is compared for three different wireless technologies: mobile WiMAX, HSPA, and LTE. All parameters for the different base station types can be found in Tables 2.2, 2.3, and 2.4. Figs. 2.2, 2.4, and 2.5 presents the power consumption PC_{area} per covered area as a function of the bit rate for respectively the macrocell, microcell, and femtocell base station. Again, PC_{area} is considered as energy efficiency metric, because the same technologies are investigated for the different base station types. This means that the bit rate offered by the base station will be the same for the different base station types, however the obtained ranges for the different bit rates will depend on the base station types.

Based on our assumptions, we found that the microcell base station is the least energy-efficient (i.e., a higher PC_{area}) than the macrocell and the femtocell base

station. PC_{area} is about 4 to 18 times lower for a macrocell base station than for a microcell base station (e.g., 1.6 mW/m^2 versus 9.2 mW/m^2 for mobile WiMAX and 3.8 Mbps) because of the higher range obtained by the macrocell base station. The range for the macrocell base station is 4 to 8 times higher than for a microcell base station depending on the considered technology because of its higher input power P_{Tx}, its higher antenna gain and its higher antenna height (Table 2.2 and 2.3).

For the macrocell and the femtocell base station, it depends on the used technology which one is the most energy-efficient. For mobile WiMAX, the femtocell base station is the most energy-efficient (PC_{area} is 0.6 mW/m^2 for 3.8 Mbps and 5.7 mW/m^2 for 24.3 Mbps versus 1.6 mW/m^2 and 8.8 mW/m^2 for the macrocell base station). PC_{area} is about 2 to 3 times lower for the femtocell base station compared to the macrocell base station. This is due to the fact that a femtocell base station consumes approximately 107 times less power than a macrcocell base station (12 W versus 1279.1 W), while the range obtained with the femtocell base station is only 7 to 9 times smaller. For HSPA, the macrocell base station is the most energy-efficient (PC_{area} is 1.3 mW/m^2 for 1.3 Mbps and 10.9 mW/m^2 for 11.3 Mbps versus 2.0 mW/m^2 and 35.0 mW/m^2 for the macrocell base station). The range of the femtocell base station is about 16 to 24 times lower than for the macrocell base station, while the power consumption of the femtocell base station is 139 times lower, resulting in a 2 to 3 times higher PC_{area} for the femtocell base station. For LTE, it depends on the bit rate if the macrocell or femtocell base station is the most energy-efficient. For a bit rate lower than 12.7 Mbps, the femtocell base station is the most energy-efficient (PC_{area} is 0.2 mW/m^2 for 2.8 Mbps versus 0.4 mW/m^2), while for a bit rate equal or higher than 12.7 Mbps the macrocell base station is the most energy-efficient (PC_{area} is 6.9 mW/m^2 for 12.7 Mbps versus 7.8 mW/m^2).

As mentioned above, for the macrocell base station, mobile WiMAX is the most energy-efficient for bit rates higher than 11.5 Mbps. For bit rates between 2.8 Mbps and 11.5 Mbps, LTE is the most energy-efficient and for bit rates below 2.8 Mbps HSPA is the most energy-efficient (only technology supporting these lower bit rates). For a microcell base station, HSPA is the most energy-efficient for bit rates below 2.8 Mbps, LTE for bit rates between 2.8 Mbps and 3.8 Mbps, and mobile WiMAX for bit rates higher than 3.8 Mbps. Finally, for a femtocell base station, HSPA is the most energy-efficient for bit rates up to 2.8 Mbps, LTE for bit rates between 2.8 Mbps and 5 Mbps and mobile WiMAX for bit rates higher than 5 Mbps.

Note that although a type of base station is less energy-efficient for a certain technology, this does not mean that it is not recommended to use it in the network to reduce power consumption. For example, for HSPA, the introduction of microcell and femtocell base station can reduce the overall network power consumption

as these types have a lower power consumption. This will be investigated in the next chapter.

2.5.4 Conclusion

In this chapter, a power consumption model for a macrocell, microcell and femtocell base station is proposed. An appropriate metric, the power consumption PC_{area} per covered area, is defined to determine the energy efficiency of each base station type. Based on this metric, the energy efficiency of different wireless technologies (mobile WiMAX, LTE, and HSPA) and of the different base station types is compared.

The lowest power consumption is obtained by the femtocell base station which consumes typically around 12 W, while the highest power consumption is obtained by the macrocell base station which has a typical power consumption of 1279 to 1673 W depending on the considered technology. The microcell base station consumes approximately 377 W.

Which technology is the most energy-efficient depends on the considered base station type and the required bit rate. E.g., for the macrocell base station, mobile WiMAX is the most energy-efficient for bit rates higher than 11.5 Mbps, LTE for bit rates between 2.8 Mbps and 11.5 Mbps, HSPA for bit rates below 2.8 Mbps. Furthermore, it depends also on the wireless technology which base station type is the most energy-efficient. For mobile WiMAX, the femtocell base station is the most energy-efficient, while for HSPA the macrocell base station is the most energy-efficient. For LTE, it depends on the bit rate which type is the most energy-efficient. However, this does not mean that it is not interesting in terms of energy efficiency and power consumption to introduce a less energy-efficient base station type in the network. Due to for example a lower power consumption, it can reduce the overall network power consumption.

The energy efficiency of a base station can be further improved by introducing MIMO. The more transmitting and receiving antennas, the more energy-efficient the base station becomes. PC_{area} can be reduced by 50 to 63% for a macrocell base station (depending on the considered technology) when using 4x4 MIMO.

The power consumption model for the different base station types and the general comparison of the energy efficiency of different technologies and base station types will be used as input for the following chapters.

References

[1] C. Patel, M. Yavuz, and S. Nanda. *Femtocells*. IEEE Wireless Communications, 17(5):6–7, October 2010.

[2] U. Barth. *Wireless networks, EARTH research project*. In ETSI Green Agenda Workshop, November 2009.

[3] L. Hérault. *Green Wireless Communications eMobility GA1*. In e-Mobility Workshop at the 4th Future Networks Concertation Meetings, Brussels, Belgium, September 2009.

[4] F. Richter, A. Fehske, and G. Fettweis. *Energy efficiency aspects of base station deployment strategies for cellular networks*. In IEEE 70th Vechicular Technology Conference Fall (VTC 2009-Fall), pages 1–5, 2009.

[5] I. Ashraf, F. Boccardi, and L. Ho. *Power savings in small cell deployments via sleep mode techniques*. In 21st Annual IEEE Symposium on Personal, Indoor and Mobile Radio Communications (PIMRC): Workshop W-Green, pages 306–310, Istanbul, Turkey, 2010.

[6] Ophir RF. *model 5303009, 5303025, 5303075, 5303018A, 5303023*, 2010.

[7] Power-One. *S series*, 2010.

[8] Daikin. *FUQ125BW13/R2Q125D7413, FHQ35BW1B*, 2010.

[9] Allgon Microwave. *AMR Transcend PLUS*, 2010.

[10] Ceragon Networks. *FibeAIR 1500P Family*, 2010.

[11] Trangobroadbandnetworks. *TrangoLINK - Giga*, 2010.

[12] L. M. Correia, D. Zeller, O. Blume, D. Ferling, Y. Jading, I. Gódor, G. Auer, and L. Van der Perre. *Challenges and Enabling Technologies for Energy Aware Mobile Radio Networks*. IEEE Communications Magazine, 48(11):66–72, November 2010.

[13] P. Chandar and S.S. Das. *Area Energy Efficiency Analysis for OFDMA Femtocell Networks*. In 11th International Symposium on Wireless Communication Systems, Barcelona, Spain, August 2014.

[14] J. Baliga, Ayre R, K. Hinton, and R.S. Tucker. *Energy Consumption in Wired and Wireless Access Networks*. IEEE Communications Magazine, 49(6):70–77, June 2011.

[15] W. Vereecken, W. Van Heddeghem, M. Deruyck, B. Puype, B. Lannoo, W. Joseph, D. Colle, L. Martens, and P. Demeester. *Power Consumption in Telecommunication Networks: Overview and Reduction Strategies*. IEEE Communications Magazine, 49(6):62–69, June 2011.

[16] L.M. del Apio, E. Mino, L. Cucala, O. Moreno, and I Berberana. *Energy Efficiency and Performance in mobile network deployments with femtocells*. In IEEE 22nd International Symposium on Personal Indoor and Mobile Radio Communications, pages 107–111, Toronto, Canada, 2011.

[17] S. Saunders. *Antennas and propagation for wireless communication systems*. Wiley, 1999.

[18] D. Plets, W. Joseph, L. Verloock, L. Martens, H. Gauderis, and E. Deventer. *Extensive penetration loss measurements and models for different building types for DVB-H in the UHF band*. IEEE Transactions on Broadcasting, 55(2):213–222, 2009.

[19] R. Krüger and H. Mellein. *UMTS introduction and measurement*. Technical report, Rohde & Schwarz, 2004.

[20] J. Hämäläinen. *Cellular Network Planning and Optimization - Part VII: WCDMA link budget*, 2008.

[21] L. Nuaymi. *WiMAX technology for broadband wireless access*. Wiley, 2007.

[22] M. Deruyck, E. Tanghe, W. Joseph, D. Pareit, I. Moerman, and L. Martens. *Performance analysis of WiMAX for mobile applications*. In IEEE Wireless Communications and Networking, pages 1–6, Sydney, Australia, April 2010.

[23] M. Hata. *Empirical Formula for Propagation Loss in Land Mobile Radio Services*. IEEE Transactions on Vehicular Technology, 29(3):317–325, August 1980.

[24] V. Erceg, L. Greenstein, S. Tjandra, S. Parkoff, A. Gupta, B. Kulic, A. Julius, and R. Bianchi. *An Empirically Based Path Loss Model for Wireless Channels in Suburban Environments*. IEEE Journal on Selected Areas in Communications, 7(7):1205–1211, July 1999.

[25] S. Bhaumik, G. Narlikar, and S. Kanugovi S. Chatoopadhyay. *Breathe to stay cool: adjusting cell sizes to reduce energy consumption*. In First ACM SIGCOMM Workshop on Green Networking, pages 41–46, New Delhi, India, 2010.

[26] COST telecommunications. *COST Action 231: Digital mobile radio towards future generation systems*. European Commission, 1999.

[27] Recommendation ITU-R P.1238-2. *Propagation data and prediction methods for the planning of indoor radiocommunication systems and radio local area networks in the frequency range 900 MHz to 100 GHz* , 19997-1999-2001.

3

Coverage-based deployment tool for energy-efficient wireless access networks

The number of mobile devices such as tablet Personal Computer (PC)s, laptops and smart phones clearly gives a boost to the growth of wireless access networks. Not only the number of devices has its influence on the traffic load on wireless access networks, but also the type of applications running on those devices. Streaming music and video, making video calls, posting photos on social network sites on the go, etc. require higher bit rates than an ordinary phone call. The use of these high-bandwidth applications results in the expansion of today's wireless access networks [1]. As wireless access networks currently consume already a large amount of power, it is important to develop energy-efficient wireless access networks in the future [2, 3].

The power consumption model for different base station types of Chapter 2 is used in the deployment tool Green Radio Access Network Design (GRAND) for design and optimization of green wireless access networks. In this section, a coverage-based algorithm is proposed which uses a genetic search algorithm. The purpose of this algorithm is to *cover* a specific (geometrical) area, here called the target area, as *energy-efficiently* as possible with a wireless technology and a minimal power consumption.

3.1 Developing energy-efficient networks with a coverage-based deployment tool

In this section, the coverage-based deployment tool is proposed. This tool can optimize the existing network of an operator towards power consumption or develop a new one with a minimal power consumption. The locations of possible base station sites and the height of the antennas on these sites are provided by the user of the tool and are assumed to be fixed. A set of the provided base station sites will eventually form the network. The network will be developed for a certain bit rate requirement provided by the user of the tool. A trade-off has to be made between the geometrical coverage and the minimal power consumption. The higher the covered area, the higher the power consumption will be as more base stations will be needed or the base stations have to transmit with a higher transmit power.

The coverage-based deployment tool uses a genetic search algorithm as it is not possible to find the perfect solution in an acceptable calculation time for the considered problem, a heuristic is used which gives a good (but maybe suboptimal) solution without being too time-consuming. The disadvantage of a genetic search algorithm is however that optimizing the different input parameters is almost a study on its own. Fig. 3.1 shows the different steps of the genetic search algorithm. Initially, all the base stations are inactive. Based on the set of possible locations, a first set (Step 1 in Fig. 3.1), here called population, of solutions is generated by using five mutations:

- Make an inactive base station active.
- Make an active base station inactive.
- Add 1 dBm to the input power of the antenna of an active base station.
- Remove 1 dBm of the input power of the antenna of an active base station.
- Changing the type of the base station (if allowed by the user of the tool).

Each solution of this first population is created independently of the other solutions of this population by using one of the five mutations described above. Which mutation is used, is determined randomly. The first two mutations influence the locations of active base stations in the network, the last one the type of base station (when allowed by the user) and the other two the input power of the antenna of the base stations. Which base station will be adapted also occurs randomly. The size of this population i.e., the number of solutions that belong to a population, has to be selected by the user at the beginning of the algorithm. Each solution of the population is a possible network to cover the target area.

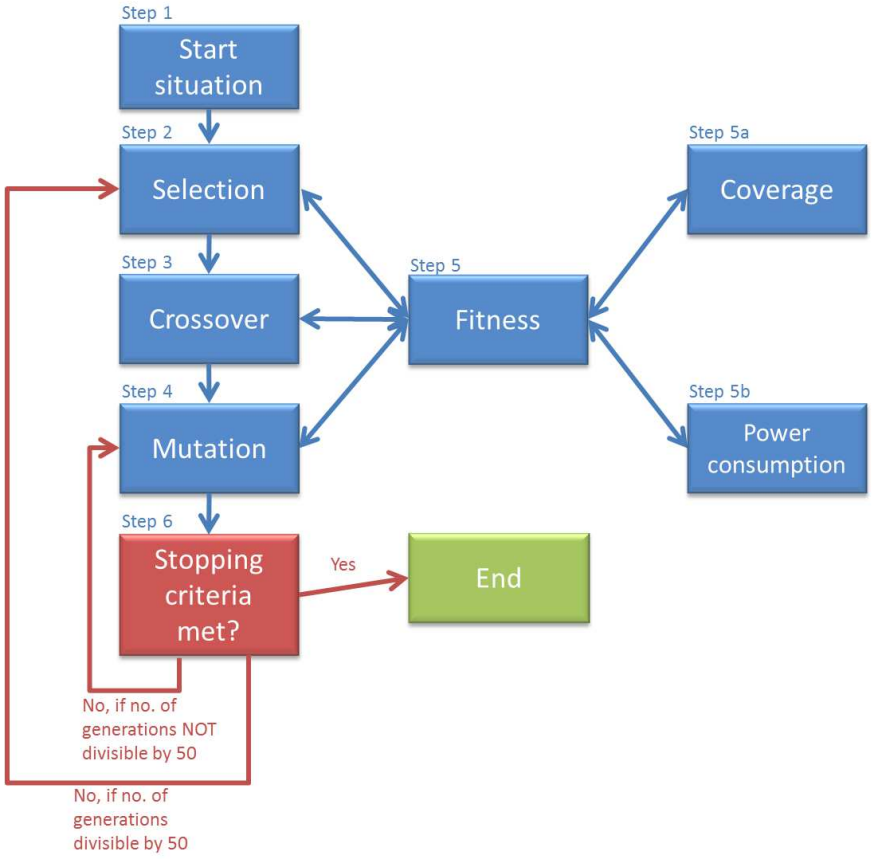

Figure 3.1: Flow chart of the coverage-based algorithm.

The initial population will be further improved through generations (Steps 2-4 in Fig. 3.1). A new generation population is created either by selecting the best solutions in the population (Step 2 in Fig. 3.1) and adding new solutions by the crossover operator until the chosen population size is reached (Step 3 in Fig. 3.1) or by mutating the current population (Step 4 in Fig. 3.1). The new population is then used in the next iteration of the algorithm until a stopping criterion is met.

As mentioned above, a new generation can be formed by selecting a number of solutions of the current generation population (Step 2 in Fig. 3.1). This selection is based on the fitness of the solution (Step 5 in Fig. 3.1) which is a function that measures the quality of the considered solution and is always problem dependent. For this problem, two different fitness functions are combined to one global fitness function. In this way, both the coverage of the target area and the associated power consumption are taken into account. The first fitness function is the coverage fit-

ness f_{cov} (Step 5a in Fig. 3.1) and is defined as:

$$f_{cov} = 100 \cdot \frac{A_{target} \cap A_{sol}}{A_{target}} \tag{3.1}$$

with A_{target} the surface of the target area to be covered (in km^2), A_{sol} the area covered by the individual solution (in km^2) and $\cap$ represents the cross-section of the two areas. f_{cov} is expressed as a percentage and indicates how good the target area is covered by the individual solution. The higher f_{cov}, the better the considered solution corresponds with the target area. The cross-section between A_{target} and A_{sol} is necessary because base stations at the boundaries of the target area will also cover parts outside the target area. Without the cross-section this results in a value of more than 100% for f_{cov} which is not desirable.

The second fitness function is the power consumption fitness f_{pow} (Step 5b in Fig. 3.1) and is defined as:

$$f_{pow} = 100 - (\frac{P_{sol}}{P_{max}} \cdot 100) \tag{3.2}$$

with P_{sol} the power consumption of the individual solution (in Watt) and P_{max} the power consumption of the network with maximal power consumption (in Watt). The network with maximal power consumption corresponds with the network whereby all possible base station locations provided by the user are used and the input power of each base station's antenna is maximal. P_{max} is then used as a reference to decide whether a solution is better than the other or not. The network with maximal power consumption is chosen as a reference instead of the one with minimal power consumption because it is not known what the most energy-efficient network is when running the algorithm.

Eq. (3.1) and (3.2) are then combined in one global fitness function f_{tot} (Step 6 in Fig. 3.1) defined as:

$$f_{tot} = f_{cov} + k(f_{cov}) \cdot f_{pow} \tag{3.3}$$

with

$$k(f_{cov}) = \begin{cases} 0, & f_{cov} < 90 \\ 5 \cdot (\frac{f_{cov}-90}{5})^2, & 90 \leq f_{cov} < 95 \\ 5, & 95 \leq f_{cov} \leq 100 \end{cases}$$

f_{tot} will have a value between 0 and 600. The maximum value (600) is obtained when both f_{cov} and f_{pow} equal 100. The higher f_{tot}, the better the solution is. This kind of global fitness function is chosen because of the trade-off between coverage and power consumption. A geometrical coverage requirement of 90% is often used by wireless operators for wireless network design. If the coverage is below 90% it is important to optimize the coverage. Therefore, a factor $k(f_{cov})$ of 0 is chosen when the coverage is below 90%. In that way, the coverage requirement

can be (easily) obtained. A coverage requirement of 95% is assumed as an excellent coverage and is therefore be chosen as an upper bound. When the coverage approaches 95%, the coverage requirement is certainly met and the most important task is to minimize the power consumption while preserving a coverage of at least 90%. The closer the coverage is to 95%, the more important it becomes to start optimizing the power consumption in the network. Therefore, the factor $k(f_{cov})$ is higher for larger values of the coverage. A quadratic function is used to assign a higher importance to higher coverage percentages. Note that the boundaries of 90% and 95% in Eq. (3.3) can be chosen freely. For the power consumption fitness function, a weighting factor 5 is considered. If this factor is too high, it is not possible to reach a good solution because if we try to optimize too much towards power consumption, a lot of coverage is lost and we have to optimize again towards power consumption. In the end, no good solution will be obtained. If we take the weighting factor too low, the algorithm does not optimize enough towards power consumption.

Based on the above defined fitness function, about 90% of the solutions will be selected for the new population (Step 2 in Fig. 3.1). The other 10%, with the lowest values for f_{tot}, will be removed from the population. To ensure that the new population has the appropriate size, new solutions will be generated by using the crossover operator (Step 3 in Fig. 3.1). Therefore, two parent solutions are chosen: one of the removed solutions of the previous generation population and one of the selected (good) solutions. Each solution consists of a number of partial solutions, which cover a smaller part of the target area. The part of the target area covered by a partial solution should be the same for all the solutions generated by our algorithm. The partial solutions of the bad parent solution are compared with the corresponding partial solutions of the good parent solution. If a partial solution of the good parent solution is better than that of the bad parent solution, the partial solution is adapted in the bad parent solution. This newly obtained solution is then added to the new generation population. The bad solution is chosen as base because in this way, the possibility that the algorithm stops in a local optimum is reduced. Note, that only every 50 generations a new generation is made based on the crossover operator (Step 8 in Fig. 3.1) as this operation is very time-consuming. After the crossover operator, each solution of the population will be mutated (Step 4 in Fig. 3.1). If no crossover operator is applied, then the previous generation will be mutated (Step 4 in Fig. 3.1). Which one of the five mutations will be used, is randomly determined, but the adaptation will only be accepted if a better global fitness (Step 6 in Fig. 3.1) is obtained.

The previous steps (Steps 2-8 in Fig. 3.1) are repeated until a stopping criterion is met (Step 7 in Fig. 3.1). The algorithm is stopped when the estimated value of the fitness of the population is not changed significantly from the estimated value of the previous population. When the estimated value of the f_{tot} distribution

function of the new population is lower than a threshold of 1% of the previous population, the algorithm is stopped. The maximum running time and the maximum number of generations can also be used as stopping criteria. The final result is then the solution from the latest generated population with the highest fitness.

3.2 Comparison between different wireless technologies

In this section, networks are developed for two different areas: a part of the city of Ghent and the Brussels Capital Region both located in Belgium. Three different wireless technologies are considered: mobile WiMAX, HSPA, and LTE. For Ghent, we will compare the different networks with only macrocell base stations and with a mixture of macrocell and microcell base stations. For Brussels Capital Region, a comparison is made between SISO and MIMO. For this study, the coverage-based deployment tool is used.

3.2.1 Application: prediction of the power consumption of a wireless access network in Ghent

We investigate how much electrical power is needed to cover a part of the city of Ghent, Belgium. The target area is shown in Fig. 3.2(a) and has a surface of 13.3 km^2. A coverage requirement of 90% is assumed. For each technology considered, a new network is deployed, once with only macrocell base stations and once with both macrocell and microcell base stations. The set of possible locations for the base stations are all the buildings in the target area with a height equal to or higher than 10 m which results in 13,437 possible locations. A subset of these locations is shown in Fig. 3.2(b). To make a fair comparison between the different technologies, a bit rate of (approximately) 5 Mbps is assumed in a 5 MHz channel. This corresponds with the 2/3 QPSK, the 3/4 QPSK and the 1/2 16-QAM modulation for mobile WiMAX, LTE, and HSPA, respectively. All other settings can be found in Tables 2.2 and 2.3 for the macrocell and microcell base station, respectively. Furthermore, the algorithm will stop when 1000 generations are reached, when the simulation lasts longer than 1 hour or when the estimated value of the f_{tot} distribution function of a new generation population is less than 1% higher than the estimated value of the f_{tot} distribution function of the previous population. The considered energy efficiency metric is here the power consumption per covered area as defined by Eq. (2.4).

Fig. 3.3 gives a visual overview of the energy-efficient network with only macrocell (a) and both macrocell and microcell base stations (b) for mobile WiMAX, resulting from the coverage-based deployment tool. Numerical results

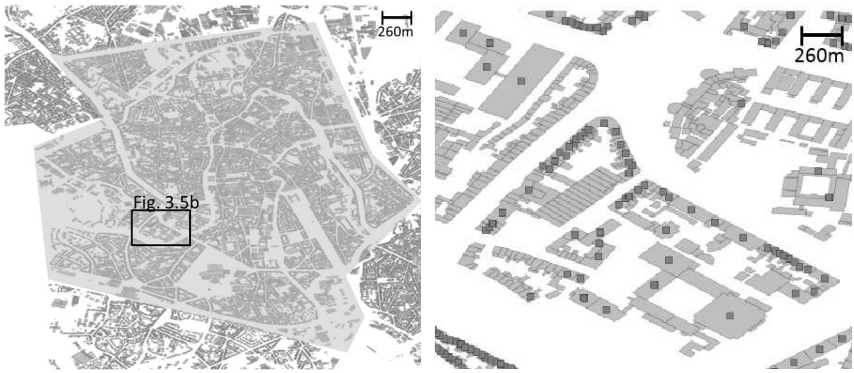

(a) (b)

Figure 3.2: Shapefile of the target area in Ghent, Belgium (a) and a subset of possible locations for the base stations (b).

for all considered technologies are summarized in Table 3.1. The results show that a higher energy efficiency (lower PC_{area} as discussed in Chapter 2 (Eq. (2.4))) is obtained when microcell base stations are introduced due to the lower total power consumption for the same coverage of the network (Table 3.1). The lowest total power consumption for combined macrocell and microcell base stations is found for LTE (81.9 kW), followed by mobile WiMAX (83.8 kW), and HSPA (178.0 kW) for the considered scenario. As discussed in Section 2.5.2.1, LTE is the most energy efficient for a macrocell base station and a 5 Mbps scenario, followed by mobile WiMAX. Table 3.1 shows that the power consumption of the networks is mainly governed by the number of macrocell base stations which is why LTE performs here the best, followed by mobile WiMAX and HSPA. For HSPA, the energy efficiency gain is very limited as the coverage of the network with both macrocell and microcell base stations is much lower than when only macrocell base stations are used (94.9% versus 97.7%).

Parameter	**mobile WiMAX macro**	**mobile WiMAX macro + micro**	**LTE macro**	**LTE macro + micro**	**HSPA macro**	**HSPA macro + micro**
Number of macrocells [-]	78	66	52	50	114	109
Number of microcells [-]	—	4	—	2	—	3
Average total power consumption [kW]	97.2	83.8	83.2	81.9	184.8	178.0
Coverage [%]	97.6	97.4	99.3	99.1	97.7	94.9
Average PC_{area} [kW/km^2]	7.5	6.5	6.3	6.2	14.2	14.1

Table 3.1: Comparison between the networks with only macrocell base stations and with both macrocell and microcell base stations for the technologies considered (5 Mbps in a 5 MHz channel).

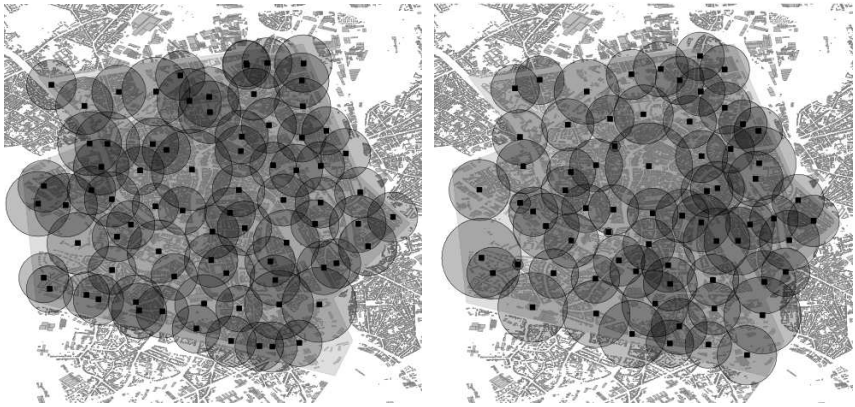

(a) (b)

Figure 3.3: Energy-efficient network with only macrocell base stations (a) and with both macrocell and microcell base stations (b) for mobile WiMAX resulting from the GRAND tool.

3.2.2 Application: prediction of the power consumption of a wireless access network in Brussels

The required electrical power needed to cover Brussels Capital Region with base stations of each technology is here investigated. For this study, a new network is deployed for each technology. However, only existing base station sites are used. The location of the existing base station sites, along with other characteristics of the base station sites, are retrieved from a shapefile from sites.bipt.be. A total number of 8095 antennas spread over 840 (macrocell and microcell) base station sites and exploited by four different operators can be found in the shapefile. Three different sorts of base stations occur in the shapefile: GPRS sites (5,262 antennas at 764 sites), UMTS sites (2,446 antennas at 538 sites) and (fixed) WiMAX sites (387 antennas at 86 sites). Some sites support more than one technology.

Fig. 3.4 shows the target area that needs to be covered which is Brussels Capital Region (149 km^2) in Belgium and is assumed to be suburban [4]. Fig. 3.4 gives also an overview of the existing base station sites in Brussels retrieved from the shapefile of sites.bipt.be. To make a fair comparison among the different technologies, a bit rate of 1 Mbps is assumed. For mobile WiMAX, the 3/4 QPSK modulation is chosen for a bandwidth of 1.25 MHz which means that 85 subcarriers out of 128 subcarriers are used, for HSPA the 1/4 QPSK modulation and for LTE the 1/2 QPSK for a bandwidth of 1.4 MHz which corresponds with 76 used subcarriers out of 128 subcarriers. The other settings for the base stations can be found in Table 2.2. The algorithm stops running when the estimated value of the f_{tot} distribution function of a new generation population is less than 1% higher

than the estimated value of the f_{tot} distribution function of the previous population. Furthermore, the algorithm will also stop when 5,000 generations are reached or when the simulation lasts longer than 14,400 s (i.e, 4 hours). During the simulations, the algorithm was always stopped by the estimated value criterion for all the considered technologies. Each population contains 100 possible solutions. The solution with the highest global fitness f_{tot} of the last generation is the final network.

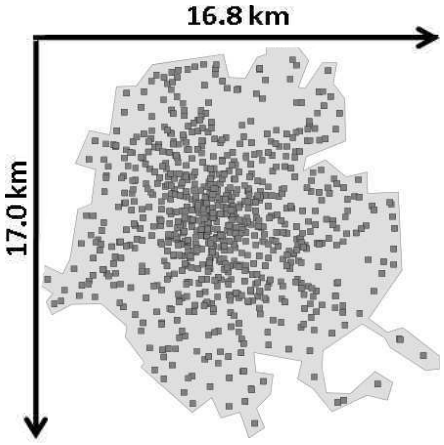

Figure 3.4: Shapefile of the target area Brussels Capital Region, Belgium and the possible base station locations.

Table 3.2 lists the numerical results for mobile WiMAX, LTE, and HSPA for both SISO and 2x2 MIMO. MIMO is here used to increase the coverage of a base station (i.e., diversity). For the SISO configuration, the best solution to cover Brussels is LTE. Higher ranges are obtained with LTE (as discussed in Section 2.5.2.1 resulting in a high energy efficiency (PC_{area} = 0.7 mW/m^2 (Chapter 2 Eq. (2.4)), a low number of used base station sites (135) and thus a low total power consumption (101.3 kW). The high ranges obtained with LTE are due to the low receiver SNR for the considered modulation and coding rate. HSPA is the second most energy-efficient technology (PC_{area} = 1.6 mW/m^2) followed by mobile WiMAX (PC_{area} = 3.2 mW/m^2) for the considered scenario. With HSPA higher ranges can be obtained than with mobile WiMAX due to the processing gain although a single HSPA base station has a higher power consumption as discussed in Section 2.5.2.1. These higher ranges result in a lower number of used base station sites (301) and thus in a lower total power consumption (224.1 kW) than for mobile WiMAX (354 sites and 450.5 kW respectively). Note that for the scenario here considered, HSPA performs better than mobile WiMAX while in Section 3.2 mobile WiMAX performed better than HSPA. The main reason is the difference

1x1 SISO	**Mobile WiMAX**	**HSPA**	**LTE**
Total power consumption [kW]	450.5	224.1	101.3
f_{cov}	94.6%	95.1%	97.8%
f_{pow}	58.0%	64.6%	84.0%
f_{tot}	335.5	418.1	518.0
Number of used sites	354	301	135
PC_{area} [mW/m^2]	3.2	1.6	0.7
2x2 MIMO	**Mobile WiMAX**	**HSPA**	**LTE**
Total power consumption [kW]	377.8	215.1	90.7
f_{cov}	96.2%	96.2%	97.4%
f_{pow}	71.6%	70.8%	87.7%
f_{tot}	454.3	450.2	535.8
Number of used sites	239	249	104
PC_{area} [kW/km^2]	2.6	1.5	0.6

Table 3.2: Comparison of the wireless technologies for the coverage of Brussels Capital Region.

in bit rate (1 Mbps here versus 5 Mbps) as also discussed in Section 2.5.2.1.

LTE is also the best solution when using 2x2 MIMO based on the assumptions made for the parameters, the considered MIMO system and a bit rate of 1 Mbps. LTE has the lowest power consumption, the highest total fitness, and needs the lowest number of base stations (Table 3.2). Table 3.2 shows that the considered technologies have a higher energy efficiency when using MIMO than for SISO. In general, a 2x2 MIMO system increases the coverage compared to a SISO system. Because of this, less base station sites are needed to cover Brussels, resulting in a lower total power consumption and thus in a higher energy efficiency.

3.3 Conclusion

In this chapter, a deployment tool for future energy-efficient wireless access networks is introduced. A coverage-based algorithm which uses a genetic search algorithm is proposed. The purpose of the genetic search algorithm is to cover a predefined (geometrical) area with a minimal power consumption.

The tool is applied on a realistic case in both Ghent and Brussels to investigate the influence of different wireless technologies (mobile WiMAX, HSPA, and LTE) on the network's energy efficiency. The highest energy efficiency for the considered cases and assumptions is obtained when using LTE. For all considered technologies, the energy efficiency can be further increased when introducing mi-

crocell base stations and MIMO in the network. It is thus recommended that future networks support both macrocell and microcell base stations and MIMO.

References

[1] Cisco. *Cisco Visual Networking Index: Global Mobile Data Traffic Forecast Update 2012-2017, White paper*. Technical report, 2012.

[2] M.A. Marsan, L. Chiaraviglio, D. Ciullo, and M. Meo. *A Simple Analytical Model for the Energy-Efficient Activation of Access Points in Dense WLANs*. In the 1st International Conference on Energy-Efficient Computing and Networking (e-Energy), pages 159–168, Passau, Germany, 2010.

[3] G. Koutitas. *Green Network Planning of Single Frequency Networks*. IEEE Transactions on Broadcasting, 56(4):541–550, 2010.

[4] J. De Bruyne, W. Joseph., L. Martens, C. Olivier, and W. De Ketelaere. *Field measurement and performance analysis of an 802.16 system in a suburban environment*. IEEE Transactions on Wireless Communication, 8(3):1424–1434, 2009.

4

Characterization and optimization of the power consumption in wireless access networks by taking daily traffic variations into account

4.1 Introduction and related work

As mentioned earlier, the base stations are responsible for a significant part of the power consumption of wireless access networks. Therefore, a lot of effort has been put in designing new power reducing techniques such as sleep modes and cell zooming or cell breathing [1–12]. Sleep modes allow that a (part of the) base station can be switched off when there is no or little activity taking place in its coverage cell. Whenever necessary, the base station is woken up. When applying cell zooming, the cell size is adjusted adaptively according to the level of activity in a base station's cell. These techniques on their own can significantly reduce the power consumption in wireless access networks and combining them allows even higher power savings. Up to now temporal variations of wireless access networks have only been studied in [4–9, 13] and not experimentally.

In this chapter, the power consumption model of chapter 2 is adapted so that it becomes load dependent. To this end, measurements are performed on an actual HSPA macrocell and microcell base station and based on these measurements the base station's power consumption is modelled as a function of the traffic load.

This model is then used in the GRAND tool of Chapter 3. The GRAND tool is here combined with an algorithm that introduces power reducing techniques in the network such as sleep modes and cell zooming. Both greenfield deployments (i.e., developing a network from scratch) and optimizing an existing operator networks are considered.

Related work Recently, more attention is drawn to the power consumption in wireless access networks. To model this power consumption, it is important to quantify the power consumption of the different components in this network. [1–4, 10–12] propose a power consumption model for today's macrocell BSs. However, [4, 10–12] does not use any measurements to establish the power consumption model. The models proposed in [1–3] are based on GSM and/or UMTS macrocell base stations, while the model described in this chapter is based on measurements on an HSPA base station. Our study shows that it is important to perform measurements to identify the relation between power consumption and traffic properly. Furthermore, a realistic HSPA traffic model can be determined instead of using theoretical traffic models as is often done in literature.

Also the possibilities of sleep modes to reduce the power consumption in wireless access networks are already investigated in a number of studies [4–7]. These studies discuss how sleep modes can be implemented and supported by the network. However, in [4–6], the energy savings in a realistic network deployment are not investigated. Our study tries to determine how much power can be saved by introducing sleep modes in a realistic network. In [7], the effect of sleep modes for different operator networks in a certain area is investigated, which is a similar study as ours. However, it is also important to investigate what the energy savings are when sleep modes are introduced in a network with a minimal power consumption (here resulting from the GRAND tool). In this way, the most energy-efficient solution for the area is considered. The algorithm developed in [7] is similar to ours, but it is assumed that the cell size of the active (non-sleeping) base stations is maximized. In our algorithm, the cell size of the active base stations is expanded as much as needed which does not necessarily correspond with the maximum cell size. Note that in this study it is not discussed how sleep modes and cell zooming should be supported by the hardware, nor the protocols that will be needed e.g., for waking up the base station when necessary. This is the scope of other studies [5–9].

The novelty of this work is that we validate our power consumption model by using measurements on an actual UMTS and HSPA base station. Furthermore, a realistic traffic model is determined and the relation between power consumption and traffic is properly identified. An extension of the coverage-based algorithm of Chapter 3 is proposed which allows to introduce sleep modes and cell zooming in a realistic network. The influence of this introduction on the power consump-

tion of three different networks is investigated: a greenfield deployment optimized towards power consumption, an existing network optimized towards power consumption, and an existing network not optimized towards power consumption.

4.2 Load-dependent power consumption model for a macrocell and microcell base station

In Chapter 2, a power consumption model for a macrocell and microcell base station has been developed. The power consumption of the power amplifier, the transceiver, and the digital signal processing can slightly vary with the load of the base station. The load is here determined by the number of users and the services they use in the base station's cell. The higher the number of users and the higher the requirement, the higher the load is. The power consumption of the components mentioned above should thus be scaled according to the load. This is done by introducing a factor F, denoted here as the load factor. The power consumption $P_{el/macro}$ of a macrocell base station for a certain time stamp t is then determined as follows (in Watt):

$$P_{el/macro}(t) = P_{el/const} + F(t) \cdot P_{el/load} \quad (4.1)$$

$$P_{el/const} = n_{sector} \cdot P_{el/rect} + P_{el/link} + P_{el/airco} \quad (4.2)$$

$$P_{el/load} = n_{sector} \cdot (n_{Tx} \cdot (P_{el/amp} + P_{el/trans} + P_{el/proc})) \quad (4.3)$$

with $F(t)$ the load factor for time stamp t and n_{sector} the number of sectors supported by the base station, n_{Tx} the number of transmitting antennas per sector, $P_{el/rect}$, $P_{el/link}$, $P_{el/airco}$, $P_{el/amp}$, $P_{el/trans}$, $P_{el/proc}$ the power consumption of, the rectifier, the microwave link (if present), the air conditioning, the power amplifier, the transceiver and the digital signal processing (in Watt), respectively.

Analogously, the power consumption $P_{el/micro}$ of a microcell base station for a time stamp t can then be calculated as follows (in Watt):

$$P_{el/micro}(t) = P_{el/const} + F(t) \cdot P_{el/load} \quad (4.4)$$

$$P_{el/const} = P_{el/rect} + P_{el/airco} \quad (4.5)$$

$$P_{el/load} = (n_{Tx} \cdot (P_{el/amp} + P_{el/trans} + P_{el/proc})) \quad (4.6)$$

with again $F(t)$ the load factor at time stamp t, n_{Tx} the number of transmitting antennas, $P_{el/rect}$, $P_{el/airco}$, $P_{el/amp}$, $P_{el/trans}$, $P_{el/proc}$ the power consumption of the rectifier, the air conditioning, the power amplifier, the transceiver and the digital signal processing (in Watt), respectively.

In terms of power consumption, the load is assumed to correspond with the number of voice calls and/or data connections. For example, if 20 voice calls occur on time stamp 1 and 30 voice calls on time stamp 2, the load on time stamp

2 will be higher than the load on time stamp 1. The duration of the call is in this way implicitly taken into account. For example, assume that 5 voice calls from time stamp 1 are still busy on time stamp 2, then this 5 voice calls are taken into account in the 30 voice calls on time stamp 2. It is thus not necessary to take into account the time duration of the voice call explicitly in the load factor. We vary the load factor F from 0 to 1. A value of 0 indicates that the load-dependent components are consuming no power i.e., they are switched off, while a value of 1 indicates that they are working on the highest power consumption level. Two scenarios are considered for determining the load factor. For the first scenario, the load factor $F(t)$ for each hour t of the day with t = 0 (i.e., 0 a.m. to 1 a.m.) .. 23 (i.e., 11 p.m. to 0 a.m.) is determined. For the second scenario, the load factor $F(t)$ will be defined as a function of the load caused by voice calls $V(t)$ at time stamp t and the load caused by data connections $D(t)$ at time stamp t. The formula will be of the following form:

$$F(t) = x \cdot V(t) + y \cdot D(t) + c \tag{4.7}$$

with $V(t)$ the load caused by voice calls ($0 \leq V(t) \leq 1$) at time stamp t and $D(t)$ the load caused by data connections ($0 \leq D(t) \leq 1$) at time stamp t. The division of load caused by voice calls and data connections is based on traffic data received from a mobile operator. The parameters x, y, and c will be determined based on measurements of both the power consumption and the voice and data traffic on an actual macrocell and microcell base station as discussed in the following sections. The measurements are necessary to relate the traffic data of the operator to the actual power consumption. The variations in power consumption can not be found in data sheets as they mostly only provide the maximum or average power consumption.

4.3 Measurements

4.3.1 Measurement procedure

To determine a model for the load factor $F(t)$, measurements are performed on an actual HSPA macrocell and microcell base station in the suburban area of Ghent, Belgium. The power consumption of the base station is measured during six days (4 weekdays and 2 weekend days). Only the power consumption of the load-dependent components (i.e., the digital signal processing, the transceiver, and the power amplifier) were included in these measurements. As DC is used in the base station, the voltage is constant (i.e., approximately 54 V for a macrocell base station and 48 V for a microcell base station) and thus only the current was measured. The power consumption $P(t)$ at a certain time instance t is then determined as fol-

lows (in Watt):

$$P(t) = V \cdot I(t) \tag{4.8}$$

with V the voltage (in Volt) and $I(t)$ the current at time t (in Ampere). The current was measured with an AC/DC current clamp (Fluke i410, accuracy 3.5% of observation).

4.3.2 Macrocell base station

Every second, the value of the current was saved, which results in 466 319 samples for the measurement period of 6 days. Fig. 4.1 shows the power consumption (in Watt) as a function of the time. In Fig. 4.1, day 1 to 5 are weekdays and day 6 is a weekend day. For the weekdays, it is noticed that the power consumption at night (i.e., from midnight to 8 a.m.) is lower than during the day (i.e., from 8 a.m. till midnight) because during the day more people are active than at night. Also during weekdays, more people are coming to town, for example, to work. For the weekend day, this difference in day-night power consumption is smaller than for weekdays.

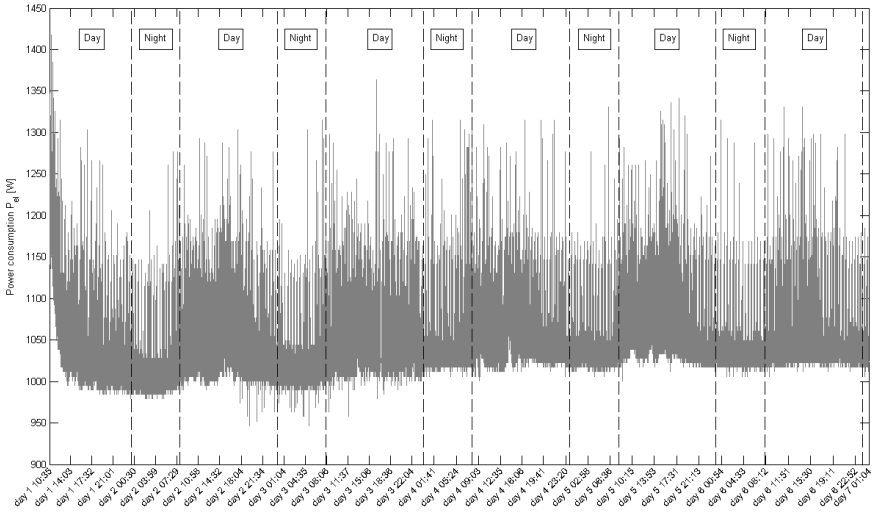

Figure 4.1: Evolution of the power consumption in time (Days 1-5 weekdays, day 6 weekend day) for a macrocell base station.

Based on the data shown in Fig. 4.1, the average power consumption per hour for weekdays and for the weekend is calculated. These averages are presented in Table 4.1. The measured equipment consumes between 1016 W and 1087 W. Determining the power consumption with our model (Eq. (4.1), $F(t)$ = 1, P_{Tx}

		Macrocell base station			Microcell base station		
Hour	**Time stamp t**	**Weekday**	**Weekend**	**Factor $F(t)$ Weekday**	**Weekday**	**Weekend**	**Factor $F(t)$ Weekday**
0 a.m. - 1 a.m.	0	1018 W	1029 W	0.94	220 W	227 W	0.96
1 a.m. - 2 a.m.	1	1017 W	1028 W	0.94	214 W	224 W	0.93
2 a.m. - 3 a.m.	2	1017 W	1027 W	0.94	221 W	220 W	0.97
3 a.m. - 4 a.m.	3	1016 W	1026 W	0.93	220 W	221 W	0.96
4 a.m. - 5 a.m.	4	1016 W	1024 W	0.93	221 W	227 W	0.97
5 a.m. - 6 a.m.	5	1017 W	1024 W	0.94	217 W	226 W	0.95
6 a.m. - 7 a.m.	6	1020 W	1025 W	0.94	224 W	218 W	0.98
7 a.m. - 8 a.m.	7	1026 W	1025 W	0.94	221 W	224 W	0.97
8 a.m. - 9 a.m.	8	1044 W	1027 W	0.96	229 W	232 W	1.00
9 a.m. - 10 a.m.	9	1057 W	1032 W	0.97	219 W	223 W	0.96
10 a.m. - 11 a.m.	10	1087 W	1031 W	1.00	225 W	225 W	0.98
11 a.m. - 12 p.m.	11	1073 W	1033 W	0.99	222 W	229 W	0.97
12 p.m. - 1 p.m.	12	1055 W	1036 W	0.97	219 W	229 W	0.96
1 p.m. - 2 p.m.	13	1060 W	1035 W	0.98	226 W	223 W	0.99
2 p.m. - 3 p.m.	14	1070 W	1037 W	0.98	219 W	222 W	0.96
3 p.m. - 4 p.m.	15	1065 W	1035 W	0.98	221 W	224 W	0.97
4 p.m. - 5 p.m.	16	1049 W	1038 W	0.97	220 W	227 W	0.96
5 p.m. - 6 p.m.	17	1044 W	1036 W	0.96	221 W	226 W	0.97
6 p.m. - 7 p.m.	18	1042 W	1034 W	0.96	222 W	223 W	0.97
7 p.m. - 8 p.m.	19	1034 W	1039 W	0.95	220 W	221 W	0.96
8 p.m. - 9 p.m.	20	1034 W	1033 W	0.95	219 W	225 W	0.96
9 p.m. - 10 p.m.	21	1033 W	1033 W	0.95	221 W	228 W	0.97
10 p.m. - 11 p.m.	22	1033 W	1030 W	0.95	219 W	228 W	0.96
11 p.m. - 0 a.m.	23	1024 W	1030 W	0.94	221 W	223 W	0.97

Table 4.1: Average power consumption per hour during weekdays and weekends for a macrocell and a microcell base station (only load dependent equipment).

= 43 dBm, including load independent equipment) and our assumptions from Table 2.1 results in a power consumption of 1673 W. Excluding the power consumption of the rectifiers, the microwave link and the air conditioning, we obtain a power consumption of 1068 W which agrees very well (standard deviation of 2.0%) with the range of power consumptions in Table 4.1. The load factor $F(t)$ for the time between 10 a.m. and 11 a.m. (t = 10) on a weekday is chosen to be 1 as this time interval corresponds with the highest power consumption. The load factor $F(t)$ for each hour of a weekday can then be determined. These load factors can be found in Table 4.1. One might argue that $F(t)$ represents the impact of the time on the power consumption of the base station rather than the impact of the load. However, a different point in time will result in a different load as shown in [14] and thus reflects $F(t)$ implicitly the impact of the load. Furthermore, it is also important that the $F(t)$ model is representative for other macrocell base stations with a similar traffic pattern in the suburban city environment as well. For other environments such as residential areas, rural terrain, industrial environment, etc., new model parameters for $F(t)$ should be determined following the above described procedure. This is a similar approach as in [14] where for each environment one site is selected to perform measurements. Note that the $F(t)$ model

depends on the expected traffic in the considered type of environment, not on the environment itself. Here, the suburban city environment is chosen as the larger cities in Belgium are considered to be suburban.

For the weekend, the fluctuations in power consumption are small as shown in Table 4.1 because the difference between the number of active users at night and during the day is smaller than for weekdays. For example, during the weekend offices are closed and less people are coming to town. Therefore, only one average load factor F is determined for the weekend. The average power consumption for the weekend is 1031 W per hour (excluding load independent equipment), which corresponds with F equal to 0.95. This F value is of course obtained by comparing the average power consumption for the weekend to the maximum power consumption of the measurements (i.e., 1087 W at 10 a.m. to 11 a.m. for a weekday).

Note that variations in traffic are not always followed by similar variations in energy consumption as already concluded by [2, 4].

4.3.3 Microcell base station

For the microcell base station, the same measurement procedure as described above for the macrocell base station is used. The microcell base station was located outdoor in a street in the city centre of Ghent, Belgium. During these measurements, 469 919 samples were obtained. Fig. 4.2 illustrates the power consumption (in Watt) as a function of time. Although the power consumption fluctuates again over time, the difference in power consumption during day and night, as noticed by the macrocell base station, is not present for the microcell base station. This is probably due to the fact that there is less traffic on the microcell base station compared to the macrocell base station.

Based on the data shown in Fig. 4.2, the average power consumption per hour for weekdays and for the weekend is calculated. These averages are presented in Table 4.1. The measured equipment consumes between 214 W and 232 W. Determining the power consumption with our model (Eq. (4.4), $F(t)$ = 1, P_{Tx} = 33 dBm, including load independent equipment) and the data from Table 2.1 results in a power consumption of 377 W. Excluding the power consumption of the rectifiers, the microwave link and the air conditioning results in a power consumption of 217 W which agrees again excellent (a standard deviation of 1.4%) with the range of power consumptions in Table 4.1. The power consumption obtained with our model corresponds with the average power consumption for weekdays during the following hours: between 5 a.m. and 6 a.m., 9 a.m. and 10 a.m., 12 p.m. and 1 p.m., 2 p.m. and 3 p.m., 8 p.m. and 9 p.m., and 10 p.m. and 11 p.m. This also validates our model. The load factor $F(t)$ for the time between 8 a.m. and 9 a.m. (t = 8) is set to be 1 as this is the time interval with the highest power consumption.

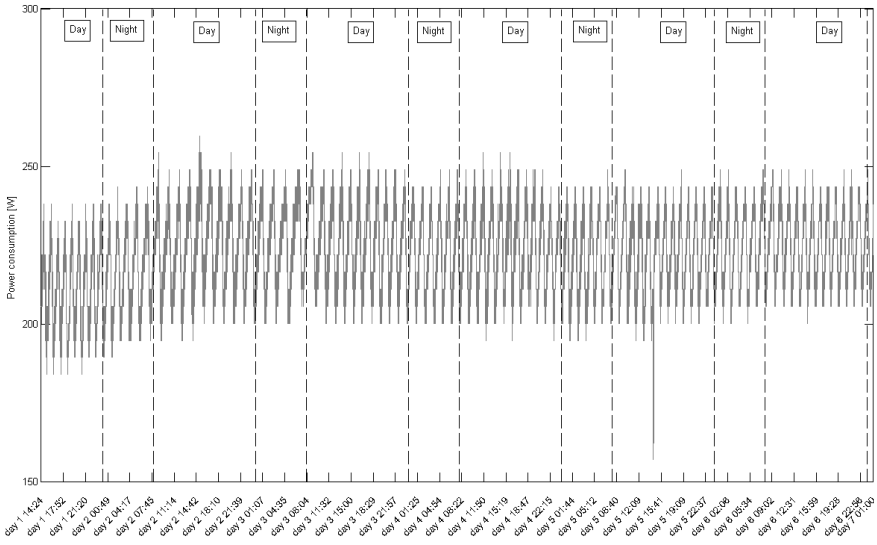

Figure 4.2: Evolution of the power consumption in time (Day 1-5 weekdays, day 6 weekend day) for a microcell base station.

The load factor for the other hours of the day can be found in Table 4.1.

For the weekend, the fluctuations in power consumption are small as shown in Table 4.1. Therefore, again only one average load factor F is determined for these hours. The average power consumption for the weekend is 225 W which corresponds with F equals to 0.98. This F value is again obtained by comparing the average power consumption for the weekend to the maximum power consumption of the measurements (i.e., 229 W at 8 a.m. to 9 a.m. for a weekday).

4.4 Relating power consumption and the number of voice and data calls

In this section, a model for the load factor $F(t)$ of the macrocell base station is determined based on the number of performed voice calls $V(t)$ and data connections $D(t)$ for a time stamp t.

4.4.1 Processing the measurement data

Based on the data from the measurements, a model for the load factor $F(t)$ is determined. The obtained power consumption values are averaged over one hour. This gives us 144 (= 6 days x 24 hours) observations for the power consumption i.e., for each hour of the measurement period one value. This will be denoted as

$P_{avg}(t)$ with t = 0 .. 143. This averaging is necessary as the power consumption will be related to the number of voice calls and data connections. The data about this number of voice calls and data connections is provided per hour by the operator.

To relate the three parameters power consumption, number of voice calls, and data connections, we normalize each parameter, by using the approach proposed in [15], as we are more interested in the relative values than the absolute ones. The normalized power consumption corresponds with the factor $F(t)$ and is obtained as follows for time stamp t:

$$F(t) = \frac{P_{avg}(t) - P_{min}}{P_{max} - P_{min}} \tag{4.9}$$

with $P_{avg}(t)$ the average power consumption for time stamp t (= 0..143), P_{min} the minimum value determined over the 144 observations of the power consumption, and P_{max} the maximum value determined over the 144 observations of the power consumption. $F(t)$ is dimensionless and yields values between 0 and 1.

Fig. 4.3 shows $F(t)$ during two of the measurement days (t = 0..47) for the considered HSPA macrocell base station. From 6 a.m. on, $F(t)$ increases significantly as during the day more people make phone calls than during the night. A higher value of $F(t)$ will result in a higher power consumption (Eq. (4.1)). In the evening, the load factor $F(t)$ decreases again. Around 7 p.m., a small peak of demand can be noted. Similar results are found for the other measurement days.

As mentioned above, also the number of voice calls and the number of data connections is normalized. The same procedure as for the power consumption is followed:

$$V(t) = \frac{V_{avg}(t) - V_{min}}{V_{max} - V_{min}} \tag{4.10}$$

$$D(t) = \frac{D_{avg}(t) - D_{min}}{D_{max} - D_{min}} \tag{4.11}$$

with $V(t)$ the normalized number of voice calls for time stamp t (= 0..143), $V_{avg}(t)$ the number of voice calls for time stamp t (= 0..143), V_{min} the minimum value determined over the 144 observations of the number of voice calls, and V_{max} the maximum value determined over the 144 observations of the number of voice calls, $D(t)$ the normalized number of data connections for time stamp t (= 0..143), $D_{avg}(t)$ the number of data connections for time stamp t (= 0..143), D_{min} the minimum value determined over the 144 observations of the number of data connections, and D_{max} the maximum value determined over the 144 observations of the number of data connections. $V(t)$ and $D(t)$ are, just as $F(t)$, dimensionless and yield values between 0 and 1.

Fig. 4.3 compares V and D with F for two measurement days of the considered HSPA macrocell base station. A similar trend as for F can be noticed. The number

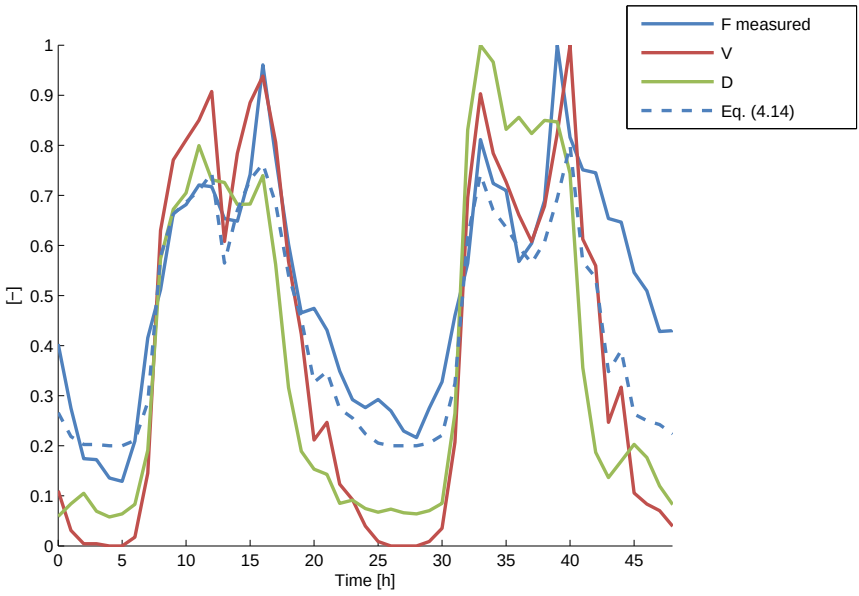

Figure 4.3: Comparison of F, V, and D as a function of time t during 48h for a HSPA macrocell base station (suburban environment, Belgium).

of voice and data calls are also higher during daytime. F and V and D will be correlated and modeled in the next section.

4.4.2 Determining a model for the load factor F

Based on the results shown in Fig. 4.3, a model for the load factor F is now determined by using linear regression. The dependent variable is F, while the two independent variables are V and D. The following formula is then obtained for F for a certain time stamp t:

$$F(t) = x \cdot V(t) + y \cdot D(t) + z \cdot V(t) \cdot D(t) + c \tag{4.12}$$

As y and z are not significantly different from zero according to t-tests (p-value = 0.7128 and 0.5044, respectively), Eq. (4.12) can be adapted to:

$$\begin{aligned} F(t) &= x \cdot V(t) + c & (4.13)\\ &= 0.6 \cdot V(t) + 0.2 & (4.14) \end{aligned}$$

with x = 0.6 and c = 0.2. The results of this model are shown in Fig. 4.3 as a function of the time and show very good agreement with the measured data.

As can be seen from the form of Eq. (4.14), the base station's power consumption depends linearly on V. In [2, 3], a similar power consumption model is proposed based on measurements of a GSM and UMTS macrocell base station. Both studies also obtained a linear relation between the traffic and the power consumption validating our model. Note that when V is equal to 0, the power consumption does not decrease to 0 W because the load-independent components (such as, the rectifier, the air conditioning, and the microwave link) still consume power and also the load-dependent components keep consuming a small amount of power (F = 0.2 for V = 0).

Note also that the parameters (x, y, z, c) depend on the performance of the components. A component of another brand or another model number can result in different values for these parameters. The values of Table 2.1 are average values obtained from data sheets from various vendors. The base station's power consumption calculated using these values agrees excellently (standard deviation of 2%) with the measured ones, here presented.

4.5 Introduction of sleep modes and cell zooming/ breathing

A promising technique to reduce power consumption in wireless access networks is the introduction of sleep modes where base stations are becoming inactive when no or little activity takes place in their coverage cells [4–7]. The base station is not completely switched off during the sleep mode as it keeps monitoring and if necessary (e.g., when a call has to be made) it can become active again. Another technique is called cell zooming or cell breathing [8] which adaptively adjust the cell size according to (amongst others) the traffic load. In this section, an algorithm is proposed combining these two techniques for power consumption reduction in a wireless access network.

The algorithm is explained based on Fig. 4.4. Fig. 4.4(a) shows the initial situation i.e., the always-on network as obtained from the GRAND tool (see Chapter 3). For each base station in the network, it is checked if it is possible to put it into sleep. However, when a base station is put into sleep, the coverage of this base station should be guaranteed by other base station(s), which are awake. To investigate if this is possible for a certain base station, here called BS_{test}, the neighboring base stations are determined as shown in Fig. 4.4(a). The range of the neighboring base stations will then be increased by adding 1 dBm to the antenna's input power of the neighboring base stations which is shown by the arrows in Fig. 4.4(b). This step is repeated until the the area of BS_{test} is covered or until the maximum input power of the antenna is reached. If the area covered by BS_{test} can be covered by extending the range of neighboring base station(s), BS_{test} will be put to sleep when the sleep threshold is met as shown in Fig. 4.4(c). The sleep threshold cor-

responds with a certain load. If the actual load on the base station is below this predefined load (i.e., the sleep threshold), it is possible for the base station to sleep. The dotted line in Fig. 4.4(c) indicates the 'old' coverage of the neighboring base stations. The traffic load of BS_{test} will be divided over the neighboring base stations. When the sleep threshold is not met, the final configuration is as shown in Fig. 4.4(a). When the sleep threshold is met, the final configuration is as shown in Fig. 4.4(c).

As discussed above, the algorithm consists of a number of steps. The different steps of the algorithm will now be discussed in detail based on the flow graph in Fig. 4.5.

First, a network is designed for a predefined area by using the GRAND tool (see Chapter 3). This tool can be used to design greenfield networks, but also enables optimizing existing networks. The input power of the (macrocell) base station antenna is limited in this first step to e.g., a certain realistic input power minus x dBm. In this way, it is possible to let cells zoom by adjusting the input power of the antenna.

Secondly, the algorithm for introduction of sleep modes and cell zooming is applied (Fig. 4.5). The different steps are now explained. For every active base station BS_i (i = 1,..,M with M the total number of base stations) in the network resulting from the GRAND tool, it is determined whether it is possible to put this base station to sleep (Fig. 4.5 Step 1). This is done by selecting the 4 closest active base stations $(BS_j)_i$ (j = 1,..,4 with j = 1 the base station the closest to BS_i and j = 4 the base station the furthest from BS_i) (Fig. 4.5 Step 2). Note that the number of closest base stations can be chosen freely. Here, 4 was chosen as this gave a good balance between performance and the computational time of the algorithm.

In the next steps, the input power of the antenna of one or more neighbouring base stations is increased. This is done as follows:

- In a first step, the input power of the antenna of one base station from the set $(BS_j)_i)$ is increased with 1 dBm i.e., applying cell zooming (Fig. 4.5 Step 3a). This will expand the range of the cell. Note that it is important to increase the input power sequential because each dBm added to the input power results in a higher power consumption (Chapter 2). This increase can be performed until the maximum input power is reached or until a solution is found (Fig. 4.5 Step 3b). A solution is found when the cell of $(BS_j)_i$ covers the cell of BS_i. If a solution is found, BS_i can be put into sleep mode and the calculation for BS_i is stopped (Fig. 4.5 Step 7). If no solution is found (Fig. 4.5 Step 3b), Step 3a of Fig. 4.5 for the other base stations from the set $(BS_j)_i$.

- If no solution can be found by expanding the range of only one base station

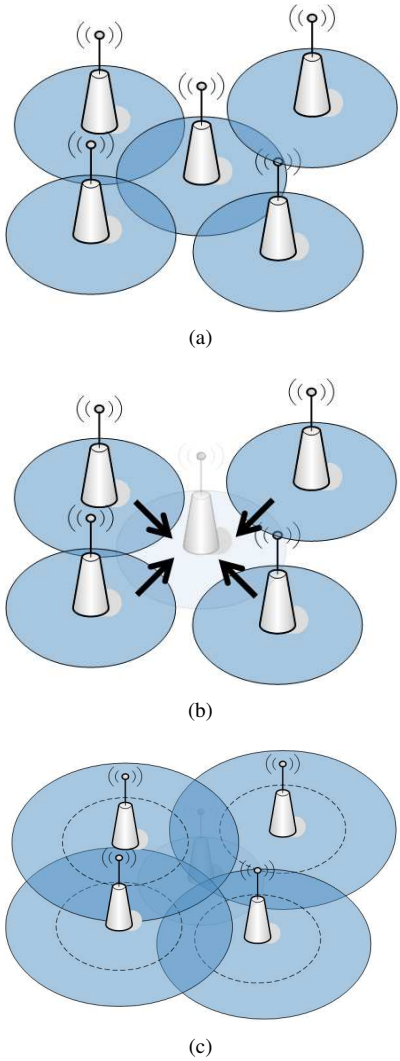

Figure 4.4: Overview of the proposed algorithm for introducing sleep modes and cell zooming: always-on configuration (a), checking if a base station can sleep (b), final configuration with base station asleep (c).

from the set $(BS_j)_i$, check if there is solution when expanding the range of *two* base stations from $(BS_j)_i$ (Fig. 4.5 Step 4a). If a solution is found (Fig. 4.5 Step 4b), stop the calculation for BS_i (Fig. 4.5 Step 7).

- If all combinations with two base stations from set $(BS_j)_i$ are checked and no solution is found (Fig. 4.5 Step 4b), check if there is a solution when

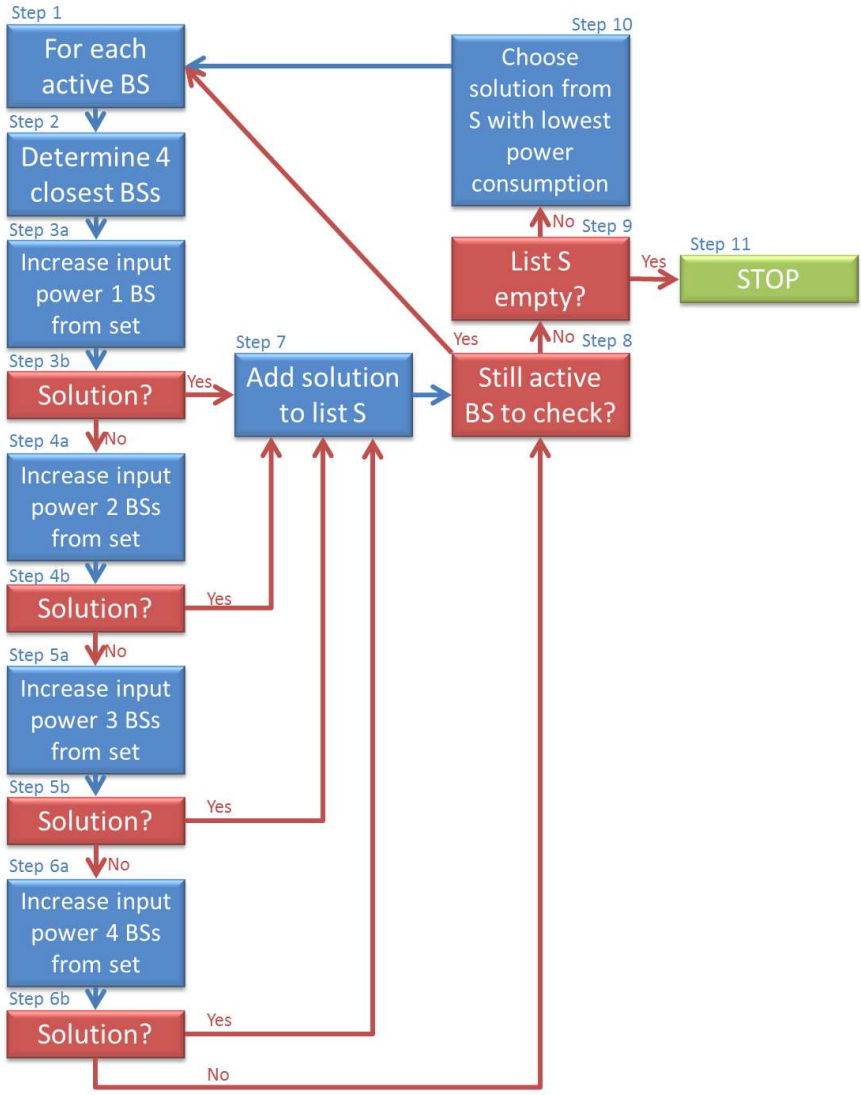

Figure 4.5: Flow diagram of the algorithm for introducing sleep modes and cell zooming in a network.

expanding the range of *three* base stations from $(BS_j)_i$ (Fig. 4.5 Step 5a). If a solution is found (Fig. 4.5 Step 5b), stop the calculation for BS_i (Fig. 4.5 Step 7).

- If all combinations with three base stations from set $(BS_j)_i$ are checked and no solution is found (Fig. 4.5 Step 5), check if there is a solution when

expanding the range of the *four* base stations from $(BS_j)_i$ (Fig. 4.5 Step 6a). If a solution is found (Fig. 4.5 Step 6b), stop the calculation for BS_i (Fig. 4.5 Step 7).

- If no solution can be found by expanding the range of the four base stations from the set $(BS_j)_i$, it is not possible to put the BS into sleep.

When the investigation is stopped for BS_i, we check if there are other active base stations in the network which have not been investigated yet (Fig. 4.5 Step 8). If so, the above described procedure (Fig. 4.5 Step 1-7) is repeated for these base stations. If not, we check if there was a solution for any of the active base stations in the network (Fig. 4.5 Step 9). If so, the solution with the lowest power consumption is determined and the corresponding base station BS_i is put into sleep (Fig. 4.5 Step 10) and the input power of the antenna of the defined base stations is increased appropriately. To determine the power consumption of a solution, the traffic load of the base station put into sleep mode is equally divided over the base stations that need to be expanded. This is a very simple approach, but it is expected that more complex approaches will not change the results as the power consumption depends linearly on the number of voice calls V (see Eq. (4.14)). The whole procedure is repeated (Fig. 4.5 Step 1-10) until it is not possible anymore to put base stations into sleep mode (Fig. 4.5 Step 9 & 11).

Note that the order in which the base stations are considered in the algorithm of Fig. 4.5 has an impact on the solution. It is of course not possible to investigate all different orders, but one way to deal with this, is to have multiple simulations.

4.6 Modeling results

4.6.1 Evolution of the power consumption during the day

In this section, it is investigated how the power consumption of a macrocell and a microcell base station fluctuates during a weekday and a weekend day. Fig. 4.6(a) presents the power consumption of a HSPA macrocell and Fig. 4.6(b) the power consumption of a HSPA microcell base station as a function of the time of the day for both a weekday and a weekend. To create Figs. 4.6(a) and 4.6(b), Eqs. (2.1) and (2.7) are used with the assumptions of Table 2.1. For F, the values of Table 4.1 are used for weekdays and F is assumed to be 0.95 and 0.98 for the macrocell and microcell base station respectively as described in Section 4.3.

For a weekday, the lowest power consumption (i.e., 1609 W) for a macrocell base station is obtained between 3 a.m. and 5 a.m. The highest power consumption (i.e., 1673 W) is found between 10 a.m. and 11 a.m. For the microcell base station, the highest power consumption (i.e., 377 W) is reached between 8 a.m.

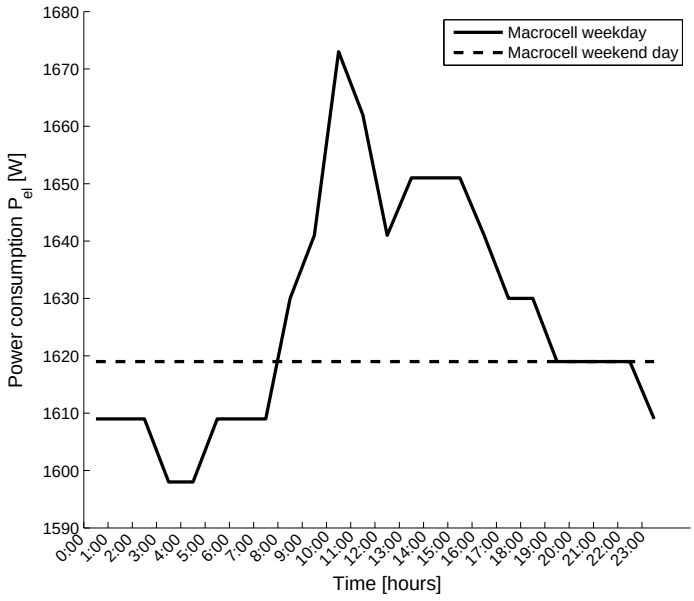

(a)

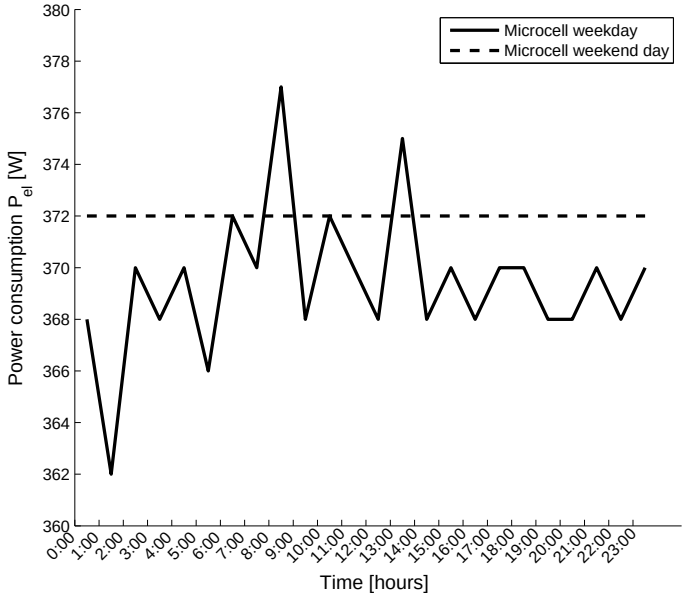

(b)

Figure 4.6: Evolution of the power consumption during a weekday and the weekend for a HSPA macrocell (a) and microcell (b) base station.

and 9 a.m. and the lowest power consumption (i.e., 362 W) between 1 a.m. and 2 a.m. However, the course of the power consumption for a microcell base station varies more than for the macrocell base station. This is due to the fact that when there is too much traffic on one of the neighbouring macrocell base stations some of the traffic is diverted to the microcell base station. In general, the fluctuations in power consumption are limited for the microcell base station compared to the macrocell base station.

4.6.2 Greenfield deployment

The power savings in a network by introducing sleep modes and cell zooming are now determined for a greenfield deployment. For this investigation, a new network is developed for the city center of Ghent, Belgium. This target area is shown in Fig. 4.7(a) and has a surface of approximately 13.3 km^2. A coverage requirement of 90% of the target area is here assumed. Furthermore, LTE is chosen as wireless technology (frequency of 2.6 GHz) and a physical bit rate of approximately 5 Mbps (in a 5 MHz channel) is provided. LTE is considered here as this technology will mostly be introduced in new network deployments. It is assumed that the (voice) traffic behaviour will not change significantly when a new technology is introduced in the network. Comparing the shape of the daily evolution of the HSPA traffic with the shape of the daily evolution of GSM as shown in [15], delivers no significant differences. Therefore, the model from the previous sections is also used here. Furthermore, it is assumed that the traffic is uniformly distributed over the area. Each base station will thus have the same traffic load at the same time when sleep modes are not activated.

The network resulting from the GRAND tool (without activation of sleep modes and cell zooming) is shown in Fig. 4.7(b). It consists of 80 macrocell base stations with a total energy consumption of 1566 kWh per day.

Fig. 4.7(c) shows the resulting network when sleep modes and cell zooming are activated. 28 base stations can be put into sleep when the sleeping conditions are met. As it is assumed that each base station has the same traffic pattern, these 28 base stations will be put into sleep mode at the same time. However, the coverage that is lost should be provided by (an)other base station(s). The algorithm shown in Fig. 4.5 determines for which base stations this is possible and for which not. The sleep threshold will be a very important parameter in determining the actual power savings in the network as is now discussed.

Fig. 4.8 shows the power savings that can be achieved by introducing sleep modes and cell zooming in the network (100% corresponds with no power consumption reduction at all). Here, we vary the sleep threshold from 0.0 to 0.3 in steps of 0.05. The daily power consumption of the network as a function of the sleep threshold is shown in Fig. 4.8. When the sleep threshold is 0.1, the network

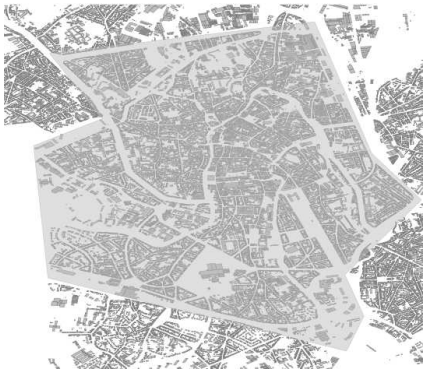

(a)

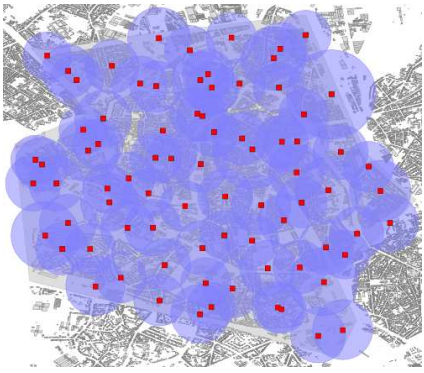

(b)

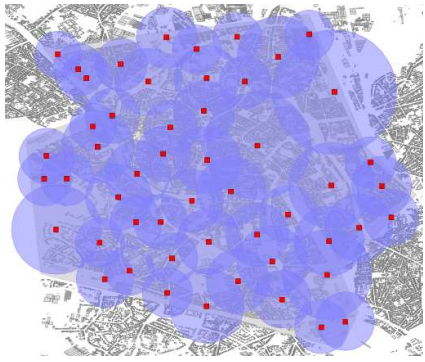

(c)

Figure 4.7: The target area (a), the greenfield network (b) for the target area resulting from the GRAND tool, and the network (c) when sleep modes and cell zooming are applied.

consumes 1432.8 kWh per day, which is 8.6% lower than without sleep modes and cell zooming. If the sleep threshold is 0.2, the network only consumes 1369.9 kWh per day which corresponds with a power saving of 12.6%. If the sleep threshold is 0.3, the network only consumes 1297.3 kWh per day which corresponds with a power saving of 13.5%. A higher power saving is achieved when a higher threshold is applied because the base stations can sleep more hours per day than for a lower threshold (Section 4.6.1). However, for a sleep threshold of 0.3, the load on the neighbouring base stations is becoming very high (load of 0.9). Therefore, it is recommended to use a sleep threshold lower than 0.3. As can be seen in Fig. 4.8, the additional saving in power consumption when increasing the sleep threshold becomes smaller and smaller from a sleep threshold of 0.15. This is due to the fact that from this threshold on it is not possible to put a lot of extra base stations

into sleep mode, as the load on the surrounding base stations becomes too high. Furthermore, remark that it is assumed that a base station in sleep mode consumes no power (both the load dependent and the load independent power consumption equal 0 W). This might however be too optimistic, but it allows us to determine the upper bounds of the power savings that can be achieved. Fig. 4.9 shows the influence of this assumption on our results. The power consumption for the sleep mode is varied between 0 W and 600 W (which corresponds with the base station's power consumption when there is no traffic (Table 2.1)) and a sleep threshold of 0.1 is assumed. The percentages show the relative daily power consumption with respect to the daily power consumption of the network without sleep modes. A linear relation between the power consumption of the sleep mode and the daily power consumption of the network is found. As mentioned above, 28 base stations can be put into sleep during 8 hours of the day (sleep threshold = 0.1). If a power consumption of 100 W is assumed for the sleep mode, this results in an extra power consumption of 22.4 kWh. The higher the power consumption during sleep mode, the lower the obtained power savings. When a base station consumes 600 W during sleep modes, the network's power consumption is the same as for the network without sleep modes.

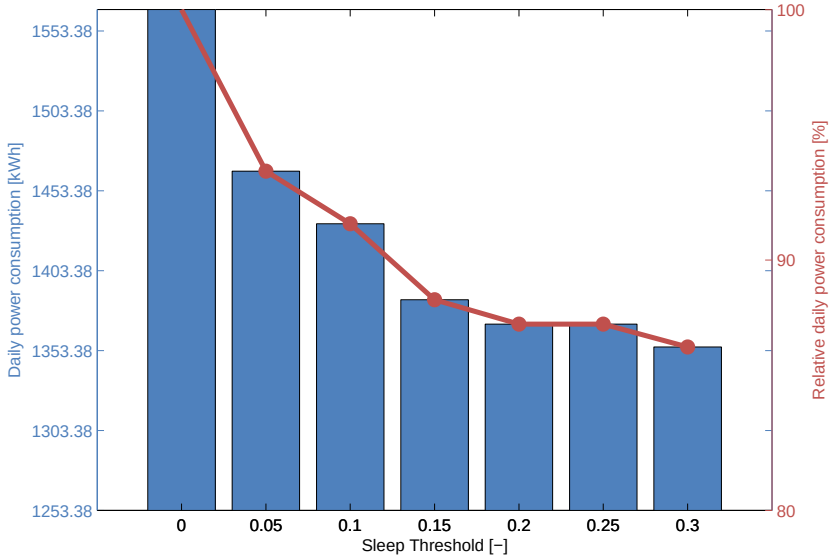

Figure 4.8: Power savings by introducing sleep modes and cell zooming in the network for varying sleep thresholds from 0 to 0.3.

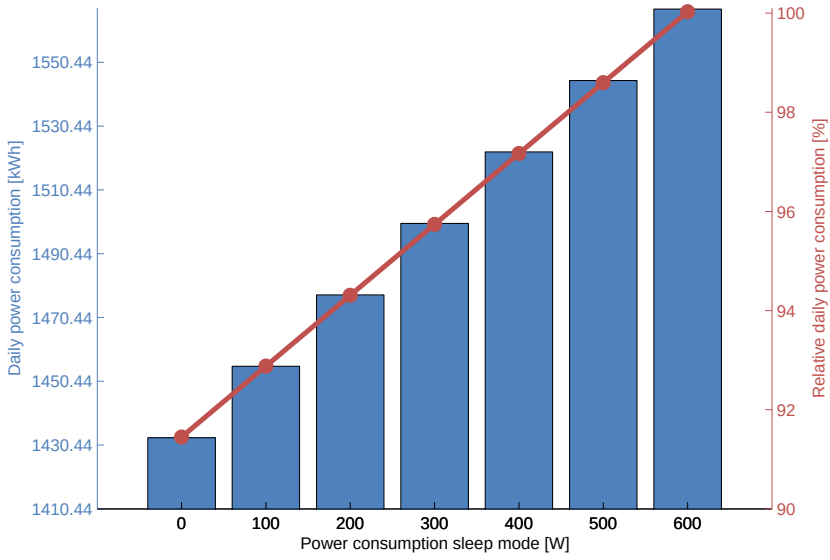

Figure 4.9: Influence of the power consumption during sleep mode on daily power consumption of the network (sleep threshold = 0.1).

Fig. 4.10 shows the evolution of the network's power consumption during a day with and without sleep modes. The power consumption during daytime (from 8 a.m. till 7 p.m.) is similar for all the investigated cases (i.e., no sleep modes and sleep modes with the considered sleep thresholds) due to the fact that for this time period V is higher than the sleep thresholds considered. At night (1 a.m. - 7 a.m.) and 11 p.m., 28 of the 80 base stations can be put into sleep (V is lower than all the sleep thresholds considered). For the other hours of the day, it depends on the sleep threshold if the 28 base stations can be put into sleep.

4.6.3 Optimizing a network

For this investigation, Brussels Capital Region, Belgium, is considered with a surface of approximately 149 km^2. Data about the base station sites is provided by Belgian Institute for Postal services and Telecommunications (BIPT). Fig. 4.11(a) shows all the 858 available base station sites in Brussels. Within this region, four different operator networks can be identified. Fig. 4.11(a) shows thus all the base stations of the four operators. Here, only one operator network (289 base stations, HSPA) is considered. All the possible locations are shown in Fig. 4.11(b) and are used as an input for the GRAND tool (Section 3.1). The GRAND tool will adapt

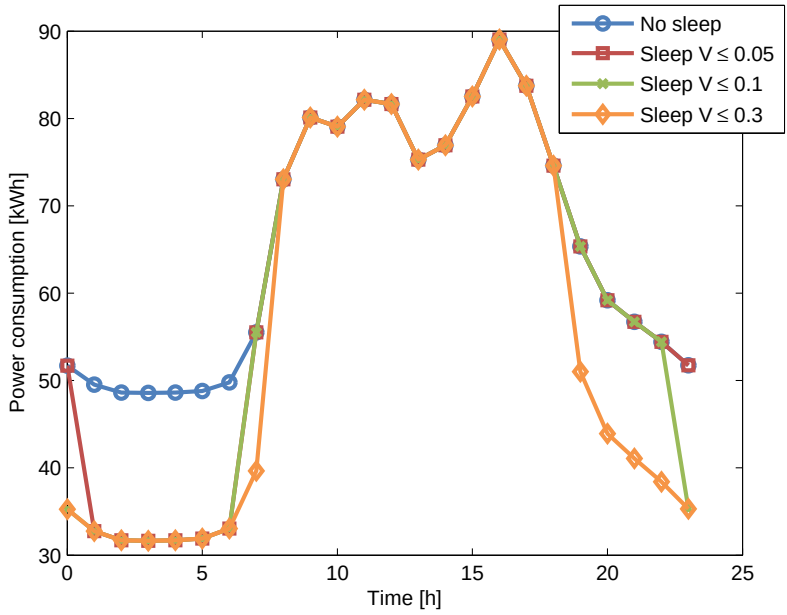

Figure 4.10: The evolution of power consumption of the network through time when sleep modes are activated and deactivated.

the operator network by adding base stations, changing the locations of base stations, or changing settings such as the input power of the antenna. The set of base stations that can be added to the network corresponds with the set of all the available base stations in the Brussels Capital Region (Fig. 4.11(a)). Furthermore, it is assumed that the traffic is uniformly distributed over the considered area for both the existing and the optimized network. The model from the previous sections will be used in this study, which is a realistic approach as only the HSPA macrocell base stations are considered for the existing network.

Fig. 4.11(c) shows the network resulting from the GRAND tool with deactivation of the sleep modes and cell zooming. This network uses only 188 base stations and has thus a daily power consumption that is 33.4% less than the power consumption of the original network (4733.4 kWh versus 7108.0 kWh) as shown in Table 4.2. Note that the optimised network with its lower power consumption still has a significant higher coverage than the original network (95.0% versus 88.7%, Table 4.2). It is thus concluded that it is useful to place the base stations properly to save power.

Fig. 4.11(d) shows the optimised network when sleep modes (sleep threshold

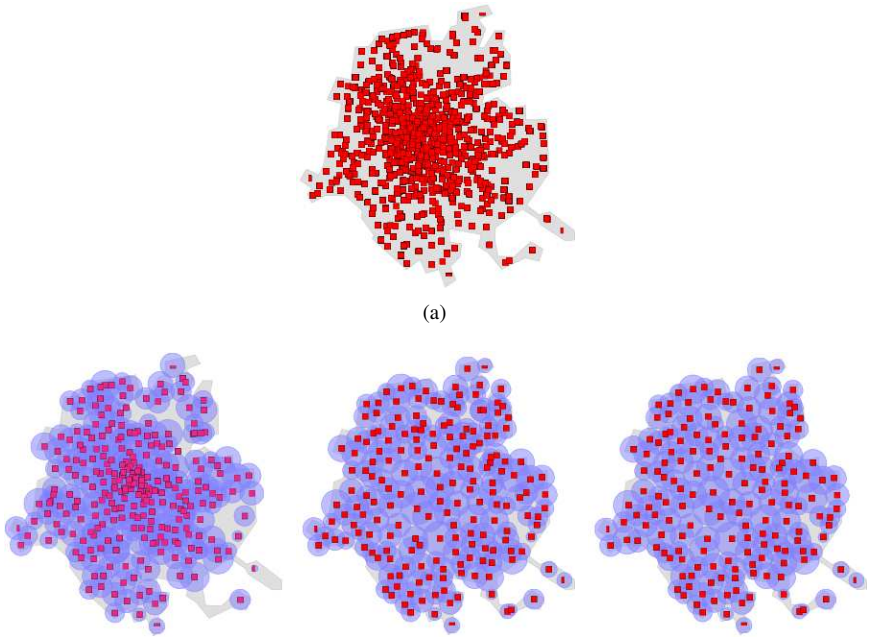

(a)

(b) (c) (d)

Figure 4.11: Brussels Capital Region: available sites (a), original operator network (b), network optimised by the GRAND tool (c), network with sleep modes and cell zooming activated.

	Original	**Optimised no sleep**	**Optimised sleep**
No. base stations	289	188	170
Coverage	88.7%	95.0%	95.0%
Daily power consumption	7108.0 kWh	4733.4 kWh	4641.4 kWh

Table 4.2: Results for the optimisation of an operator network in the Brussels Caption Region.

of 0.1) and cell zooming are activated. 18 base stations can sleep when the traffic is below the sleep threshold of 0.1 (Table 4.2). This results in a daily power consumption of 4641.4 kWh (Table 4.2) which is 1.9% lower than the optimised network without activating sleep modes and 33.4% lower than the original operator network. Again it is concluded that it is recommended to add sleep modes and cell zooming into the networks, although the savings are limited. Today's operator networks are currently thus not optimised towards power consumption. Remark, that introducing sleep modes and cell zooming in the network also needs extra

management in the network.

For comparison, it is also determined how much power can be saved when introducing sleep modes in the original operator network without first optimizing the network. Assuming a sleep threshold of 0.1, this results in a daily power consumption of 6526.5 kWh (versus 7108.0 kWh for the original network). A reduction of about 8% is thus obtained.

4.7 Conclusion

In this chapter, a power consumption model as a function of the traffic load and temporal variations is designed for a macrocell and microcell base station based on measurements on an actual base station. This model allows us to investigate the evolution of the power consumption during the day and to develop energy-efficient wireless access networks by combining the GRAND tool, which develops an always-on network with a minimal power consumption for a predefined area, and an algorithm that introduces power reducing techniques in the network such as sleep modes and cell zooming.

Two cases are investigated. In the first case, a completely new LTE network is developed for the city center of Ghent. By introducing sleep modes and cell zooming in this network, the power consumption can be reduced up to 13.5% (depending on the used sleep threshold) compared to the network without sleep modes and cell zooming. In the second case, an existing operator network for Brussels Capital Region is optimised. Applying GRAND on this network results in a reduction of 33.4% for the daily power consumption. The introduction of sleep modes and cell zooming causes an additional saving of 1.9% compared to the optimised network. A careful selection of the base station locations can already result in a significant saving (33.4% as shown by the results from the GRAND tool). In current networks, this can be done by site sharing. For future networks, it is recommended that sleep modes and cell zooming are supported. Also for existing networks (without optimizing the base station locations), introducing sleep modes and cell zooming can result in a reduction of 8% of the daily power consumption (depending on the considered threshold). In general, we conclude that a careful selection of the base station locations results in a significant power consumption saving. This saving can be extended by introducing sleep modes and cell zooming in the network.

References

[1] O. Arnold, F. Richter, G. Fettweis, and O. Blume. *Power consumption modeling of different base station types in heterogeneous cellular networks*. In Future Network and Mobile Summit, pages 1–8, Florence, Italy, 2010.

[2] C. Peng, S-B. Lee, S. Lu, H. Luo, and H. Li. *Traffic-driven power savings in operational 3G cellular networks*. In Proceedings of the 17th Annual Conference on Mobile Computing and Networking (MobiCom), Las Vegas, Nevada, 2011.

[3] J. Lorincz, T. Garma, and G. Petrovic. *Measurements and modelling of base station power consumption under real traffic loads*. Sensors, 12(4):4281–4310, 2012.

[4] G. Micallef, P. Mogensen, and H-O. Scheck. *Cell size breathing and possibilities to introduce cell sleep mode*. In 16th European Wireless Conference, pages 111–115, Lucca, Italy, 2010.

[5] L. Correia, D. Zeller, O. Blume, D. Ferling, Y. Jading, I. Gódor, G. Auer, and L. Van der Perre. *Challenges and enabling technologies for energy aware mobile radio networks*. IEEE Communications Magazine, 48(11):66–72, 2010.

[6] L. Saker, SE. Elayoubi, and T. Chahed. *Minimizing energy consumption via sleep mode in green base station*. In IEEE Wireless Communications and Networking Conference (WCNC), pages 1–6, Sydney, Australia, 2010.

[7] E. Oh, B. Krishnamachari, X. Liu, and Z. Niu. *Toward dynamic energy-efficient operation of cellular network infrastructure*. IEEE Communications Magazine, 49(6):56–61, 2011.

[8] Z. Niu, Y. Wu, J. Gong, and Z. Yang. *Cell zooming for cost-efficient green cellular networks*. IEEE Communications Magazine, 48(11):74–79, 2011.

[9] L. Saker and SE. Elayoubi. *Sleep mode implementation issues in green base stations*. In 21st Annual IEEE International Symposium on Personal, Indoor and Mobile Radio Communications (PIMRC), pages 1681–1686, Istanbul, Turkey, 2010.

[10] D. Tsilimantos, J.-M. Gorce, and E. Altman. *Stochastic Analysis of Energy Savings with Sleep Mode in OFDMA Wireless Networks*. In IEEE INFOCOM - 32nd International Conference on Computer Communications, pages 1097–1105, Turin, Italy, 2013.

[11] L. Suarez, L. Nuaymi, and J.-M. Bonnin. *Analysis of the overall energy savings achieved by green cell-breathing mechanisms*. In Sustainable Internet and ICT for Sustainability (SustainIT), pages 1–6, Pisa, Italy, 2012.

[12] L. Suarez, L. Nuaymi, and J.-M. Bonnin. *Analysis of a Green-Cell Breathing Technique in a hybrid access network environment*. In IFIP Wireless Days, pages 1–6, Valencia, Spain, 2013.

[13] Y. Su, P. Yu, Z. Jiang, W. Li, and X. Qiu. *A Distributed Energy Saving Mechanism in Wireless Access Network*. In 15th Asia-Pacific Network Operations and Management Symposium (APNOMS), pages 1–3, Hiroshima, Japan, 2013.

[14] W. Joseph, L. Verloock, E. Tanghe, and L. Martens. *In-situ measurement procedures for temporal RF electromagnetic field exposure of the general public*. Health Physics, 96(5):529–542, 2009.

[15] W. Joseph and L. Verloock. *Influence of mobile phone traffic on base station exposure of the general public*. Health Physics, 99(5):631–638, 2010.

5

Reducing the power consumption in LTE and LTE-Advanced wireless access networks using a capacity-based deployment tool

The last few years have seen a tremendous increase in the number of mobile users, with global mobile phone penetration increasing from 20 percent in 2003 to 67 percent in 2009 [1]. Mobile devices have also become more powerful, allowing users to not only make phone calls on the go, but also to check their email, streaming music and video, video conferencing, surfing the web, visiting social networks, etc. This is of course only possible if the network is capable of supporting this amount of traffic. To this end, new wireless technologies such as LTE(-Advanced) have been introduced.

In this chapter, we investigate how energy-efficient LTE-Advanced (Release 10) access networks can be designed to improve energy efficiency compared to LTE (Release 8/9) networks. LTE-Advanced introduces three additional functionalities that can influence the energy efficiency [2]:

- Carrier Aggregation (CA) whereby the bit rate is increased by letting the base station transmit multiple LTE carriers (here also called component carrier), each with a bandwidth up to 20 MHz.

- heterogeneous networks which consists in LTE-based networks typically of

a two-layered network with macrocell (or eNodeB) and femtocell (or home-eNodeB) base stations. Although LTE already supports this functionality, LTE-Advanced improves the handling of interference between the different cells.

- extended support for MIMO.

The influence of the three above described features on the energy efficiency of a single base station and the network is here investigated. For the study on the network level, a capacity-based deployment tool is proposed. The purpose of this algorithm is to *respond* to the instantaneous *bit rate request* of the users in a geometrical area as *energy-efficiently* as possible rather than providing coverage to a certain area as in the coverage-based algorithm of Chapter 3. The power consumption models of Chapter 2 are used to evaluate the power consumption of the network.

Although some researchers have studied the energy efficiency of heterogeneous LTE and LTE-Advanced networks [3–5], to the best of our knowledge, no one has compared the energy efficiency of LTE and LTE-Advanced or the effect of LTE-Advanced's main functionalities on energy efficiency.

5.1 Developing energy-efficient networks by a capacity-based deployment tool

In this section, the capacity-based deployment tool is discussed, which allows to develop future wireless access networks optimized towards power consumption and that respond to the instantaneous bit rate requirement of the users active in the considered area.

5.1.1 Generating traffic loads

As mentioned above, the proposed deployment tool is capacity-based, meaning that the network responds to the instantaneous bit rate request of the user active in the considered area. Therefore, it is important to have realistic data about the traffic generated by the users active in the considered area. This data will be delivered in the form of traffic files to the algorithm for developing the network described in the next section. A traffic file contains information about the number of active users, the location of each user, and the bit rate requested by each user for a certain time stamp. Fig. 5.1 shows the flow diagram for generating a traffic file.

First, the considered area for which the network has to be developed (Fig. 5.1 Input 1) is needed. Within this area, a number of users will be active. The *maximum number of users* determines the maximum number of users that are simul-

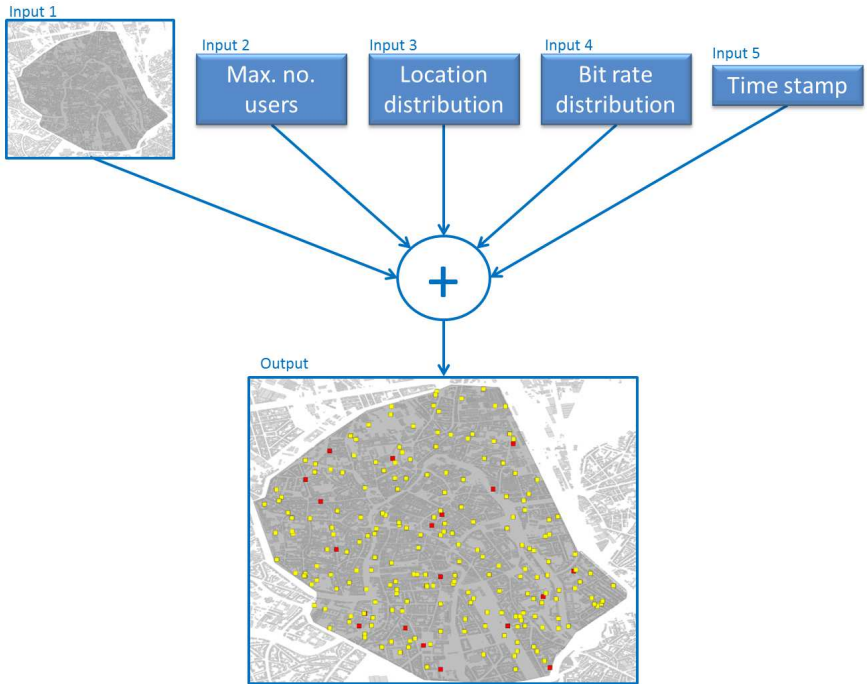

Figure 5.1: Schematic for generating realistic traffic (yellow squares in output = users requiring 64 kbps, pinks squares in output = users requiring 1 Mbps).

taneously active. This number will of course vary during the day. Therefore, it is also important to know for which time stamp during the day the traffic is generated (Fig. 5.1 Input 5). The function used here is based on traffic data received from a Belgian operator. Fig. 5.2 presents the variation of the maximum number of simultaneously active users during the day for the area shown in Fig. 5.1 (Input 2). These results are confirmed by [6, 7]. To determine the location of each user, a *location distribution* is used (Fig. 5.1 Input 3) for the considered area. Note that for another area e.g., an area with a mixture of suburban and rural parts, a different approach could be used as the user density in the suburban part will be higher than in the rural part. Finally, the bit rate of each user is defined by the *bit rate distribution* (Fig. 5.1 Input 4). A certain part of users requires 64 kbps to make a phone call, while the other part of the users requires 1 Mbps for transferring data. These bit rates are realistic values for the proposed applications in the current networks [1]. Depending on the considered time stamp during the day (Fig. 5.1 Input 5), the ratio of users requiring 64 kbps and users requiring 1 Mbps will vary. Note, that a different bit rate distribution can also be considered.

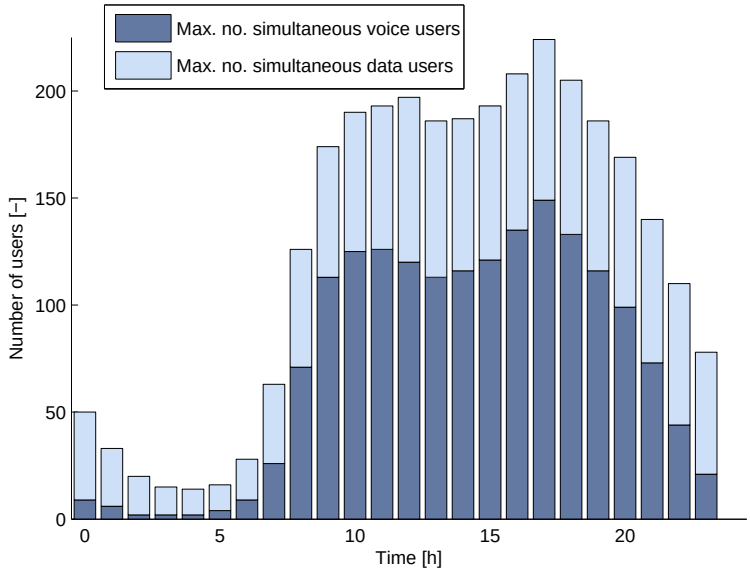

Figure 5.2: Example of the maximum number of simultaneously active users during the day for the area shown in Fig. 5.1 (Input 1 & Output).

When combining all the inputs described above, a traffic file can be generated. The block 'output' in Fig. 5.1 gives an example of the traffic generated for the time interval from 5 to 6 p.m. which is the busiest time interval during the day as shown in Fig. 5.2. The squares in Fig. 5.1 show the location of the users. A red square corresponds with a user requesting 64 kbps, while a yellow square corresponds with a user requiring 1 Mbps.

5.1.2 Optimizing towards power consumption

The different steps of the algorithm will be explained based on Fig. 5.3. The input is the generated data from the previous section, along with a shape file containing detailed 3D information about the buildings in the chosen environment (i.e., location, shape, height, etc.), a file with possible base station locations, and an xml file containing different parameters characterizing the wireless technology and the power consumption of the base station.

As mentioned above, different distributions are combined to generate the traffic data. Therefore, it is important to have multiple simulations in order to obtain a good estimation of the median value for the different output parameters. The following steps will thus be repeated n times, with n the total number of simulations. When a new simulation is started, we assume that all the base stations are asleep.

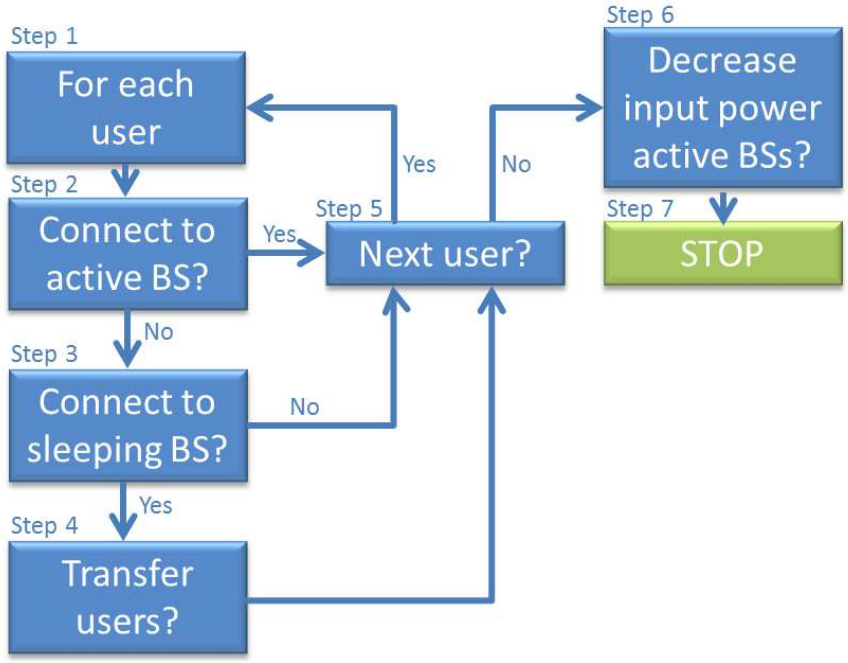

Figure 5.3: Flow diagram of the capacity-based algorithm for optimizing towards power consumption.

As our tool is capacity-based, we will try to connect each user active in the considered area to a certain base station (Fig. 5.3 Step 1). The next steps will thus be repeated m times, with m the number of users active in the considered area. When connecting a user to a base station, there are two options: a user can be connected to a base station that is already active (Fig. 5.3 Step 2) or we will need to wake up a base station that is currently sleeping (Fig. 5.3 Step 3). In terms of power consumption, it is more energy-efficient to connect a user to an active base station instead of waking a new one up. Increasing the antenna's input power results in an electric power increase up to 468 W (when increasing the antenna's input power from 1 dBm to 43 dBm for a SISO base station) while waking a base station up results in an additional electric power of 920 W which is a factor of approximately 2 higher (assuming that a base station consumes 45% of its power while in sleep mode as proposed in [8]). Therefore, this is first checked (Fig. 5.3 Step 2). We try to connect the user to the base station from which the user experiences the lowest path loss (which has also to be lower than the maximum allowable path loss to which a transmitted signal can be subjected while still having a sufficient signal quality at the receiver side to offer the bit rate requested by the user). If a base

station can not cover the user due to the path loss, we also check if increasing the input power of the antenna (if possible) can solve this. When a suitable base station is found, the user is connected to this base station. To calculate the path loss, we determine if we have a Line-of-Sight (LoS) or non-Line-of-Sight (nLoS) situation. Therefore, a straight line between the user and the considered base station is determined. By using the shape file of the environment, we know if this line crosses a building or not. If so, the WI nLoS propagation model is used, otherwise the WI LoS propagation model [9].

When the user can not be connected to an active base station, it is checked if we can wake a sleeping base station up (Fig. 5.3 Step 3). The same procedure is followed here: the user will be connected to the base station from which he/she experiences the lowest path loss (which is lower than the maximum allowable path loss) and that can support the bit rate requested by the user. Again, the optimal input power of the antenna is determined, so that the user is covered. When a suitable base station is found, the base station will be woken up and the user will be connected to this base station. In order to spread the load on the active base stations in the network, it is checked if users that are already covered by other base stations can be transferred to this new active base station (Fig. 5.3 Step 4). This can of course only be the case when the path loss experienced from this new base station is lower than the path loss experienced from the old base station and if the new base station can support the requested bit rate.

When the user can not be covered by any base station (active or by waking one up), it is not possible to serve this user.

If the procedure described above ends for the considered user, it is checked if there are still other users to cover (Fig. 5.3 Step 5). If so, Step 2 and if necessary Step 3 and 4 will be repeated. If not, a final check will be performed (Fig. 5.3 Step 6). For this final check, we analyze all active base stations and check if the input power of the antenna can be reduced. It is of course important that all users connected to a base station are still covered with the requested bit rate after decreasing the input power of the antenna. After this check, the development of the network for this simulation ends. When there are still simulations to be done, Steps 1 to 4 are repeated, otherwise, the calculation stops (Fig. 5.3 Step 7).

5.2 Influence on the power consumption of the individual base station

The influence of the three above mentioned features of LTE-Advanced on the power consumption and energy efficiency of a single base station is now investigated. The energy efficiency is here defined by Eq. (2.7). The values of the different link budget parameters are shown in Tables 2.2 and 2.4 for the macrocell and femtocell base station, respectively. Another important difference between

the macrocell and the femtocell base station is the maximum number of served users. The smallest unit to which user traffic can be allocated is Physical Resource Block (PRB), consisting of 12 carriers. For each bandwidth, we divide the number of carriers used by 12 to determine the number of PRBs. Futhermore, we assume that each PRB has a different user. For the macrocell base station, this results in a maximum of 18, 36, 75, 150, 225, and 300 users, for a respective bandwidth of 1.4, 3, 5, 10, 15, and 20 MHz. For a femtocell base station, the number of users is typically limited to 16 (independent of the bandwith) [10]. We use this information for the numerical investigation.

5.2.1 Carrier aggregation

In this section, it is investigated how the energy efficiency is influenced by adding carrier aggregation. When carrier aggregation is applied, multiple carriers are sent to the user to increase the bandwidth and thus the bit rate [2]. However, possible drawbacks of carrier aggregation are: the vulnerability to loss in the throughput, interference coordination, the incompatibility with user equipment, etc.

Fig. 5.4 shows the energy efficiency for some modulation schemes supported by LTE(-Advanced) for both macrocell and femtocell base stations in a 5 MHz channel. Note that the energy efficiencies in Fig. 5.4 indicated as LTE apply to Release 8/9, while all these energy efficiencies are applicable to Release 10 as Release 10 is backwards compatible which does not necessarily result in a similar energy efficiency. We also indicated how much carriers are aggregated for LTE-Advanced.

For each scenario in Fig. 5.4, a higher modulation scheme and/or coding rate results in a lower energy efficiency. For example, an LTE-Advanced macrocell base station with a CA of two 5 MHz component carriers results in an EE = 0.5 (km$^2\cdot$ Mbps)/W for a coding rate of 2/3 and a modulation of QPSK i.e., 2/3 QPSK versus 0.2 (km$^2\cdot$ Mbps)/W for 2/3 64-QAM because a higher modulation scheme and coding rate lead to a shorter range for a higher bit rate. The decrease in range is higher than the increase in bit rate, leading to a lower energy efficiency as the power consumption and the number of served users remain the same.

When comparing LTE and LTE-Advanced, Fig. 5.4 shows that higher bit rates can be obtained even for a higher energy efficiency by using CA. E.g., for a macrocell base station and 1/2 QPSK, EE = 0.4 (km$^2\cdot$ Mbps)/W for LTE versus 2.1 (km$^2\cdot$ Mbps)/W when aggregating 5 component carriers of 5 MHz. This is due to the fact that CA does not influence the obtained range nor the number of served users. Introducing CA has little impact on the base station's power consumption because CA corresponds in practice to a multicarrier (not aggregated) configuration, which is already supported by LTE or to a base station supporting multiple frequency bands depending on which type of CA is considered [2]. The

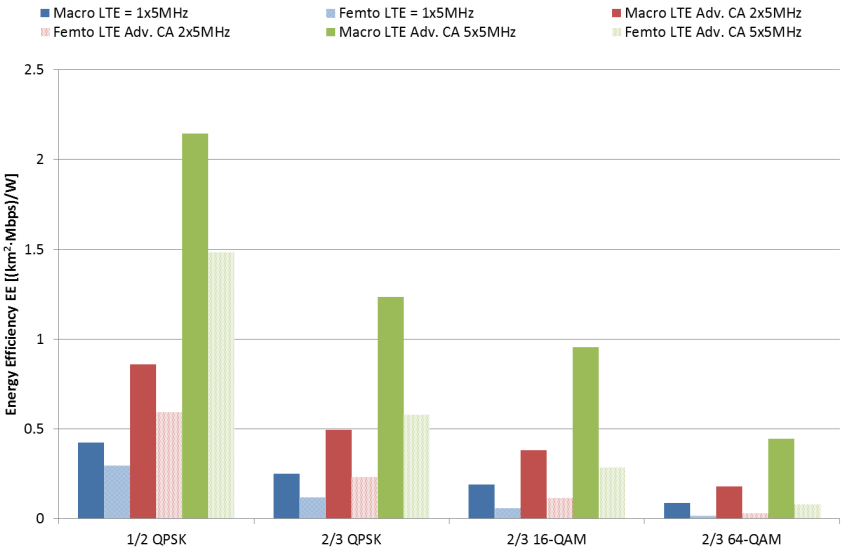

Figure 5.4: Energy efficiency EE of LTE and LTE-Advanced in a 5 MHz channel.

extra power consumed for processing will thus be negligible compared to the base station's power consumption. It is concluded that in terms of the base station's energy efficiency, it might be interesting to immediately implement LTE-Advanced in the network, without introducing Release 8/9. Similar results can be obtained for the other bandwidths.

5.2.2 MIMO

Here, the influence of the extended support for MIMO on the energy efficiency is studied for both spatial diversity and spatial multiplexing. Fig. 5.5(a) shows the influence of spatial diversity on the energy efficiency for different MIMO modes and both the macrocell and femtocell BS. A bit rate of 2.8 Mbps in a 5 MHz channel is considered. SISO is used as reference scenario.

Fig. 5.5(a) shows that the higher the number of transmitting and receiving antennas, the higher the energy efficiency. For the macrocell base station, the energy efficiency increases up to 433% when using 8x8 MIMO. In Eq. (2.7), P_{el} is 2 times higher, while the range R is 3 times higher, resulting in a 5 times higher energy efficiency. For the femtocell base station, the energy efficiency increases even up to 454.6% (or 5.75 times).

Fig. 5.5(b) shows the results for spatial multiplexing. 1/3 QPSK and a 5 MHz channel are considered. Again, a higher number of transmitting and receiving

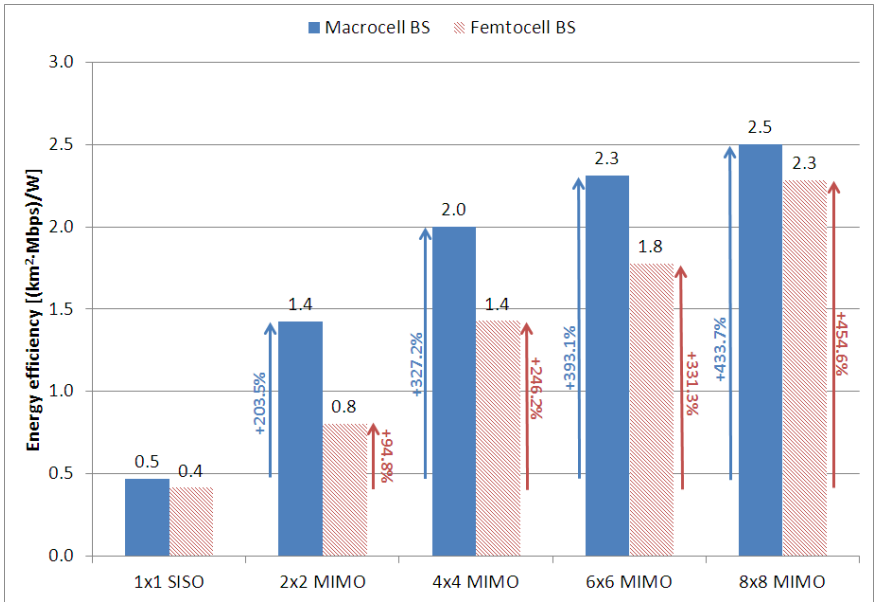

(a)

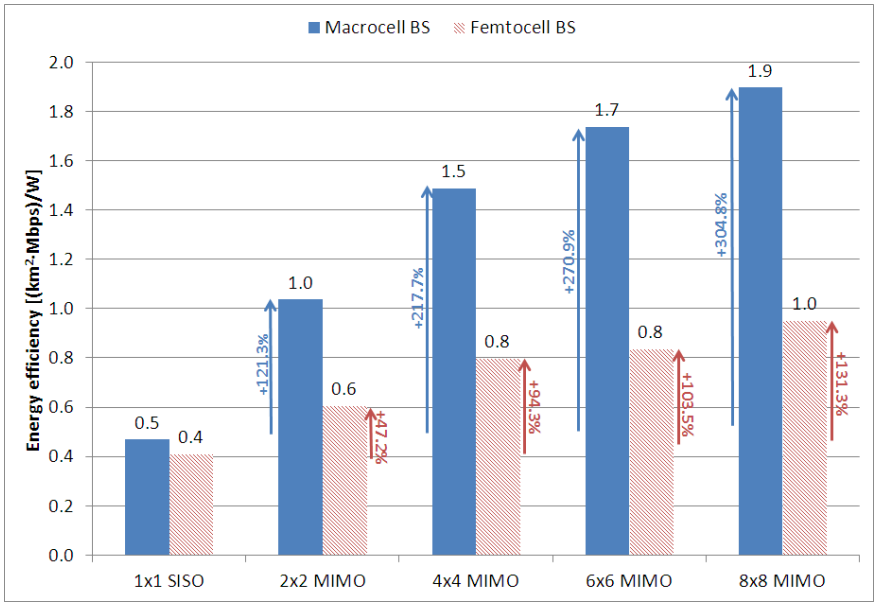

(b)

Figure 5.5: Influence of spatial diversity (a) and spatial multiplexing (b) on the energy efficiency for different MIMO modes using 1/3 QPSK in a 5 MHz channel.

antennas results in a higher energy efficiency. For the macrocell base station, a maximum increase of 304.8% (or about 4 times) is found due to an 8 times higher bit rate while the power consumption increases only 2 times. For a femtocell base station, the energy efficiency gain is maximum 131.3% (or 2.5 times). The highest energy efficiency gain is obtained by using MIMO for spatial diversity.

5.2.3 Heterogeneous deployments

Fig. 5.4 suggests that a femtocell base station is less energy efficient than a macrocell base station. However, this is not always the case. Fig. 5.6 compares the energy efficiency of LTE-Advanced macrocell and femtocell base stations as a function of attainable bit rates. To obtain Fig. 5.6, the bit rate is first defined when aggregating sequentially one to five component carriers with equal bandwidth. We considered all possible bandwidths. Next, for each possible bit rate and each base station type, we selected the most energy-efficient solution.

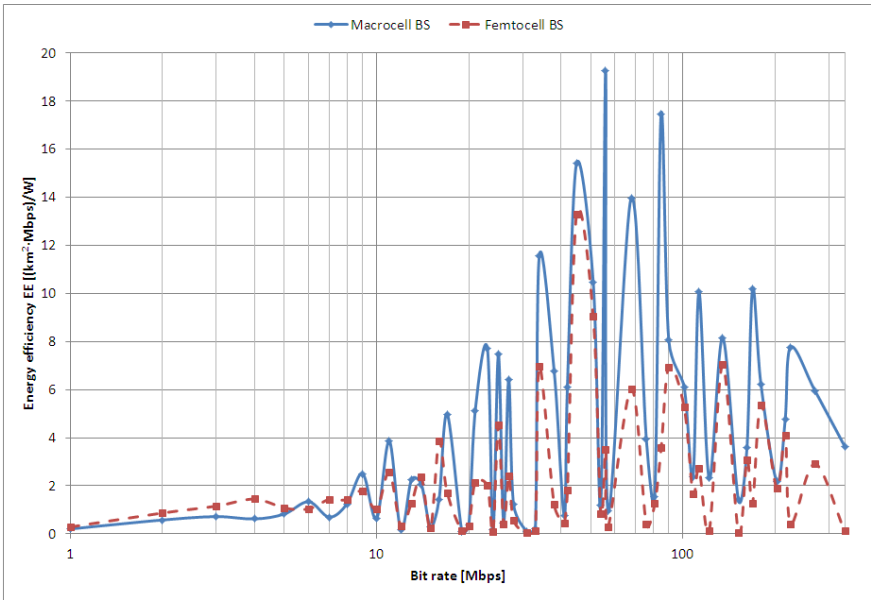

Figure 5.6: Comparison of the energy efficiency of an LTE-Advanced macrocell and femtocell base station for different bit rates.

Fig. 5.6 shows that the bit rate determines which base station type is the most energy efficient. For bit rates higher than 20 Mbps, the macrocell base station is the most energy efficient (EE = 7.5 (km^2· Mbps)/W versus 4.5 (km^2· Mbps)/W for 25 Mbps) due to its longer range and higher number of served users (despite

its higher power consumption). Below 20 Mbps, there is no unambiguous answer. In some cases, the macrocell base station is most energy efficient (for example, for 5 Mbps), while in other cases the femtocell base station is most energy efficient (for example, for 13 Mbps).

With carrier aggregation, we can obtain high bit rates even with a lower modulation scheme or bandwidth. For example, aggregating three 15 MHz carriers with 4/5 16-QAM gives us 122 Mbps, while aggregating five 20 MHz carriers with 2/3 QPSK gives us 113 Mbps, and aggregating four 20 MHz carriers with 1/2 16-QAM gives us 135 Mbps. Because of the higher modulation scheme, the range is much lower for 122 Mbps (141.3 m) than for 133 and for 122 Mbps (respectively, 398.0 m and 327.2 m), resulting in a lower energy efficiency, which is responsible for the up-and-down behavior in Fig. 5.6.

Although future networks will obviously include different base station types, we will need a good estimation of the required bit rate, coverage, and number of served users to determine which type is most suitable in each network location to reduce the network's power consumption. Because demand varies over time as shown in Fig. 5.2, both base station types must be deployed in the network, with the optimal combination resulting in a more energy-efficient network. We can find this optimal combination by placing macrocell base stations to cover the area first, and then femtocell base stations to provide coverage in the *coverage holes* i.e., the areas that are not covered by macrocell base stations. Furthermore, we can extend the macrocell base station's capacity as needed using femtocell base stations in the coverage cell of the macrocell base stations.

5.3 Influence on the power consumption of the network

In the previous section, the influence of carrier aggregation, heterogeneous networks, and MIMO on the power consumption and energy efficiency of a single LTE-Advanced base station was investigated. We will now investigate the influence of these three features on the power consumption and energy efficiency of the complete network. To this end, the capacity-based deployment tool described in Section 5.1 will be used.

5.3.1 Configuration

For this study, an outdoor suburban area of 6.85 km^2 in Ghent, Belgium is selected which is shown in Fig. 5.7. The possible locations (75 locations) for the base stations are indicated by red squares and are existing locations from Belgian mobile operators. Furthermore, we consider an LTE-Advanced network at 2.6 GHz. The different link budget parameters can be found in Tables 2.2 and 2.4 for the macro-

cell and femtocell base station, respectively. For the MIMO gain, the theoretical MIMO gain of Eq. (2.14) is assumed.

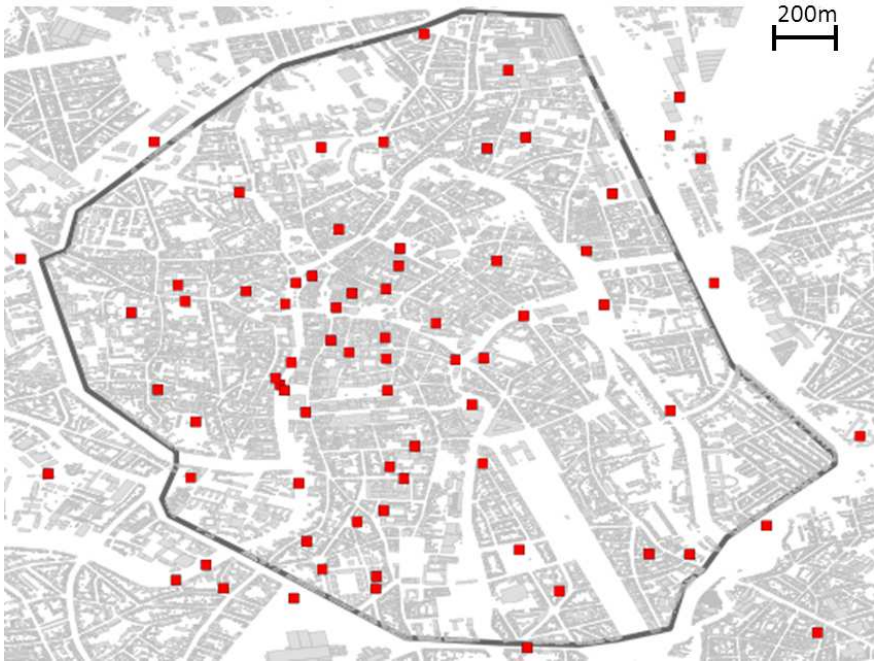

Figure 5.7: The selected suburban area of 6.85 km^2 in Ghent, Belgium.

5.3.2 Reference scenario

The reference scenario used in this study is the scenario whereby the developed networks consist of only macrocell base stations not supporting carrier aggregation nor MIMO.

All the results will be presented as the 50^{th} and 95^{th} percentile calculated over the 40 simulations (as discussed in Section 2.14). As the network responds to the instantaneous bit rate requirements of the users active in the area, the number of selected base stations in the network will vary during the day, resulting in a varying power consumption, and thus energy efficiency, of the network. Fig. 5.8 shows the evolution of both the power consumption (left blue axis) and the energy efficiency (right red axis) during the day for both the 50th and the 95th percentile. The power consumption is the highest during daytime (from 10 a.m. till 8 p.m.). The energy efficiency reaches its highest level around 5 p.m. when the highest number of users is active in the network. On the other hand, the energy efficiency is the

lowest around 3 a.m. to 4 a.m. when the lowest number of users is active in the network. Although the power consumption is higher around 5 p.m. than around 3 a.m. to 4 a.m., a higher energy efficiency is obtained due to better performance of the network (higher offered capacity, higher number of users served, and a higher coverage).

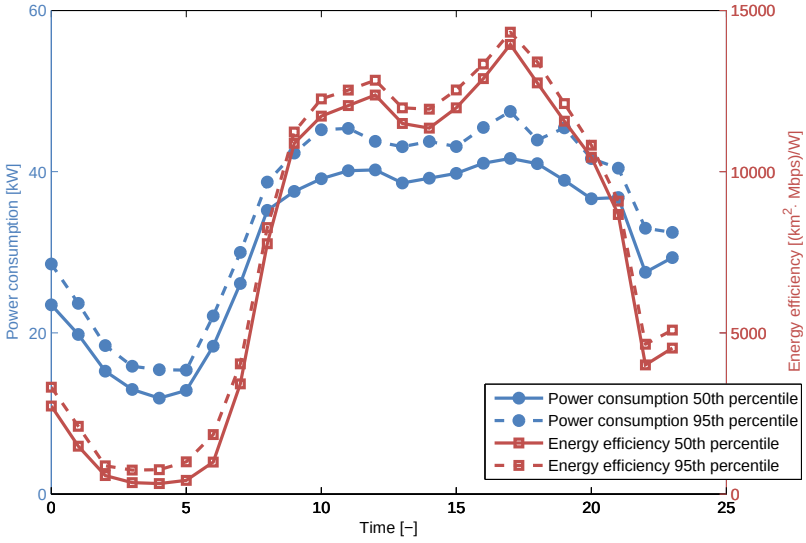

Figure 5.8: Evolution during the day of the 50th and the 95th percentile of the power consumption (blue left axis) and the energy efficiency (red right axis) for the reference scenario.

Fig. 5.9 shows the network obtained from one simulation case for four different time intervals during the day. The red squares indicate the location of the base stations, while the blue triangles indicate the location of the users. For the networks at 12 a.m. and 6 p.m., of course much more active BSs are required than at 12 p.m. and 6 a.m. because of the higher number of active users (Fig. 5.9). Note that for each time interval, 40 simulations will be performed and thus 40 networks will be designed for each time interval. From now on, only two time intervals will be considered: the 4-5 a.m. time interval with the lowest number of active users (i.e, 14 users) and the 5-6 p.m. time interval with the highest number of active users (i.e., 224 users). The results will be presented as the 50^{th} (p_{50}) and 95^{th} (p_{95}) percentile calculated over the 40 simulation cases for each time interval. For each considered time interval, the standard deviation σ_{PC} and σ_{EE} and the 90% confidence intervals CI_{PC} and CI_{EE} of the power consumption and the

energy efficiency respectively, calculated over the 40 simulations is given. σ_{PC} is between 1.6 kW and 2.8 kW for the 4-5 a.m. time interval and between 2.5 kW and 5.6 kW for the 5-6 p.m. time interval which amounts to approximately 10% of the obtained p_{50} value due to the considered distributions (user, location, and bit rate distribution). Furthermore, the power consumption reduction and the energy efficiency improvement compared to the reference scenario will be determined for each scenario.

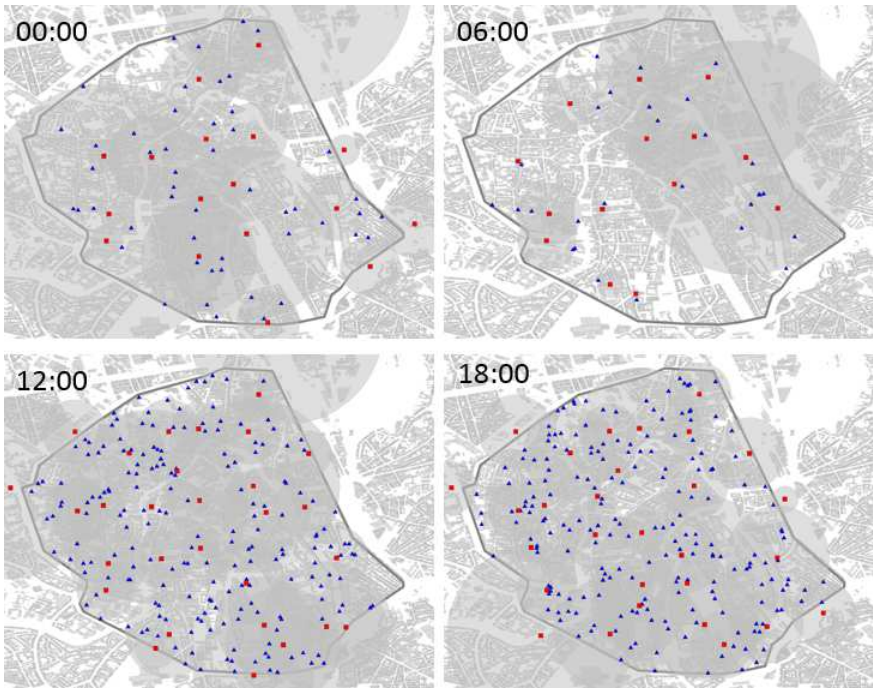

Figure 5.9: Overview of the network obtained by one simulation for different time intervals during the day (red square = base station location, gray circle = range of the base station, and blue triangle = user location).

5.3.3 Carrier aggregation

Tables 5.1 and 5.2 show the results for both the power consumption (PC) and the energy efficiency (EE) for the two selected time intervals i.e., 4 a.m. to 5 a.m. (lowest number of active users) and 5 p.m. to 6 p.m. (highest number of active users), respectively when applying carrier aggregation compared to the reference scenario. 2 up to 5 carriers of 5 MHz are aggregated in this comparison and only macrocell base stations are considered. Figs. 5.10 and 5.11 give an overview of

the individual parameters (number of active base stations (a), network power consumption (b), number of users served by the network (c), and the capacity offered by the network (d)) for the two selected time intervals.

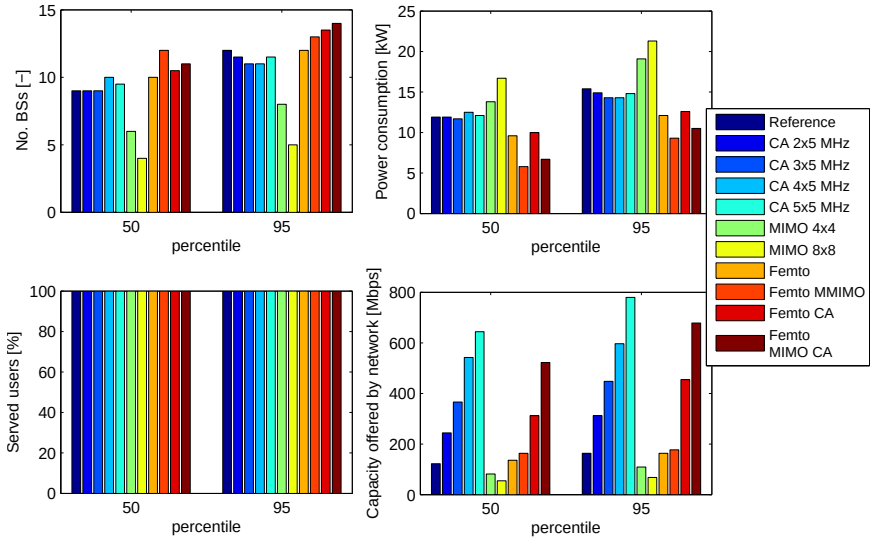

Figure 5.10: Comparison of different parameters (number of used base stations (a), power consumption (b), percentage of users served (c), and capacity offered by the network (d)) for the time interval *4 a.m. to 5 a.m.* for the different scenarios.

Based on Tables 5.1 and 5.2, it is concluded that the more carriers are aggregated, the more energy-efficient the solution becomes. Aggregating 5 carriers results for the considered case in an energy efficiency improvement up to 400% (Table 5.2) due to the fact that a higher number of aggregated carriers results in a higher offered bit rate per base station for the same base station's power consumption (CI_{PC} is approximately the same for the considered CAs) and thus in a higher network capacity (Figs. 5.10 (d) and 5.11 (d)). When aggregating two 5 MHz carriers, the capacity offered by the network multiplies by approximately 2; analogously when aggregating 5 carriers the capacity offered by the network multiplies by approximately 5. For all considered scenarios, all users active in the selected area are covered for the 4-5 a.m. time interval and 97% for the 5-6 p.m. time interval (Figs. 5.10 (a) and 5.11 (a)). For the 5-6 p.m. time interval, 3% of the users can not be covered, because the locations where new base stations can be il-

Table 5.1: Comparison of the power consumption and energy efficiency for the time interval *4 a.m. to 5 a.m.* for the different scenarios and difference with respect to the reference scenario.

Scenario	PC p_{50}/p_{95} [kW]	σ_{PC} [kW]	CI_{PC} [kW]	EE p_{50}/p_{95} $[(km^2 \cdot Mbps)/W]$	CI_{EE} $[(km^2 \cdot Mbps)/W]$	σ_{EE} $[(km^2 \cdot Mbps)/W]$	ΔPC p_{50}/p_{95} [%]	ΔEE p_{50}/p_{95} [%]
Reference	11.9/15.4	1.8	12.1 ± 0.5	324.4/755.9	378.0 ± 43.3	167.0	—/—	—/—
CA 2x5 MHz	11.9/14.9	1.6	11.9 ± 0.4	592.8/1528.7	718.0 ± 93.3	359.7	0/3.2	82.7/102.2
CA 3x5 MHz	11.7/14.3	1.7	11.9 ± 0.4	862.5/1700.7	966.2 ± 107.8	415.7	1.7/7.1	165.9/125.0
CA 4x5 MHz	12.5/14.3	1.8	11.8 ± 0.5	1278.2/2688.3	1381.0 ± 157.4	607.2	-5.0/7.1	294.02/255.6
CA 5x5 MHz	12.1/14.8	1.6	12.1 ± 0.4	1375.3/3333.2	1556.9 ± 199.3	768.8	-1.7/3.9	324.03/341.0
MIMO 4x4	13.8/19.1	2.6	14.0 ± 0.7	295.2/431.2	300.2 ± 18.5	71.2	-16.0/-24.0	-9.0/-43.0
MIMO 8x8	16.7/21.3	2.8	17.0 ± 0.7	191.0/235.9	197.7 ± 8.4	32.5	-40.3/-38.0	-41.1/-66.4
Femto	9.6/12.1	1.7	9.6 ± 0.5	332.3/913.0	407.1 ± 69.3	267.4	19.3/21.4	2.4/20.8
Femto MIMO	5.8/9.3	1.8	5.8 ± 0.5	475.7/1711.5	643.7 ± 121.0	466.8	51.3/39.6	46.6/126.4
Femto CA	10.0/12.6	1.7	9.8 ± 0.4	784.5/1656.0	837.1 ± 106.7	411.5	16.0/18.2	141.8/119.1
Femto CA MIMO	6.7/10.5	1.9	6.7 ± 1.9	1197.9/5164.4	1851.0 ± 371.0	1430.7	43.7/31.8	292.3/583.2

PC = Power Consumption, σ_{PC} = standard deviation of PC, CI_{PC} = 90% confidence interval of PC, Δ_{PC} = relative PC reduction, EE = energy efficiency, σ_{EE} = standard deviation of EE, CI_{EE} = 90% confidence interval of EE, Δ_{EE} = relative EE gain.

Table 5.2: Comparison of the power consumption and energy efficiency for the time interval *5 p.m. to 6 p.m.* for the different scenarios and difference with respect to the reference scenario.

Scenario	PC p_{50}/p_{95} [kW]	σ_{PC} [kW]	CI_{PC} [kW]	EE p_{50}/p_{95} $[(km^2 \cdot Mbps)/W]$	CI_{EE} $[(km^2 \cdot Mbps)/W]$	σ_{EE} $[(km^2 \cdot Mbps)/W]$	ΔPC p_{50}/p_{95} [%]	ΔEE p_{50}/p_{95} [%]
Reference	41.6/47.5	3.0	41.7 ± 0.8	13945/14328	13884 ± 82.8	319.4	—/—	—/—
CA 2x5 MHz	38.5/42.7	2.7	38.4 ± 0.7	28043/28899	27875 ± 191.7	739.4	7.5/10.1	101.1/101.7
CA 3x5 MHz	38.4/42.8	2.7	38.4 ± 0.7	41733/43771	41801 ± 320.5	1235.9	7.7/9.9	199.3/205.5
CA 4x5 MHz	39.1/45.0	3.2	39.2 ± 0.8	55676/57927	55650 ± 380.4	1466.8	6.0/5.3	299.3/304.3
CA 5x5 MHz	38.7/43.9	2.5	39.0 ± 0.6	69575/72291	69646 ± 423.7	1634.0	7.0/7.6	398.9/404.5
MIMO 4x4	60.4/65.4	3.3	59.7 ± 0.9	7198.5/7715.2	7221.0 ± 74.2	286.3	-45.2/-37.7	-48.4/-46.2
MIMO 8x8	91.1/100.5	5.6	90.5 ± 1.5	4260.6/4509.5	4257.9 ± 39.9	153.8	-119.0/-111.6	-69.4/-68.5
Femto	39.4/43.5	3.0	39.3 ± 0.8	27563/31295	28273 ± 491.6	1895.8	5.3/8.4	97.7/118.4
Femto MIMO	32.9/37.4	2.9	32.5 ± 0.7	35060/40157	35000 ± 818.5	3156.5	20.9/21.3	151.4/180.3
Femto CA	39.6/42.8	2.6	39.3 ± 0.7	85314/108200	86606 ± 2768.7	10677	4.8/9.9	511.8/655.2
Femto CA MIMO	33.1/37.5	2.5	33.0 ± 0.7	122180/148100	12347 ± 3798.4	14648	20.4/21.1	776.2/933.6

PC = Power Consumption, σ_{PC} = standard deviation of PC, CI_{PC} = 90% confidence interval of PC, Δ_{PC} = relative PC reduction, EE = energy efficiency, σ_{EE} = standard deviation of EE, CI_{EE} = 90% confidence interval of EE, Δ_{EE} = relative EE gain.

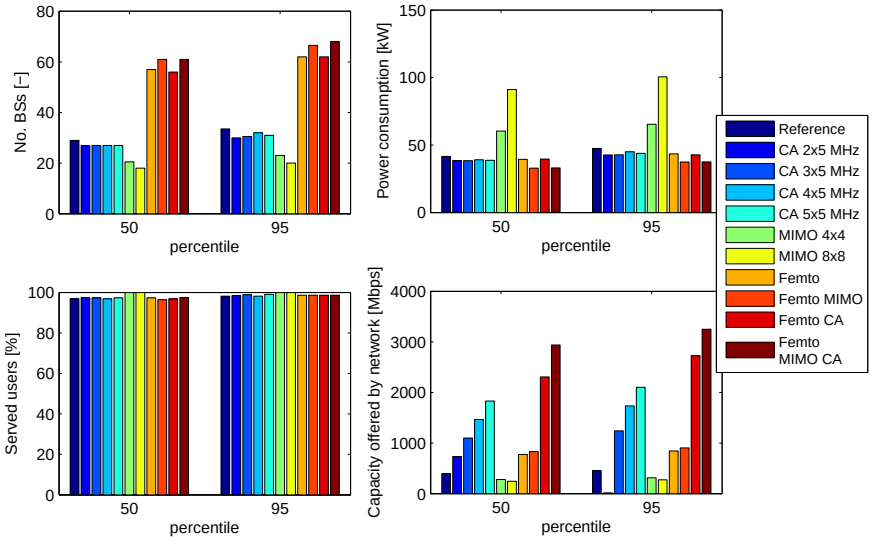

Figure 5.11: Comparison of different parameters (number of used base stations (a), power consumption (b), percentage of users served (c), and capacity offered by the network (d)) for the time interval *5 p.m. to 6 p.m.* for the different scenarios.

luminated are limited, and the path loss experienced by the user from base stations on these locations is higher than the maximum allowable path loss (Section 5.1).

For the selected area, carrier aggregation does not result in a lower power consumption for the 4-5 a.m. interval. The same number of base stations (9 as shown in Fig. 5.10 (a)) is used for the different scenarios where carrier aggregation is applied as for the reference scenario because the capacity per base station is here not the most limiting factor to develop the network but the range per base station. For the 5-6 p.m. time interval, a small power consumption reduction (about 7%) is obtained as the introduction of carrier aggregation results in a smaller number of base stations (27 versus 29 for the reference scenario, Fig. 5.11 (a)).

5.3.4 MIMO

The second feature that is investigated is MIMO. Tables 5.1 and 5.2 also list the values for the power consumption and the energy efficiency compared to the reference scenario for the 4-5 a.m. and the 5-6 p.m. time interval respectively. Three different cases are studied: SISO which corresponds with the reference scenario, 4x4 MIMO, and 8x8 MIMO. Spatial diversity is used, so a higher range will be obtained when applying MIMO. Figs. 5.10 and 5.11 give again an overview of the individual parameters for the two selected time intervals. The results for the

energy efficiency parameter in Tables 5.1 and 5.2 show that for the selected area, MIMO does not lead to a higher energy efficiency.

For the 4-5 a.m. interval, the energy efficiency is decreased with 9% to 43% by introducing 4x4 MIMO when taking the p_{50} and p_{95} values into account compared to the reference scenario. For the 5-6 p.m. interval, a decrease of approximately 47% is obtained. For 8x8 MIMO, these reductions are even higher: 41% (p_{50}) to 66% (p_{95}) for the 4-5 a.m. interval and approximately 69% for the 5-6 p.m. interval. In general, it is concluded that the energy efficiency for the considered case decreases when applying MIMO for the case here considered. As applying MIMO results in a higher range per base station, fewer base stations are needed to cover all the users in the area (Figs. 5.10 (a & c) and 5.11 (a & c)) and thus less capacity is available in the network (Figs. 5.10 (d) and 5.11 (d)) resulting in a lower energy efficiency. When using 4x4 MIMO, the number of used base stations is reduced by approximately 30% (for the 4-5 a.m. and 5-6 p.m. interval), resulting in approximately the same reduction in network capacity. When using 8x8 MIMO, the number of base stations is even further reduced compared to the reference scenario: by approximately 57% and 39% for the 4-5 a.m. and 5-6 p.m. interval respectively, resulting also in approximately the same reduction in network capacity. Despite the reduction in number of base stations, no power reduction is found. This is due to the fact that the extra power consumption needed to support the multiple antennas is too high for the considered case.

5.3.5 Heterogeneous deployments

In this section, the influence on the power consumption and energy efficiency of introducing femtocell base stations in the network is studied. The results for these parameters compared to the reference scenario are listed in Tables 5.1 and 5.2 for the 4-5 a.m. and the 5-6 p.m. time interval, respectively. Five different scenarios are investigated: (i) the network consisting of only macrocell base stations without carrier aggregation and MIMO (i.e., the reference scenario), (ii) the combination of macrocell and femtocell base stations both not supporting carrier aggregation and MIMO, (iii) the combination of macrocell and femtocell base stations where the femtocell base station supports 4x4 MIMO (spatial diversity), (iv) the combination of macrocell and femtocell base stations where the femtocell base station aggregates 5 carriers of 5 MHz, and (v) the combination of macrocell and femtocell base stations where the femtocell base station supports both carrier aggregation and MIMO. Although the femtocell base station is seen as an indoor device, we here consider it to be outdoor or at least its antenna is placed outdoor. Tables 5.1 and 5.2 show that introducing femtocell base stations in the network has a high influence on the energy effciency. When introducing femtocell base stations without carrier aggregation and MIMO, an energy efficiency improvement of 2% (p_{50}) to 21% (p_{95}) is obtained for the 4-5 a.m. interval and 98% (p_{50}) to 118% (p_{95}) for

the 5-6 p.m. interval. This is due to the lower power consumption of the femtocell base station compared to the macrocell base station is significantly lower (12 W versus 1674 W, Chapter 2) resulting in a network power consumption reduction (Tables 5.1 and 5.2) of approximately 20% for the 4-5 a.m. time interval and 5% (p_{50}) to 8% (p_{95}) for the 5-6 p.m. time interval compared to the reference scenario, although a higher number of base stations is used (Figs. 5.10 (a) and 5.11 (a)). For the 5-6 p.m. time interval, the number of used base stations is increased by 85% (p_{95}) to 97% (p_{50}), while the number of used base stations is approximately the same for the 4-5 a.m. time interval as for the reference scenario to cover the same number of users (i.e., 100% for the 4-5 a.m. interval and 97% for the 5-6 a.m. interval (Figs. 5.10 (a) and 5.11 (a)). Note, that this collection of used base stations consists of both macrocell and femtocell base stations, while the collection for the reference scenario consists only of macrocell base stations. Furthermore, this large number of base stations also provides a higher network capacity thus resulting in a higher energy efficiency (non-overlapping CI_{EE}). For the 5-6 p.m. interval, the network capacity increases by 86% (p_{95}) to 97% (p_{50}) compared to the reference scenario. For the 4-5 a.m. interval, the increase is only 0% (p_{95}) to 11% (p_{50}) compared to the reference scenario as the number of base stations is approximately the same as for the reference scenario.

Comparing the scenario with MIMO and the scenario with carrier aggregation shows that introducing femtocell base stations supporting MIMO influences the power consumption the most. CI_{PC} when using MIMO is significantly lower than when using carrier aggregation which is preferable as this shows that there is less uncertainty about the obtained power consumption value. Furthermore, the CI_{PC} when using carrier aggregation is similar to the CI_{PC} when using femtocell base stations without supporting MIMO or carrier aggregation. A reduction of 32% (p_{95}) to 44% (p_{50}), respectively 21% (p_{50} and p_{95}), is obtained for the scenario with femtocell base stations supporting MIMO for the 4-5 a.m., respectively the 5-6 p.m. time interval, versus approximately 17% respectively 5% (p_{50}) to 10% (p_{95}) for the scenario with femtocell base stations supporting carrier aggregation (Tables 5.1 and 5.2). Due to MIMO, the range of the femtocell base stations is increased and more femtocell base stations (with a lower power consumption) than macrocell base stations are used although the total number of used base stations does not decrease (Figs. 5.10 (a) and 5.11 (a)). In contrary, introducing femtocell base stations supporting carrier aggregation influences the energy efficiency most. An energy efficiency improvement of 292% (p_{50}) to 583% (p_{95}), respectively 512% (p_{50}) to 655% (p_{95}), is found for the 4-5 a.m. and 5-6 p.m. time interval versus 119% (p_{95}) to 142% (p_{50}) and 151% (p_{50}) to 180% (p_{95}) when introducing femtocell base stations supporting MIMO (Tables 5.1 and 5.2). The CI_{EE} differs significantly between the different scenarios. As carrier aggregation increases the capacity per base station, the overall capacity of the network

increases, resulting in a high energy efficiency.

The best results are obtained when introducing both carrier aggregation and MIMO. For this scenario, the consumed power is similar as for the scenario when supporting only MIMO as CI_{PC} overlaps significantly, but the energy efficiency improvement is much higher (CI_{EE} is significantly higher) when supporting both MIMO and carrier aggregation as supporting carrier aggregation results in a higher capacity per base station and MIMO in a higher range per base station.

5.4 Influence of the sleep mode power consumption

In the discussions above, we assumed that the unselected base stations consume no power which is of course an ideal situation. We will now investigate the influence of the base station's power consumption during sleep mode on the network's power consumption. Fig. 5.12 shows the obtained network power consumption (50th percentile) for all of the above described scenarios for the 5 p.m. to 6 p.m. time interval (except for 3, 4 and 5 component carriers as these give the same results as for 2 x 5 MHz CA as discussed later). The x-axis shows how much power a base station consumes during sleep mode with respect to the power consumption during active operation. For example, a value of 10% means that the base station consumes 10% of 1672 W (i.e., the power consumption during operation). A value of 0% means that the sleeping base station consumes no power, while a value of 100% means that the sleeping base station consumes the same amount of power as an active base station. In [8], a realistic value of 45% of the operational power consumption is obtained for the power consumption during sleep mode. For a base station using MIMO, it is assumed that during sleep mode the base station can turn off all the extra antennas and thus the same power consumption as for a SISO base station is considered during sleep mode. In [11], three different sleep modes are considered for a femtocell base station: stand-by mode with a power consumption of 50% of its operational consumption and a wake-up time of 0.5 s, sleep mode with a power consumption of 15% and a wake-up time of 10 s, and off-line mode with a power consumption of 0 W and a wake-up time of 30 s.

In general, the network's power consumption in Fig. 5.12 increases when the amount of power that is consumed during sleep mode increases. This linear relation is self-evident because the power consumption during sleep mode is fixed and can not be optimized by our tool. Only the power consumed by active base stations can be tuned. Furthermore, for values lower than 85% the lowest power consumption is obtained when aggregating 2 carriers of 5 MHz while for values equal or higher than 85% the reference scenario consumes the lowest amount of power. As mentioned above (Table 5.2), the reference scenario uses 29 base stations (consuming 41.6 kW) while the carrier aggregation scenario uses 27 base

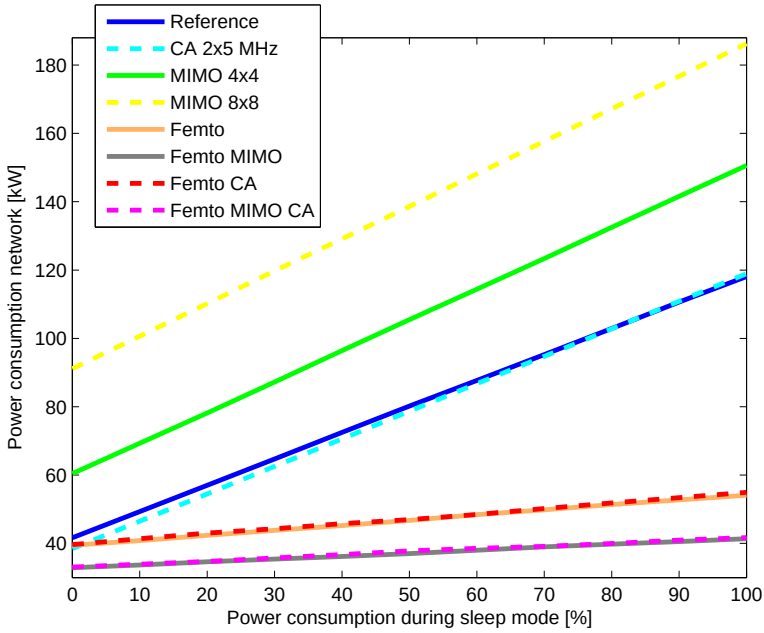

Figure 5.12: Influence of the (50th percentile) power consumption of the sleeping base stations on the network's power consumption for the *5 p.m. to 6 p.m.* time interval.

stations (consuming 38.5 kW). The carrier aggregation scenario will thus have a higher sleeping power consumption than the reference scenario as it has more sleeping base stations (48 versus 46). For a value higher than 85 %, the difference in the power consumption of the sleeping base stations (68.2 kW versus 65.4 kW for the reference scenario and 85%) exceeds the difference in power consumption of the active base stations resulting in a lower overall network power consumption for the reference scenario. The same result is obtained for the other carrier aggregation scenarios. The two considered MIMO scenarios do not overlap with the reference scenario because the difference in power consumption of the active base stations is already too high compared to the reference scenario.

For the scenarios involving femtocell base stations, we have used the same ratio of femtocell base stations to macrocell base stations for the sleeping base stations as for the active base stations. For example, if 10% of the active base stations is a femtocell base station and 90% a macrocell base station, than 10% of the sleeping base stations is also a femtocell base station and 90% a macrocell base station. The percentage for the power consumption during sleep mode is of course kept the same for the femtocell and the macrocell base station. For a value of 20%

and the ratio of 90% mentioned above, 10% of the sleeping base stations will consume 20% of 12 W (femtocell base station) and 90% of the sleeping base stations will consume 20% of 1672 W (macrocell base station). Note, that we have also added the reference scenario in Fig. 5.12. However, this is a purely macrocell base station scenario and thus all sleeping base stations are assumed to be macrocell base stations which clarifies the higher network's power consumption obtained by the reference scenario. This is also the reason why the power consumption during sleep mode influences more the network's power consumption than for the femtocell base station scenarios (steeper curve).

The scenarios using femtocell base stations without carrier aggregation and MIMO and with carrier aggregation (but without MIMO) show similar results because they use approximately the same number of active base stations (56-57) resulting in a similar power consumption (39.4-39.6 kW, Table 5.2). The difference in power consumption of the active base stations is again too high to obtain any overlap with the other two femtocell base station scenarios which also have similar results as already discussed in the previous section (Table 5.2).

From now on, the value of 45% of the operational power consumption obtained by [8] will be assumed for the power consumption during sleep mode. For this value, the network power consumption for the reference scenario amounts to 76.4 kW compared to 41.6 kW for the ideal situation when the sleeping base stations consume no power and 118.1 kW when all base stations are active.

5.5 Different energy efficiency metrics

In section 2.4, we discussed the need of an appropriate energy efficiency metric. Seven different energy efficiency metrics were proposed. Table. 5.3 compares the results for the above described scenarios (5-6 p.m. time interval) for the energy efficiency metrics introduced in Section 2.4: PC_{area} (Eq. (2.4)), PC_{users} (Eq. (2.5)), $PC_{bitrate}$ (Eq. (2.6)), $PC_{product_1}$ (Eq. (2.7)), PC_{norm} (Eq. (2.8)), PC_{sum} (Eq. (2.9)), and $PC_{product_2}$ (Eq. (2.10)). For PC_{norm} and PC_{sum}, the following is assumed: A_{max} is the surface of the considered area, B_{max} corresponds with the capacity offered by the network when each base station is active and aggregates 5 carriers of 5 MHz with the highest possible modulation scheme and coding rate, U_{max} is the number of simultaneous active users (which depends on the time interval) in the considered area, and P_{max} equals the electical power consumed by the network when each base station is active and supporting 8x8 MIMO.

All metrics agree on the fact that the scenario with femtocell base stations supporting MIMO and carrier aggregation is the most energy-efficient. However, they do not agree on the sequence of the other scenarios. The metrics involving

Scenario	PC_{area} [km^2/W]	PC_{users} [1/W]	$PC_{bitrate}$ [Mbps/W]	$PC_{product_1}$ [(km$^2\cdot$ Mbps)/W]	PC_{norm} [-]	PC_{sum} [-]	$PC_{product_2}$ [(km$^2\cdot$ Mbps)/W^3]
Reference	0.16	5.2	9.5	13945	757.2	25583	8.0
CA 2x5 MHz	0.18	5.7	19.0	28043	1522.7	28629	19.0
CA 3x5 MHz	0.18	5.7	28.5	41733	2266.1	29517	28.9
CA 4x5 MHz	0.17	5.6	38.2	55676	3023.2	29588	36.5
CA 5x5 MHz	0.17	5.6	47.6	69757	3777.9	30618	46.2
MIMO 4x4	0.11	3.7	4.7	7198.5	390.9	17897	2.0
MIMO 8x8	0.1	2.5	2.8	4260.6	231.3	11838	0.5
Femto	0.17	5.5	19.6	27563	1496.7	27688	18.3
Femto MIMO	0.19	6.6	25.3	35060	1903.8	30501	31.9
Femto CA	0.17	5.5	58.6	85314	4632.5	32897	54.4
Femto CA MIMO	0.20	6.6	87.9	122180	6634.2	37998	112.6

Table 5.3: Comparison of different energy efficiency metrics for the considered scenarios and the *5 p.m. to 6 p.m.* time interval.

covered area PC_{area} and served users PC_{users} show similar results. As users are uniformly distributed over the area, the users can be everywhere in the considered area and thus results a higher number of served users also in a higher coverage of the area. $PC_{bitrate}$ shows a different sequence in terms of energy efficiency. The higher the capacity offered by the network, the better it performs in terms of $PC_{bitrate}$. Adding carrier aggregation has thus a big influence on the $PC_{bitrate}$ metric. Similar results as for the $PC_{bitrate}$ are obtained by the $PC_{product_1}$ metric, although this metric combines covered area, number of served users, and bit rate. The difference between the minimal and maximal value of PC_{area} and PC_{users} amounts to 62.5%, while for $PC_{bitrate}$ this difference is significant higher (96.8%). It is thus obvious for the case here considered, that $PC_{product_1}$ will be influenced mostly by the bit rate parameter.

Table. 5.3 shows that similar results are obtained with the metrics combining the number of served users, offered bit rate, covered area, and power consumption. The scenario with femtocell base stations supporting both carrier aggregation and MIMO performs for all four metrics the best and also the sequence in terms of energy efficiency is the same for all four parameters. Note that the absolute values between the different scenarios differ from metric to metric. However, the absolute values are here less important. The purpose of the metric is to define which scenario performs the best. The algebraic composition is thus of minor importance as long as the relative results remain the same.

In general, all these metrics express energy efficiency. However, we suggest to use the $PC_{product_1}$ metric as this combines all considered performance metrics. As an alternative also PC_{norm}, PC_{sum}, or $PC_{product_2}$ can be used, but they give the same information as the $PC_{product_1}$ metric. In this chapter, the $PC_{product_1}$ energy efficiency metric is considered.

5.6 Conclusion

In this chapter, we investigated the influence of three main functionalities (carrier aggregation, MIMO, and heterogeneous networks) of the LTE-Advanced standard on the power consumption and energy efficiency on the base station level and on the network level. For the study on the network level, a capacity-based deployment tool is proposed. The purpose of this algorithm is to respond to the instantaneous bit rate request of the users in a geometrical area as energy-efficiently as possible rather than providing coverage to a certain area as in the genetic search algorithm. The network is developed for a realistic suburban case in Ghent, Belgium.

For a single base station, we found that, in general, a higher bit rate results in a lower energy efficiency. However by using carrier aggregation, LTE-Advanced allows to obtain higher bit rates for even a higher energy efficiency. The type of base station (macrocell or femtocell base station) that is the most energy-efficient

depends on the bit rate. MIMO can also increase the energy efficiency of a single base station.

For the network, the highest power reduction and energy efficiency improvement is obtained when applying the three features together i.e., a heterogeneous network whereby the femtocell base station supports both carrier aggregation and MIMO. Adding femtocell base stations without MIMO and carrier aggregation can already reduce the power consumption significantly. Furthermore, introducing femtocell base stations only supporting carrier aggregation has the highest influence on the energy efficiency, while introducing femtocell base stations only supporting MIMO has the highest influence on the power consumption.

Based on this study, it is recommended for future wireless access networks to take the advantage of LTE-Advanced incoperated features, especially the introduction of femtocell base stations, to reduce the power consumption of the network.

References

[1] Cisco. *Cisco Visual Networking Index: Global Mobile Data Traffic Forecast Update 2012-2017, White paper*. Technical report, 2012.

[2] E. Dahlman, S. Parkvall, and J. Sköld. *4G LTE/LTE-Advanced for Mobile Broadband*. Academic Press, 2011.

[3] M.W. Arshad, A. Vastberg, and T. Edler. *Energy Efficiency Improvement through Pico Base Stations for a Green Field Operator*. In IEEE Wireless Communications and Networking Conference, pages 2224–2229, Paris, France, 2012.

[4] L.M. del Apio, E. Mino, L. Cucala, O. Moreno, and I Berberana. *Energy Efficiency and Performance in mobile network deployments with femtocells*. In IEEE 22nd International Symposium on Personal Indoor and Mobile Radio Communications, pages 107–111, Toronto, Canada, 2011.

[5] C. Khirallah, J.S. Thompson, and D. Vukobratović. *Energy Efficiency of Heterogeneous Networks in LTE-Advanced*. In IEEE Wireless Communications and Networking Conference, pages 53–58, Paris, France, 2012.

[6] W. Joseph and L. Verloock. *Influence of mobile phone traffic on general public base station exposure*. Health Physics, 99(5):361–638, 2010.

[7] A. Gati, A. Hadjem, M.F. Wong, and J. Wiart. *Exposure Induced by WCDMA Mobile Phones in Operating Networks*. IEEE Transactions on Networks, 8(12):5723–5727, 2009.

[8] M.J. Gonzalez, D. Ferling, W. Wajda, A. Erdem, and P. Maugars. *Concepts for Energy Efficient LTE Transceiver Systems in Macro Base Stations*. In Future Network & Mobile Summit, Warsaw, Poland, 2011.

[9] COST telecommunications. *COST Action 231: Digital mobile radio towards future generation systems*. European Commission, 1999.

[10] Y. Hou and D.I. Laurenson. *Energy Efficiency of High QoS Heterogeneous Wireless Communication Network*. In IEEE 72nd Vehicular Technology Conference Fall, pages 1–5, Ottawa, 2010.

[11] W. Vereecken, I. Haratcherev, M. Deruyck, W. Joseph., M. Pickavet, L. Martens, and P. Demeester. *The Effect of Variable Wake Up Time on the Utilization of Sleep Modes in Femtocell Mobile Access Networks*. In 9th International Conference on Wireless On-demand Network Systems and Services, pages 63–66, Courmayeur, Italy, 2012.

6

Optimizing the network towards both power consumption and electromagnetic exposure of human beings

As already discussed before, in the last few years, the worldwide use of wireless devices has grown considerably. Laptops, tablets, smartphones, etc. have entered into our daily life. Due to this growth, wireless access networks have also been expanding significantly in order to serve all mobile users. However, wireless access networks, and more specifically the base stations of these networks, are currently already very large power consumers as we have determined in the previous chapters. As it is expected that the amount of wireless devices, customers, and traffic will further increase in the coming years, it is very important to develop and implement energy-efficient wireless access networks in the near future [1, 2]. In addition to this, people are becoming more and more concerned about the health effects that can be caused by the electromagnetic radiation of these networks; so on the other side, it is also important to minimize the exposure of human beings to these networks.

In this chapter, the capacity-based deployment tool of Chapter 5 is further extended to take also human exposure to electromagnetic fields of base stations into account. First, we propose an approach to minimize power consumption while satisfying a certain exposure limit. Second, an approach to minimize the exposure

of human beings is proposed and finally an algorithm for optimizing towards both power consumption and exposure of human beings is introduced.

6.1 Optimizing towards power consumption while satisfying a certain exposure limit

The algorithm described in this section minimizes the network's power consumption while satisfying a certain exposure limit per antenna. The same approach as in Section 5.1 is used, however, an extra step will be added in the beginning of the algorithm. In this step, we determine for each base station the maximum Equivalent Isotropically Radiated Power (EIRP), here denoted as $EIRP_{max}$, satisfying the considered exposure limit E_{lim} per antenna [3]. Once $EIRP_{max}$ is known, the maximum input power of the antenna can be calculated, and the network can be developed by using the procedure described in Section 5.1 with the obtained limitations for the antenna's input power of each base station.

To determine $EIRP_{max}$, three extra inputs for the algorithm are needed: a grid over the considered area to evaluate the exposure, a distance d_s (in m), which defines the minimal separation between the human from the base stations that will be installed, and the maximally allowed electric-field strength E^{ds}_{max} (in V/m) at distance d_s from the base station. For each base station, the path loss PL_{ds} (in dB) at distance d_s is determined and by using the following formula $EIRP_{max}$ (in dBm) is calculated [3]:

$$EIRP_{max} = 43.15 + 20 \cdot log_{10}\frac{E^{ds}_{max}}{f} + PL_{ds} \tag{6.1}$$

with f the frequency of the considered technology (in MHz).

Note that the above proposed algorithm is an extension of the capacity-based algorithm of Section 5.1. This means that the algorithm is also capacity-based and realistic traffic data is needed as input. To generate this traffic, the procedure in Section 5.1.1 is used here as well.

6.2 Optimizing towards exposure of human beings

Fig. 6.1 shows the flow diagram of the approach followed to design wireless access networks with a minimal exposure for human beings which is based on the algorithm proposed in [3] and the capacity-based algorithm of Section 5.1. Realistic traffic is again generated by using the algorithm in Section 5.1.1.

In the first step (Fig. 6.1 Step 1), the network will be created where the EIRP of the base stations is limited to x dBm. In this way, a network containing many low-power base stations is obtained which is, in terms of minimal exposure, preferred

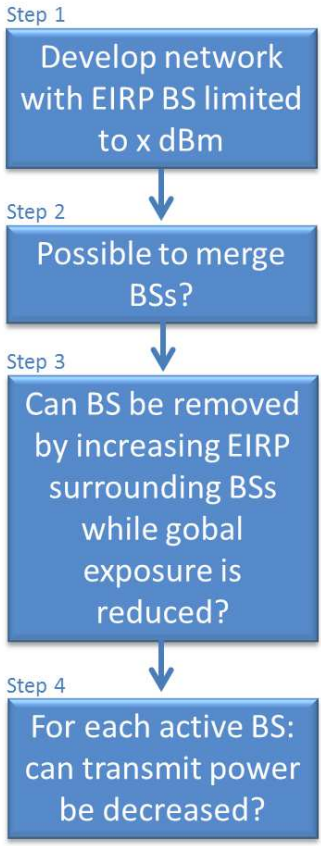

Figure 6.1: Flow diagram of the capacity-based deployment tool designing wireless access networks with a minimal exposure of human beings.

over a network with a few high-power base stations. The algorithm discussed in Section 5.1 can be used in this step.

In the second step (Fig. 6.1 Step 2), it is investigated if two base stations can be merged into one base station with whether or not a higher transmit power. Only those pairs of base stations are investigated whereby the base stations are laying in 125% of their range from each other [3]. This value gives us a good trade-off between not excluding possible mergeable base stations and not needlessly investigating all base station pairs. To determine the location of the new base station, a list of users that are not covered anymore when removing the base station pair is composed. These users need to be covered by a new base station that has a low transmit power. To this end, the algorithm determines for each base station location the highest path loss obtained between that location and the uncovered

users. The base station location that has the lowest value (and can provide the required capacity) will be able to cover the users with the lowest transmit power and will thus be added as new base station to the network. This will occur only when the global exposure of the network E_M, which is a weighted average of the median electric-field strength E_{50} and the 95%-percentile value of the field strengths E_{95}, is lower than before the merge [3]:

$$E_M = \frac{w_1 \cdot E_{50} + w_2 \cdot E_{95}}{w_1 + w_2} \tag{6.2}$$

with w_1 and w_2 weighting factors for the 50%-percentile value E_{50} and the 95%-percentile value E_{95} respectively. In this way, the median exposure of the network (E_{50}) and the maximum exposure values of the network (E_{95}) are taken into account [3]. Here, we assume an equal impact of E_{50} and E_{95} on the metric and set both w_1 and w_2 at a value of 0.5.

The third step (Fig. 6.1 Step 3) investigates if it is possible to remove a base station by increasing the transmit power of the surrounding base stations. The algorithm starts with the base station covering the lowest number of users because this case has the highest chance that the users are covered by other base stations. All users that are covered by the base station under investigation need to be covered by another base station. Therefore, the transmit power of a surrounding base station is increased until all users are covered or until all its capacity is consumed or until the maximum allowable transmit power is reached. When there are still uncovered users, the transmit power of the next surrounding base station is increased. A base station that has already increased its transmit power will not be considered anymore in further investigations. The adaptation of the network will only be accepted when the global exposure of the network is lower than before.

In the fourth and last step (Fig. 6.1 Step 4), it is checked if the transmit power of each base station can be decreased while still serving the users.

6.3 Optimizing towards both power consumption and exposure of human beings

In the previous algorithms, we focused on the optimization towards one parameter: power consumption or global exposure. We now propose an algorithm that optimizes towards both power consumption and global exposure.

Again, the capacity-based algorithm of Section 5.1 is slightly adapted. In the capacity-based algorithm, we tried to connect as much as possible each user to an active base station because it is more energy-efficient to connect to an active base station than waking up a new one as discussed in Section 5.1. However, here a base station can connect to any base station, an active one or by waking up a sleeping one, as long as the experienced path loss is lower than the maximum allowable

path loss. In the ideal case, it will be possible for the user to connect to multiple base stations. To decide which is the best option to connect to, a fitness function is used. This fitness function is similar as the one used in the coverage-based algorithm (Section 3.1), however, different parameters will be taken into account. The global fitness function used here is:

$$f_{tot} = w_1 \cdot (1 - \frac{P}{P_{max}}) \cdot 100 + w_2 \cdot (1 - \frac{E_M}{E_{max}}) \cdot 100 \tag{6.3}$$

with w_1 and w_2 weight factors between 0.0 and 1.0 (boundaries included), P the power consumption of the network, P_{max} the maximum power consumption of the network (i.e., when all base stations are active with maximal input power of the antenna and consuming maximum power according to the settings (e.g., MIMO)), E_M expressed by Eq. (6.2) and E_{max} the global exposure of the network assuming that all base stations are transmitting at the highest possible power. f_{tot} give us a value between 0.0 and 200.0 (boundaries included). The higher f_{tot}, the better the performance of the network. The user will connect to the base station that delivers the highest f_{tot}. If this base station is currently asleep, it will obviously be awakened and we check if it is possible to move users from other base stations to this base station. A user will only change from base station when a lower f_{tot} is obtained. Furthermore, also the antenna's input power of the base station is tuned. Only the process of choosing to connect to which base station is slightly adapted compared to the algorithm of Section 5.1, the rest of the algorithm remains the same.

6.4 Comparison optimizing towards power consumption and exposure of human beings

In the following sections, the power consumption and the global exposure is evaluated when developing networks towards minimal power consumption only, towards minimal power consumption while satisfying a certain exposure limit, and towards minimal global exposure only. The tools of Section 5.1 and the ones discussed above are used for this investigation.

6.4.1 Selected scenario and assumptions

The algorithms will be illustrated on the same case as in Section 5.3.1 for an outdoor suburban area in Ghent, Belgium (Fig. 5.7). Here, only the time stamp of the day with the maximum number of users (i.e., 5-6 p.m. time interval with 224 users) is considered, so the worst-case scenario is investigated. Furthermore, LTE-Advanced is used as wireless technology with a frequency of 2.6 GHz and a bandwidth of 5 MHz, supporting 4x4 MIMO. The other link budget parameters can be found in Table 2.2. Only macrocell base stations are considered.

For evaluating the exposure, we use a grid with a distance of 50 m between two different grid points in both x- and y-direction as shown in Fig. 6.2. This results in a total of 2737 grid points. The exposure of a certain base station will not be taken into account for the grid points within a distance of 25 m from that specific base station as it is assumed that no human will be closer to the base station than the predefined distance. To determine the electric-field strength of a single antenna and the combined electric-field strength from multiple sources, the approach of [3] is followed.

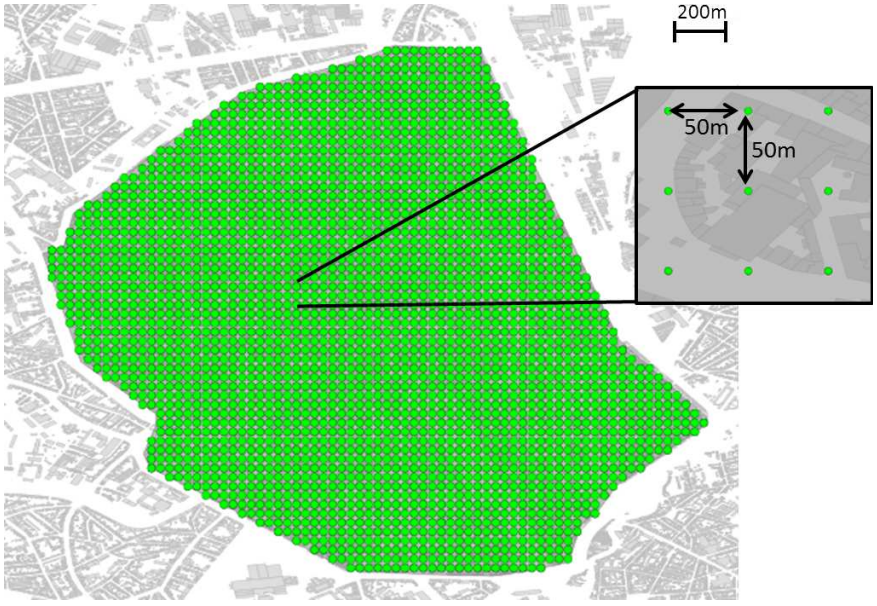

Figure 6.2: Grid used to evaluate the exposure in the Ghent area, Belgium.

Three different networks will thus be developed for this scenario: one optimized towards power consumption, one optimized towards power consumption satisfying an electric field of 4.48 V/m per antenna at 2.6 GHz (Flemish exposure norm [4]), and one optimized towards global exposure. 40 simulations are needed per considered optimization (Chapter 3). For the optimization towards minimal global exposure, the maximum input power of the antenna is limited to 40 dBm. For the network's power consumption, it is assumed that sleeping base stations consume 45% of their active maximal SISO power consumption (Section 5.4). Furthermore, 4x4 MIMO is considered.

6.4.2 Optimization towards power consumption versus power consumption satisfying a certain exposure limit versus global exposure optimization

Table 6.1 lists an overview of the different performance parameters (number of active base stations BS, power consumption PC, obtained electric-field strength E_M, and percentage of users served) for the three different optimizations. For each parameter (except for the number of active base stations and the user coverage for which we only show the 50th percentile), the 50th (p_{50}) and 95th (p_{95}) percentile, and the 90% confidence interval CI calculated over the 40 simulations is shown. The probability density function of the obtained field exposure is shown in Fig. 6.3.

Scenario	BS [-]	PC p_{50} [kW]	PC p_{95} [kW]	CI_{PC} [kW]	E_M p_{50} [mV/m]	E_M p_{95} [mV/m]	CI_{E_M} [mV/m]	Cov. users [%]
Power consumption	20	101.0	105.0	$\pm$0.9	269.2	312.9	$\pm$8.6	100
Power consumption satisfying 4.48 V/m	21	104.7	109.5	$\pm$1.0	259.0	293.4	$\pm$5.2	100
Exposure	41	118.3	125.3	$\pm$1.0	120.7	146.9	$\pm$3.1	100

Table 6.1: Overview of the performance of the developed network (40 simulations) when optimizing towards power consumption, power consumption satisfying 4.48 V/m, and global exposure.

As expected, the lowest power consumption in Table 6.1 is of course obtained when optimizing towards this parameter. The power consumption amounts to 101 kW (p_{50}), while a power consumption of 105 kW and 118 kW is obtained when satisfying 4.48 V/m and optimizing towards exposure, respectively. This lower power consumption is because the networks optimized towards power consumption use only 20 active base stations, while for the last case, the network requires even up to 41 active base stations. Due to this lower number of active base stations, a higher input power of the base station's antenna will be necessary to cover the users. This higher input power results unfortunately in the highest global exposure of the considered optimizations (Fig. 6.3 and Table 6.1). An average value of 269 mV/m and a maximum of 313 mV/m is obtained. Note that the exposure limit of 4.48 V/m is also fulfilled here.

The lowest field exposure (121 mV/m on average and 147 mV/m maximum) is obtained, as expected, when optimizing towards global exposure. To obtain this low exposure, a low input power per base station is used, resulting in a total number of 41 active base stations. This leads to a higher power consumption i.e., 118 kW, than when optimizing towards power consumption.

A compromise between optimizing towards power consumption and global exposure is optimizing towards power consumption while satisfying an exposure

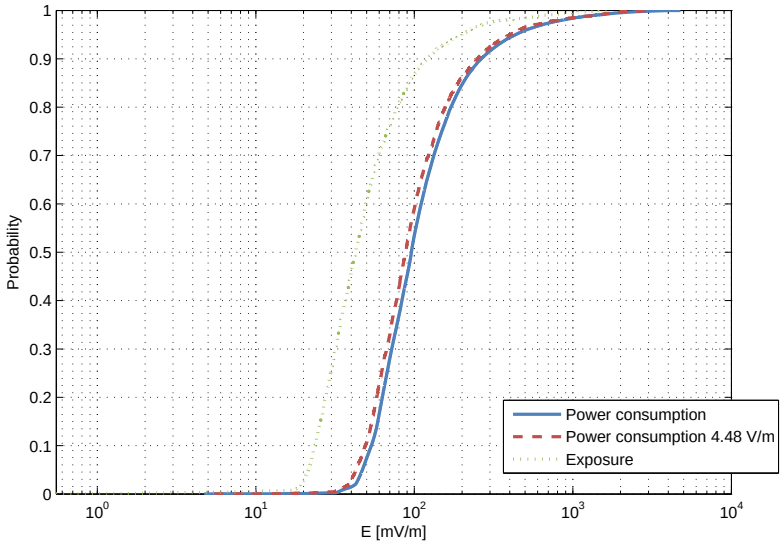

Figure 6.3: Cumulative density function of the obtained exposure when optimizing towards (i) power consumption, (ii) power consumption satisfying 4.48 V/m, and (iii) global exposure.

limit. As shown in Fig. 6.3, the field exposure of this network (259 mV/m on average and 293 mV/m maximum) is between the field value of the networks optimized towards power consumption and global exposure. The field strength obtained when optimizing towards global exposure is however 2 times lower than when optimizing towards power consumption while satisfying a certain exposure limit. Also the power consumption (105 kW) is between the values for the other two networks. In general, a network optimized towards power consumption consists of a low number high-power base stations, while a network optimized towards global exposure consists of a high number low-power base stations.

6.4.3 Influence of limiting the antenna's input power when optimizing towards exposure

As discussed in Section 6.2, in Step 1 of the algorithm a network is developed with limited input power for the antenna. Table 6.2 shows the results when limiting the input power to 30, 35, and 40 dBm. All other parameters remain the same as described in Section 6.4.1.

Although a stricter limitation of the antenna's input power results in a higher number of active base stations (41 for 40 dBm, 44 for 35 dBm, and 45 for 30 dBm),

Scenario	BS [-]	PC p_{50} [kW]	PC p_{95} [kW]	CI_{PC} [kW]	E_M p_{50} [mV/m]	E_M p_{95} [mV/m]	CI_{E_M} [mV/m]	Cov. users [%]
Exposure 40 dBm	41	118.3	125.3	$\pm$1.0	120.7	146.9	$\pm$3.1	100
Exposure 35 dBm	44	119.0	130.4	$\pm$1.9	106.1	119.9	$\pm$2.2	96.0
Exposure 30 dBm	45	118.2	129.5	$\pm$2.4	68.3	78.3	$\pm$1.6	83.7

Table 6.2: Influence of limiting the antenna's input power on the performance of the network (40 simulations) when optimizing towards global exposure.

there is almost no difference in power consumption. This is due to the fact that a lower input power of the antenna results in a lower power consumption (Section 2.1), but also in a lower range per base station, requiring more base stations to cover the users and thus no power consumption reduction is found. The global exposure on the other hand is more influenced by limiting the power. For 40 dBm, a maximum value of 147 mV/m is found, while for 30 dBm, a maximum value of 120 mV/m is obtained. This is quite obvious because as mentioned earlier, a network with a high number of low-power base stations is more desirable in terms of exposure than a network with a low number of high-power base station. However, note that when limiting the power to 30 dBm, the user coverage is drastically decreased to 84%, while for 35 dBm a value of 96% is obtained which is still acceptable. For 40 dBm, all users are covered.

6.4.4 Influence of the minimal distance d_s between base station and the general public

When developing the network (and evaluating the global exposure), a minimal distance d_s between the base station and the human is assumed. Within distance d_s of the base station, it is assumed that no general public will be present and that the norm of [4] does not have to be satisfied. Here, we investigate how this assumption influences our results. For this study, the network optimized towards power consumption satisfying 4.48 V/m per antenna is considered. Three different values for d_s are investigated: 5 m, 15 m, and 25 m. All other parameters remain the same as described in Section 6.4.1. Table 6.3 lists the obtained results.

The larger the proximity d_s of the general public to the base station, the less base stations are active: 34 for 5 m, 23 for 15 m, and 20 for 25 m. This is due to the fact that when a human is closer to the base station, he/she experiences a higher electric-field and thus the algorithm will limit the base station's EIRP (and thus the antenna's input power) more. This limitation in EIRP results in a lower range per base station and thus more base stations will be needed, resulting in a similar power consumption for the different scenarios. However, the global exposure is lower for a lower d_s as for a lower d_s the antenna's input power is more limited resulting in

Scenario	BS [-]	PC p_{50} [kW]	PC p_{95} [kW]	CI_{PC} [kW]	E_M p_{50} [mV/m]	E_M p_{95} [mV/m]	CI_{E_M} [mV/m]	Cov. users [%]
Power consumption 4.48 V/m d_s = 25 m	20	104.7	109.5	±1.0	259.0	293.4	±5.2	100
Power consumption 4.48 V/m d_s = 15 m	23	96.3	98.9	±0.8	176.9	193.8	±2.4	99.6
Power consumption 4.48 V/m d_s = 5 m	34	103.9	108.7	±0.9	80.2	84.7	±1.1	85.3

Table 6.3: Influence of the minimal distance d_s between base station and human on the performance of the network.

a network with a higher number of low-power base stations. A maximum value of 85 mV/m is found for 5 m, while for 25 m a maximum value of 293 mV/m is obtained. Note again, that the user coverage for 5 m is significantly lower than for 15 m and 25 m. Due to the limitation of the antenna's input power, it is not possible anymore to cover all users.

6.4.5 Influence of the distance between the grid points

Another input parameter for the above described algorithms is the grid to evaluate the global exposure of the developed network. In this section, we investigate the influence of the distance d between two grid points. Three distances are considered: 10 m, 30 m, and 50 m. The network optimized towards power consumption satisfying 4.48 V/m is considered. All other parameters remain the same as described in Section 6.4.1. Table 6.4 lists the results.

Scenario	BS [-]	PC p_{50} [kW]	PC p_{95} [kW]	CI_{PC} [kW]	E p_{50} [mV/m]	E p_{95} [mV/m]	CI_E [mV/m]	Cov. users [%]
Power consumption 4.48 V/m d = 50 m	20	104.7	109.5	±1.0	259.0	293.4	±5.2	100
Power consumption 4.48 V/m d = 30 m	20	104.7	109.5	±1.0	259.1	286.6	±5.4	100
Power consumption 4.48 V/m d = 10 m	20	104.7	109.5	±0.8	259.2	288.7	±4.7	100

Table 6.4: Influence of the distance between the grid points on the performance of the network.

Table 6.4 shows that the distance between the grid points does not influence the performance parameters (power consumption and global exposure) significantly. This is quite obvious as the purpose of the grid is only to evaluate the global exposure. It does not have a direct influence on the development of the network as for example, the input power of the antenna.

6.5 Comparison optimizating towards both power consumption and exposure of human beings

As concluded in Section 6.4.2, a network optimized towards power consumption consists of a low number high-power base stations, while a network optimized towards global exposure consists of a high number of low-power base stations. These two parameters, power consumption and global exposure, impose thus contradicting restrictions on the network. A trade-off will thus have to be made when optimizing towards both power consumption and global exposure. In this section, we will investigate this trade-off by varying the weight factors of Eq. (6.3). The algorithm described in Section 6.3 is used for this investigation.

Table 6.5 lists the results when optimizing towards power consumption (w_1 = 1 and w_2 = 0) with the algorithm of Section 6.3 and towards global exposure (w_1 = 0 and w_2 = 1). Comparing those results with the results of Table 6.1 obtained with the algorithms of Section 5.1 and 6.2, which optimize only towards power consumption and global exposure, respectively, are similar as it should be. When optimizing towards power consumption and global exposure (w_1 = 0.5 and w_2 = 0.5; both parameters are assumed to be equally important), a compromise is obtained. The maximum power consumption is slightly higher than when optimizing only towards power consumption (106 kW versus 108 kW for p_{95}) but significantly lower than when optimizing towards global exposure (127 kW). Analogously, a maximum global exposure of 208 mV/m (p_{95}) is found versus 353 mV/m and 175 mV/m when optimizing only towards power consumption and global exposure, respectively.

Parameters	BS [-]	PC p_{50} [kW]	PC p_{95} [kW]	CI_{PC} [kW]	E_M p_{50} [mV/m]	E_M p_{95} [mV/m]	CI_{E_M} [mV/m]	Cov. users [%]
Power consumption $w_1 = 1, w_2 = 0$	20	100.1	105.5	$\pm$0.9	268.2	353.2	$\pm$9.3	100
$w_1 = 0.5, w_2 = 0.5$	23	101.1	107.6	$\pm$1.1	163.1	207.7	$\pm$6.4	100
Exposure $w_1 = 0, w_2 = 1$	38	120.9	127.1	$\pm$1.7	104.2	175.0	$\pm$9.1	100

Table 6.5: Overview of the results when optimizing the network towards power consumption, global exposure, and towards both parameters.

Fig. 6.4 shows the influence of varying the w_1 and w_2 parameter of Eq. (6.3). In each figure, the influence of varying the w_2 factor for a fixed w_1 on the power consumption and the global exposure is shown. The blue full line represents the 50th percentile along with the obtained 90% confidence interval and the red dashed line represents the 95th percentile.

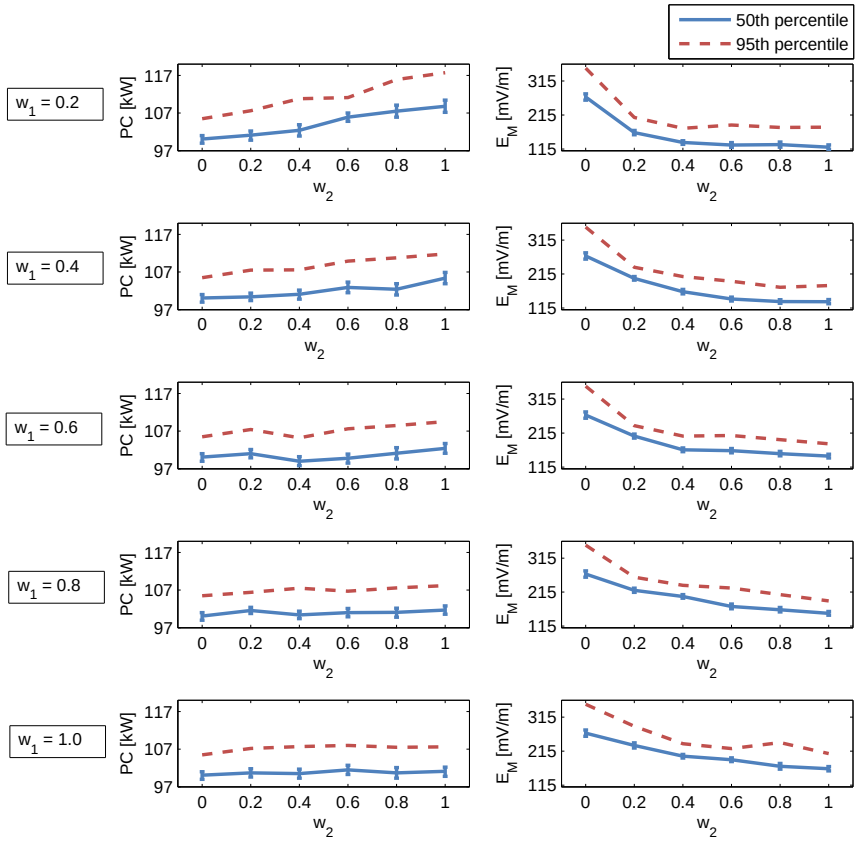

Figure 6.4: Influence of the w_1 and w_2 weight factors of Eq. (6.3) on the performance of the developed network.

Fig. 6.4 shows that for a fixed w_1, a higher w_2 results in a lower global exposure E_M (in mV/m), but also as expected in a higher power consumption PC (in kW). For example, for $w_1 = 0.2$ and $w_2 = 0.2$, a power consumption of 100 kW (p_{50}) and a global exposure of 163.1 mV/m (p_{50}) is obtained versus 108 kW and 45 mV/m for $w_1 = 0.2$ and $w_2 = 0.8$. Analogously, a higher w_1 for a fixed w_2 results in a lower power consumption but also in a higher global exposure. For example, for $w_1 = 0.2$ and $w_2 = 0.8$, a power consumption of 108 kW (p_{50}) and a global exposure of 45 mV/m (p_{50}) is obtained versus 100 kW and 51 mV/m for $w_1 = 0.8$ and $w_2 = 0.8$. Note however that the influence of varying weight factors is limited when optimizing towards both power consumption and global exposure. A

minimum value of 100 kW (p_{50}, w_1 = 0.6 and w_2 = 0.4) and 44 mV/m (p_{50}, w_1 = 0.2 and w_2 = 0.6) is obtained versus a maximum value of 108 kW (p_{50}, w_1 = 0.2 and w_2 = 0.8) and 70 mV/m (p_{50}, w_1 = 0.8 and w_2 = 0.2). The higher one of the two weight factors, the less influence the other weight factor has.

In general, the following guidelines can be used for choosing the weight factors:

- Optimizing towards power consumption: w_1 = 1 en w_2 = 0
- Optimizing towards global exposure: w_1 = 0 en w_2 = 1
- Optimizing towards power consumption and global exposure (equal important): $w_1 = w_2$
- Optimizing towards power consumption and global exposure when power consumption is more important: $w_1 > w_2$
- Optimizing towards power consumption and global exposure when exposure is more important: $w_1 < w_2$

6.6 Conclusion

In this chapter, four different algorithms are proposed to develop future green wireless access networks. Each algorithm optimizes towards another parameter: power consumption, power consumption while satisfying a certain exposure limit, global exposure, and both power consumption and global exposure.

Comparing the results of the first three algorithms shows that when optimizing towards power consumption, the network consists of a low number of high-power base stations, while optimizing towards global exposure results in a network consisting of a high number of low-power base stations. When optimizing towards power consumption while satisfying a certain exposure limit, a compromise between the other two optimizations is obtained, although the field values are a factor 2 higher compared to the optimization towards global exposure.

We have discussed a fourth algorithm that optimizes the network towards both power consumption and global exposure. By choosing the appropriate weight factors, the required trade-off between the importance of optimizing towards power consumption and towards global exposure is obtained.

References

[1] M.A. Marsan, L. Chiaraviglio, D. Ciullo, and M. Meo. *A Simple Analytical Model for the Energy-Efficient Activation of Access Points in Dense WLANs*. In the 1st International Conference on Energy-Efficient Computing and Networking (e-Energy), pages 159–168, Passau, Germany, 2010.

[2] G. Koutitas. *Green Network Planning of Single Frequency Networks*. IEEE Transactions on Broadcasting, 56(4):541–550, 2010.

[3] D. Plets, W. Joseph, K. Vanhecke, and L. Martens. *Exposure Optimization in Indoor Wireless Networks by Heuristic Network Planning*. Progress in Electromagnetics Research, 139:445–487, 2013.

[4] *Besluit van de Vlaamse Regering van 19 november 2010 tot wijziging van het besluit van de Vlaamse Regering van 1 juni 1995 houdende algemene en sectorale bepalingen inzake milieuhygiëne wat betreft de normering van vast en tijdelijk opgestelde zendantennes voor elektromagnetische golven tussen 10 MHz en 10 GHz.*

7 Conclusions and future research

In this final section, overall conclusions of the research performed in this dissertation are summarized.

7.1 Conclusions

The last few decades, a considerable increase in mobile devices ranging from mobile phones and smart phones, over laptops and tablets, to smart watch and fitness devices has been noticed. Besides this, these devices are becoming very powerful, allowing also more demanding services such as streaming music and videos, video calling, etc. These two trends have of course their influence on the wireless access networks serving those mobile devices. The network will not only have to expand in size to cope with these extra demands but also has to provide a higher capacity to keep the end user satisfied. In 2008, communication networks were already responsible for 15% of the ICT power consumption, moreover, 77% of this consumption was caused by telecommunication operator networks. To preserve our fossil fuels and reduce CO_2 emission, every aspect of our society has to contribute and thus it is important to develop in the future wireless access networks with a minimal power consumption. On the other side, more people are becoming concerned about the health effects of those networks. Exposure awareness to electromagnetic fields is currently growing, so also wireless access networks with a minimal global exposure for human beings are desirable in the future. The main focus of this dissertation is to design future green wireless access networks opti-

mizing both power consumption and electromagnetic exposure for human beings.

A wireless access network consists of many base stations, often of different types. When developing and evaluating the network's power consumption, it is thus important to quantify the power consumption of a base station (type). In Chapter 2, the architecture of three base station types (macrocell, microcell, and femtocell base station) is determined and based on this architecture, a power consumption model is defined for each base station type. A typical power consumption of 12 W, 377 W, and 1279-1673 W is obtained for a femtocell, microcell, and macrocell base station, respectively. Furthermore, appropriate energy efficiency metrics are defined to determine and compare different wireless technologies and base station types. Which technology the most energy-efficient is depends on the considered base station type and the required bit rate. For example, for a macrocell base station, mobile WiMAX is the most energy-efficient for bit rates higher than 11.5 Mbps, LTE for bit rates between 2.8 and 11.5 Mbps, and HSPA for bit rates below 2.8 Mbps. Furthermore, it depends also on the wireless technology which base station type is the most energy-efficient. However, this does not mean that it is not interesting in terms of energy efficiency and power consumption to introduce a less energy-efficient base station type in the network. Due to for example a lower power consumption, it can reduce the overall network power consumption. To increase the energy efficiency of a single base station, MIMO can be used. The power consumption per covered area is reduced by 50 to 63% for a macrocell base station when supporting 4x4 MIMO.

Chapter 3 proposes a deployment tool for the design of future wireless access networks with a minimal power consumption. A coverage-based algorithm is proposed which uses a genetic search algorithm. The purpose of this tool is to cover a specific (geometrical) area as energy-efficiently as possible for a certain predefined bit rate. The power consumption model of Chapter 2 is used by both algorithms when developing and evaluating the network.
The coverage-based algorithm is applied on a realistic case. For an area in Ghent (Belgium), a greenfield deployment is considered, while for Brussels Capital Region (Belgium) the existing network is optimized towards power consumption. The performance of different wireless technologies is again studied. The highest energy efficiency for the considered cases and assumptions is obtained for LTE. For all considered cases, the energy efficiency can be further increased when introducing microcell base stations in the network and when the base stations support MIMO. It is recommended for future networks to support both macrocell and small-cell base stations.

In Chapter 4, measurements were performed on an actual macrocell and mi-

crocell base station. These measurements allowed us to validate the power consumption model of Chapter 2. Furthermore, the influence of traffic variations on the base station's power consumption are investigated and an appropriate power consumption model is proposed. An extension of the coverage-based algorithm of Chapter 3 combining sleep modes and cell zooming (or cell breathing) which are two power reducing techniques is presented.
For the case in Ghent, introducing sleep modes and cell zooming, results in a power consumption reduction of 14% (depending on the considered sleep threshold) compared to the network without these power reducing techniques. For the case in Brussels, optimizing towards power consumption (without sleep modes and cell zooming) reduces already the consumed power by 33%. An additional saving of 2% can be obtained when using sleep modes and cell zooming, while a saving of 8% is found for existing networks without optimizing the base station locations. A careful selection of the base station locations can thus already result in a significant saving. In current networks, this can be done by site sharing. For future networks, it is recommended that sleep modes and cell zooming are supported.

Chapter 5 studies the influence of three features added to LTE-Advanced on the power consumption and energy efficiency and compares it to the performance of LTE. These three features are carrier aggregation whereby the bit rate offered by the base station can be increased, improved support for heterogeneous networks consisting of a mixture of macrocell and femtocell base stations, and extended support for MIMO up to 8 transmitting and 8 receiving antennas. The investigation is performed on the base station level and on the network level. For the network level, a capacity-based deployment tool is proposed. This tool develops networks with a minimal power consumption but responds to the instantaneous bit rate requests of the users active in the considered area, rather than providing coverage to a certain area as in the coverage-based deployment tool. The tool is applied on a realistic case in Ghent, Belgium.
For a single base station, in general, a higher bit rate results in a lower energy efficiency. However, by using carrier aggregation, LTE-Advanced allows to obtain higher bit rates for even a higher energy efficiency. The type of base station (macrocell or femtocell base station) that is the most energy-efficient depends on the bit rate. MIMO can also increase the energy efficiency of a single base station. For the investigation on the network level, the highest power reduction and energy efficiency improvement is obtained when applying the three features together i.e., a heterogeneous network where the femtocell base station supports both carrier aggregation and MIMO. Adding femtocell base stations without MIMO and carrier aggregation can already reduce the power consumption significantly. Furthermore, introducing femtocell base stations only supporting carrier aggregation has the highest influence on the energy efficiency, while introducing femtocell base

stations only supporting MIMO has the highest influence on the power consumption.
We recommend for future wireless access networks to take the advantage of LTE-Advanced incoperated features (carrier aggregation, heterogeneous networks, and extended support for MIMO), especially the introduction of femtocell base stations, to reduce the power consumption of the network.

In Chapter 6, three extensions of the capacity-based deployment of Chapter 5 are proposed. The first extension develops networks optimized towards power consumption but while satisfying a certain exposure limit, while the second extension optimizes networks towards global exposure for human beings. The last extension develops future green wireless access networks whereby the network is optimized towards both power consumption and global exposure.
Comparing the results of the first three algorithms shows that when optimizing towards power consumption, the network consists of a low number of high-power base stations, while optimizing towards global exposure results in a network consisting of a high number of low-power base stations. When optimizing towards power consumption while satisfying a certain exposure limit, a compromise between the other two optimizations is obtained, although the field values are a factor 2 higher compared to the optimization towards global exposure.
The previous results show that optimizing towards both power consumption and global exposure is a complex process as the optimization towards each parameters results in conflicting requirements for the network. A trade-off between these two parameters have to be made. We have shown that by choosing appropriate weight factors for evaluating the performance of the network during the design phase, the required trade-off between the importance of optimizing towards power consumption and towards global exposure can be obtained. This last algorithm allows to design the desired future green wireless access networks minimizing power consumption and global exposure.

7.2 Future research

Wireless access networks are of course still evolving. A newly added feature is 'relaying' where the mobile device communicates with a relay node instead of directly with the base station as we discussed in Chapter 1. In the future, these relay nodes can be integrated in vehicles, placed on robots or it can also be another mobile device such as a smart phone or a tablet. These 'new types of base stations' can move around during communication compared to the currently deployed base stations which will of course influence the network's coverage, the capacity offered in the different parts of the network, and the global exposure. This influence

should clearly be studied, along with how this can be taken into account when designing networks. Furthermore, appropriate models should be developed for the power consumption of these new types of base stations and it should be investigated if it is possible to reduce the power consumption and improve the energy efficiency when introducing these new types of base stations into the network.

The commercial market for mobile communication is of course not limited to one operator. Some of those operators are virtual operators, using the infrastructure of other operators, however, there are still multiple operators each having their own network. Due to this, the frequency band for a certain wireless technology has to be divided between them. Currently, a new idea i.e., co-primary shared access, is being raised to actually share the frequency band between operators rather than dividing it between them. In this way, a better spectrum utilization is obtained and operators can cope better with temporary peaks. It should be investigated how co-primary shared access can be taken into account when developing future networks, and how this can reduce the power consumption and improve the energy efficiency of those networks.

In this dissertation, only the downlink communication (from the base station to the mobile device) is considered. One of the biggest challenges for the future is probably to consider the uplink communication (from the mobile device to the base station) as well. This means that an appropriate power consumption model has to be defined for the mobile device. Defining such a power consumption model is not such an obvious task because of the huge range of mobile devices. Not only mobile phones, smart phones, tablets, and laptops can be considered as mobile devices; within each category there also exist a tremendous range of products. Furthermore, the power consumed by the mobile device is very dependent on the user behavior. Also the uplink absorption due to the radiation of the mobile device should be taken into account. Not only the absorption by the whole body should be considered, but also the localized absorption in for example the head should be considered.

Finally, we have only considered outdoor environments. In an ideal situation, our deployment tool can be extended or combined with an indoor network planning tool. In this way, it is possible to investigate how the signals from the outdoor base stations propagates through the indoor environment and how to adapt the outdoor network to provide also indoor coverage. The exposure of indoor and outdoor users can be compared. Furthermore, the global exposure of the network's outdoor antennas can be evaluated in the indoor environment. Also the influence of indoor relays can be investigated.